UNIVERSIDADE DE LISBOA

FACULDADE DE CIÊNCIAS

Search for new modulators of Phe508del-CFTR retention at the plasma membrane of epithelial cells

" Documento Definitivo"

Doutoramento em Biologia
Especialidade de Biologia de Sistemas

Ana Margarida Fernandes Pereira de Matos

Tese orientada por:
Prof. Doutor Paulo Matos (Orientador) e
Prof. Doutor Rainer Pepperkok (Co-Orientador)

Documento especialmente elaborado para a obtenção do grau de doutor

2018

UNIVERSIDADE DE LISBOA

FACULDADE DE CIÊNCIAS

Ciências
ULisboa

Search for new modulators of Phe508del-CFTR retention at the plasma membrane of epithelial cells

Doutoramento em Biologia

Especialidade de Biologia de Sistemas

Ana Margarida Fernandes Pereira de Matos

Tese orientada por:

Prof. Doutor Paulo Matos (Orientador) e
Prof. Doutor Rainer Pepperkok (Co-Orientador)

Júri:

Presidente:

- Doutor Rui dos Santos Malhó, Professor Catedrático e Presidente do Departamento de Biologia Vegetal da Faculdade de ciências da Universidade de Lisboa

Vogais:

- Doutor Duarte Custal Barral, Professor auxiliar convidado da Nova Medical School da Universidade Nova de Lisboa
- Doutora Maria João Aleixo da Silva, Investigadora auxiliar do Instituto de Nacional de Saúde Dr. Ricardo Jorge
- Doutora Filipa Fernandes Mendes, Investigadora auxiliar do Instituto Superior Técnico da Universidade de Lisboa
- Doutor Carlos Miguel Ribeiro da Silva Farinha, Professor auxiliar com agregação da Faculdade de Ciências da Universidade de Lisboa
- Doutor Paulo Henrique Carrasquinho de Matos, Investigador FCT "nível incial" da Faculdade de Ciências da Universidade de Lisboa, Orientador

Documento especialmente elaborado para a obtenção do grau de doutor

Bolseira de doutoramento, financiada pela Fundação para a Ciência e a Tecnologia do Ministério da Ciência, Tecnologia e Ensino Superior, Bolsa PD/BD/52490/2014.

2018

De acordo com o disposto no artigo 24º do Regulamento de Estudos de Pós-Graduação da Universidade de Lisboa, Despacho nº 7024/2017, publicado no Diário da República – 2ª Série – nº 155 – 11 de Agosto de 2017, foram utilizados nesta dissertação resultados incluídos nos seguintes artigos:

1. Loureiro CA, **Matos AM**, Dias-Alves A, Pereira JF, Uliyakina I, Barros P, et al. A molecular switch in the scaffold NHERF1 enables misfolded CFTR to evade the peripheral quality control checkpoint. *Sci. Signal.* **8(377),** ra48 (2015)

2. **Matos AM**, Combination therapy in Phe508del CFTR: how many will be enough? *J. Lung Health Dis.* **2,** 9–16 (2018)

3. **Matos AM**, Gomes-Duarte A, Faria M, Barros P, Jordan P, Amaral MD, et al. Prolonged co-treatment with HGF sustains epithelial integrity and improves pharmacological rescue of Phe508del-CFTR. *Sci. Rep.* **8,** 13026 (2018)

No cumprimento do disposto da referida deliberação, a autora esclarece serem da sua responsabilidade, exceto quando referido o contrário, a execução das experiências que permitiram a elaboração dos resultados apresentados, assim como a interpretação e discussão dos mesmos. Os resultados obtidos por outros autores foram incluídos com a autorização dos mesmos para facilitar a compreensão dos trabalhos e estão assinalado s nas respetivas figuras.

“Science is not only compatible with spirituality;
it is a profound source of spirituality.”

Carl Sagan

Index

Agradecimentos

Se há alguém a quem tenho verdadeiramente de agradecer é ao meu orientador Paulo Matos. Durante estes 4 anos de doutoramento aprendi imenso, não só na bancada, mas principalmente na maneira de pensar. O Paulo é um verdadeiro orientador, no sentido mais literal da palavra: genuinamente preocupado e sempre disponível; cheio de ideias e sugestões; genial e inovador na maneira de pensar. Além de ser um ótimo cantor nos tempos mortos de confocal! Muito obrigado pela boa disposição, imensa paciência e todo o tempo investido em mim e no meu trabalho. Ao meu co-orientador, Rainer Pepperkok, que embora esteja noutro país esteve sempre disponível para me ajudar e aconselhar.

Se esta tese ganhou forma foi sem dúvida com um grande trabalho de equipa. E tenho que o agradecer às minha colegas de bancada, sempre disponíveis a ajudar. Patrícia, Vânia, Andreia, Joana, Márcia e Claúdia, agradeço as conversas, as dicas e o apoio constante. Grata também por aturarem as minhas maluquices e particularidades. No fundo eu acho que vocês até vão sentir falta do cheiro a caril e das sessões na sala coração pacífico. Falando desta sala não posso deixar de agradecer ao Peter Jordan, uma pessoa que me inspira na maneira de ser e de estar. No fundo fui calhar a um grupo de trabalho já por si diferente e bastante adequado a mim, no melhor dos sentidos. Não me esqueço também das alunas de mestrado que passaram pela orientação do Paulo, e que por isso trabalharam muito próximas de mim e do meu trabalho. Andreia e Vanessa, é bem possível que tenha aprendido mais com vocês do que vocês comigo. Aos meus co-autores, muitos dos quais foram mencionados acima, foi um prazer trabalhar convosco. Que haja muitas Nature-Cell no nosso futuro.

Aos meus colegas de doutoramento, pioneiros do BioSys, um agradecimento especial ao Hugo, Paulo, Nikhil, Joana e Sara. Foi muito bom ter-vos ao meu lado durante esta jornada. E como cabeças de cartaz!

Ao meu marido e filho, que dão sentido à minha vida. Aos meus pais, que sempre deram muita importância à minha formação e futuro, agradeço ter chegado até aqui. A toda a minha família, eu sei que estão orgulhosos de mim. E aos meus amigos, que eu adoro e compreendem inteiramente quem eu sou.

No fundo passaram-se quatro anos em que comecei como uma miúda e saí uma mulher. Muito obrigado a todos vós que me acompanharam, é com imensa gratidão que olho para trás e me apercebo do que ganhei em ter feito este caminho.

Abbreviations

ABC transporter	ATP-binding cassette transporter
AON	Oligoribonucleotide
ASL	Airway Surface Liquid
ATP	Adenosine Triphosphate
BHK	Baby Hamster Kidney cells
C-terminal	Carboxyl-Terminal
C1199Tiam1	GDP-to-GTP Exchange Factor Tiam1
C4	Corrector corr-4a
CAL	CFTR-associated ligand
Calpain 1	Calcium-Activated Neutral Proteinase 1, catalytic subunit
CCS	combined confidence score (CCS)
CF	Cystic Fibrosis
CFTR	Cystic Fibrosis Transmembrane conductance Regulator
cGMP	cyclic Guanosine Monophosphate
CHIP	Carboxyl terminus of Hsc70 Interacting Protein
CHX	Cycloheximide
CK18	Cytokeratin 18
CK8	Cytokeratin 8
Cl^-	Chloride
DAVID	Database for Annotation, Visualization and Integrated Discovery
DMSO	Dimethylsulfoxide
Dox	Doxycycline
DSP	Dithiobis Succinimidyl Propionate
EB	EZR binding site
EMA	European Medicines Agency
EMT	Epithelial-Mesenchymal Transition
ENaC	Epithelial Sodium Channel

ER	Endoplasmic Reticulum
ERAD	Endoplasmic Reticulum Associated Degradation
ERM	ezrin-radixin-moesin (ERM)
ERQC	Endoplasmic Reticulum Quality Control
EZR	Ezrin
F-actin	Filamentous Actin
FBS	Fetal Bovine Serum
FDA	Food and Drug Administration
FERM domain	Four point one, ERM domain
FEV_1	Forced Expiratory Volume in One Second
Fsk	Forskolin
GDP	Guanosine Diphosphate
GEF	Guanine Nucleotide Exchange Factor
Gen	Genistein
GFP	Green Fluorescent Protein
Glut1	Glucose Transporter 1
GSNOR	S-nitrosoglutathione reductase
GTPases	Guanosine Triphosphatases
HCO_3^-	Bicarbonate
HGF	Hepatocyte Growth Factor
HS-YFP	Halide-Sensitive Yellow Fluorescent Protein
Hsc70	Heat Shock Cognate 70-kD protein
inh172	CFTR 172 Inhibitor
IP	Immunoprecipitation
IPO5	Importin 5
mChF Phe508del-CFTR	mCherry-Flag-Phe508del-CFTR
mChF wt-CFTR	mCherry-Flag-wt-CFTR
MEM	Minimal Essential Medium
N-terminal	Amino-Terminal
NBDs	Nucleotide-Binding Domains
NHERF1	Na+/H+ exchange regulatory factor 1
PBMC	Peripheral Blood Mononuclear Cells

PCS	Protein Confidence Score
PDZK1	PDZ domain-containing protein in kidney 1
PDZK2	PDZ domain-containing protein in kidney 2
Phe508del	Deletion of a Phenylalanine Residue at Position 508
PIP_2	l-α-phosphatidylinositol-4,5-bisphosphate
PIP5K	Phosphatidylinositol 4-phosphate 5-kinase
PKC	Protein Kinase C
PM	Plasma Membrane
PPQC	Peripheral Protein Quality Control
R	Regulatory Domain
Rme-1	Receptor Mediated Endocytosis 1
ROCK	Rho-kinase
rPhe508del	rescued Phe508del
sGC	Soluble Guanylate Cyclase
Shank2	SH3 and Ankyrin repeats containing protein 2
TBCP2	MeOx6-THF19-MeOx6
TEER	Transepithelial Electrical Resistance
Tet-ON	Tetracycline-Inducible
TJ	Tight-Junction
TMDs	Transmembrane Domains
TS	Thermal Shift
VX-661	Tezacaftor
VX-770	Ivacaftor
VX-809	Lumacaftor
WB	Western Blot
YFP	Yellow Fluorescent Protein

Summary

Cystic fibrosis (CF) is a complex inherited disorder caused by mutations in the cystic fibrosis transmembrane conductance regulator (CFTR) gene. Around 2000 disease causing mutations are known for this gene, which encodes a Chloride (Cl^-) channel expressed at the plasma membrane (PM) of epithelial cells. The most frequent CFTR mutation, the deletion of phenylalanine 508 (Phe508del), causes the protein to misfold and be prematurely degraded. Low temperature or pharmacological "correctors" can partly rescue Phe508del-CFTR processing defect and enhance the channel traffic to the cell surface. Nevertheless, the rescued channels show partial channel function and a highly decreased PM half-life, due to accelerated endocytosis and fast turnover. Given this accelerated endocytic rate, new strategies aiming to retain rescued Phe508del-CFTR at the cell surface could be relevant as to enhance the efficacy of currently available pharmacological correctors. For that reason, the major objective of this dissertation is to identify novel cellular pathways or key interactors for the modulation of CFTR surface retention.

Previous results from the host laboratory had showed that stimulation of endogenous RAC1 by Hepatocyte Growth Factor (HGF) signaling potentiated the retention of rescued Phe508del-CFTR at the PM by promoting an interaction between the actin-binding adaptor ezrin (EZR) and the Na+/H+ exchange regulatory factor-1 (NHERF1), enhancing CFTR anchoring to the actin cytoskeleton. In **chapter 2** we showed that the mechanism behind this stabilization lies on a conformational change in NHERF1, triggered by EZR activation upon RAC1 signaling, which is then able to bind and stabilize misfolded CFTR at the PM. However, HGF/RAC1 signaling pathway is known to have proliferative and pleiotropic biological functions, which limit its application for therapeutic intervention. Therefore, in **chapter 3**, we investigated the effect of HGF treatment in epithelium-like cellular models, in combination with the most common administrated drugs. Contrary to what would be commonly assumed, we found that prolonged co-administration of HGF actually prevented previously unrecognized epithelial dedifferentiation effects of prolonged exposure to the FDA-approved Phe508del-CFTR corrector VX-809. It also significantly increased the Phe508del-CFTR functional rescue by the FDA- and EMA-approved VX-809/VX-770 drug combination, preventing the destabilization of the PM rescued channels by prolonged exposure to the VX-770 potentiator drug. These results suggest that HGF co-administration could indeed be beneficial for CF patients and should be further clinically explored.

Lastly, since we showed that the type of protein interactions that wt- and rescued Phe508del-CFTR establish at the cell surface can be major determinants of their different PM stabilities, in **chapter 4** we identified, for the first time, the core components of the macromolecular complexes assembled around wt- and rescued Phe508del-CFTR proteins at the PM. By identifying exclusive PM interactions between rescued Phe508del-CFTR, NHERF1 and EZR, we were able to recognize Calpain 1 as a key contributor for the decreased surface stability of pharmacologically rescued Phe508del-CFTR, probably acting through the disruption of the EZR-actin cytoskeleton binding.

Keywords

Cystic Fibrosis, CFTR, Phe508del, Plasma Membrane Stabilizers, CFTR interactome.

Resumo

A Fibrose Quística (FQ) é uma doença hereditária, letal, cujo nome deriva do aspeto quístico e fibroso do pâncreas dos portadores da doença. É uma das doenças genéticas mais comuns, afetando aproximadamente 70.000 pessoas em todo o mundo, com maior expressão na população caucasiana. Em Portugal estima-se que nasçam cerca de 30 a 40 crianças com FQ por ano. A doença é causada por alterações que ocorrem num único gene – o gene CFTR (do inglês, ***C**ystic **F**ibrosis **T**ransmembrane **C**onductance **R**egulator*). Este gene codifica um canal de cloreto (Cl^-), expresso maioritariamente na membrana apical das células epiteliais. As mutações neste canal levam a uma secreção deficiente de Cl^- no epitélio, causando um desequilíbrio eletrolítico que provoca várias manifestações sistémicas. Os sistemas mais afetados são o pulmonar e gastrointestinal, onde muco extremamente viscoso é acumulado, causando infeções e inflamações pulmonares crónicas e obstrução pancreática com consequente malnutrição. A principal causa de morte por FQ é a falência pulmonar, sendo a esperança média de vida atual entre os 35 e os 40 anos de idade.

À data existem mais de 2000 mutações descritas para o gene CFTR. A mutação mais frequente é uma deleção de um resíduo de fenilalanina na posição 508, chamada Phe508del, estando presente em 85% dos doentes em pelo menos num alelo. Em Portugal os números indicam que esta está presente em cerca de 85% dos doentes com FQ. Esta mutação provoca, em primeira instância, defeitos no processamento (*folding*) da CFTR, impedindo que esta atinja a membrana plasmática (MP). Adicionalmente, as poucas moléculas CFTR-Phe508del que conseguem chegar à superfície das células apresentam defeitos de função, ao nível da abertura do canal, bem como um tempo de semi-vida na membrana (estabilidade na MP) bastante reduzido, quando comparado com a CFTR normal. Atualmente existem compostos capazes de promover o resgate parcial do *folding* da CFTR-Phe508del e o seu tráfego para a MP (denominados "corretores", como o VX-809) e a abertura do canal na MP (denominados "potenciadores", como o VX-770). No entanto, não existe de momento qualquer composto que aumente o tempo de semi-vida e a estabilidade do canal na MP. Nesse sentido, o principal objetivo desta dissertação é identificar novos modeladores ou vias celulares que aumentem a retenção na MP da CFTR-Phe508del resgatada farmacologicamente.

É sabido que o canal CFTR está associado a várias outras proteínas, formando um grande complexo proteico à superfície das células. Estas interações entre proteínas são determinantes para a função e regulação do canal na MP. De acordo com este conhecimento, o laboratório de acolhimento mostrou, anteriormente, que a ativação da via RAC1 regula a ancoragem da CFTR-Phe508del à MP e ao citoesqueleto de actina mediante a sua interação com duas proteínas adaptadoras, a ezrina (EZR) e o NHERF1 (do inglês Na/H exchanger regulatory factor 1). Este aumento da ancoragem ao citoesqueleto de actina deriva da ativação da proteína EZR, que após estimulada pelo RAC1 adquire uma conformação aberta e ativa, o que promove uma maior afinidade tanto para a ligação à actina como para a ligação ao complexo NHERF1-CFTR, prevenindo a endocitose do canal CFTR mutante. Usando o fator de crescimento de hepatócitos (HGF), um conhecido ativador do RAC1 endógeno, foi possível observar um aumento de estabilidade três vezes maior na retenção da CFTR-Phe508del resgatada farmacologicamente em células epiteliais tratadas com HGF, em comparação com células não tratadas com o fator. Assim sendo, no **capítulo 2** desta dissertação, foi aprofundada

a interação entre as proteínas CFTR-Phe508del, EZR e NHERF1, com o objetivo de compreender o mecanismo molecular que leva ao aumento da estabilidade do canal após a ativação da via HGF/RAC1. Demonstrámos que a ligação da EZR ativa à proteína NHERF1 promove uma mudança de conformação na mesma, levando a uma mudança de ligação da CFTR do domínio NHERF1-PDZ1 para o NHERF1-PDZ2. Esta mudança na estrutura do complexo proteico CFTR-NHERF1, induzida pelo RAC1, antecipa e previne a deteção pelos mecanismos de controlo periférico de proteínas anómalas (PPQC, do inglês Peripheral Protein Quality Control), levando a uma menor taxa de endocitose e, consequentemente, a um aumento da estabilidade da CFTR-Phe508del resgatada.

Contudo, embora tenhamos mostrado e caracterizado que a via HGF/RAC1 promove a estabilidade da CFTR mutada à superfície das células, devido à descrita pleiotropia funcional do HGF e a sua associação ao desenvolvimento de certas neoplasias, a aplicabilidade deste fator em terapias é limitada. Assim sendo, no **capítulo 3** desta dissertação procedeu-se ao estudo do efeito do tratamento, tanto agudo como prolongado, do HGF em modelos celulares de epitélio polarizado, em combinação com o tratamento com VX-809 e/ou VX-770. Tanto o tratamento de HGF agudo como o prolongado aumentaram os níveis de CFTR-Phe508del funcional à superfície das células, quando combinado com os fármacos VX-809 e VX-770, aprovados para a tratamento de doentes com a mutação Phe508del pelas entidades reguladoras FDA e EMA. Curiosamente, tendo já sido descrita uma destabilização por parte do potenciador VX-770 na CFTR-Phe508del resgatada por VX-809, o triplo co-tratamento com HGF teve um efeito protetor na estabilidade da CFTR-Phe508del. Mais importante, ao invés de promover a desdiferenciação e proliferação das células epiteliais polarizadas, o tratamento prolongado com HGF teve o efeito contrário, prevenindo o aumento dos marcadores Ki-67 e CK8 que, surpreendentemente, aumentaram com a exposição prolongada de VX-809 e VX-770. Em conjunto, estes resultados sugerem que a co-administração de HFG com fármacos corretores e potenciadores poderá ser benéfica para pacientes com FQ.

Tendo-se anteriormente demonstrado que as interações entre a CFTR e as proteínas que compõem o seu complexo macromolecular à superfície das células são importantes para a estabilidade do canal, no **capítulo 4** propusemos estudar em detalhe os seus componentes, com o objetivo de identificar novos modeladores da retenção da CFTR na MP. Para isso, isolámos e identificámos as proteínas que compõem os complexos macromoleculares associados à CFTR em CFTR-wt e em CFTR-Phe508del resgatada pela baixa temperatura ou o fármaco VX-809, usando ferramentas bioinformáticas para identificar diferenças entre os mesmos. Tendo como base as interações exclusivas entre as proteínas EZR, NHERF1 e a CFTR-Phe508del resgatada identificámos a protease Calpain 1 como um modelador da estabilidade do canal na membrana. Ao diminuirmos a quantidade e função desta proteína observámos um aumento substancial na abundância, função e retenção na MP da CFTR-Phe508del resgatada. Sabendo que a EZR é um substrato conhecido da protease Calpain 1 (*Calcium-Activated Neutral Proteinase 1*), mostrámos que, à superfície das células, a EZR aumenta quando diminuímos a quantidade de Calpain 1 disponível, não sendo observadas quaisquer diferenças na quantidade de NHERF1. Assim sendo, propusemos que a Calpain 1 é um regulador negativo da estabilidade da CFTR-Phe508del na MP, atuando através da proteólise da proteína EZR, destabilizando o seu complexo macromolecular. Como a Calpain 1 foi identificada como sendo uma proteína exequível de ser farmacologicamente modelada pela base de dados chEMBL, o

seu estudo pode vir a ser importante para o desenvolvimento de novas terapias que promovam a estabilidade na MP da CFTR.

Em resumo, esta dissertação cumpriu os objetivos propostos, dado que identificou e caracterizou vários modeladores da retenção da CFTR-Phe508del resgatada farmacologicamente para a superfície das células. Estes resultados abrem portas para o estudo e desenvolvimento de novas terapias combinadas, pois, como anteriormente referido, neste momento não existe qualquer composto disponível que aumente o tempo de semi-vida e a estabilidade do canal na MP. Algumas das implicações deste estudo não são exclusivas apenas para a mutação Phe508del, podendo também ser aplicados a outras mutações que diminuam a estabilidade da proteína CFTR, como a mutação c.120del23 e Q1412x.

Palavras-Chave

Fibrose Quística, CFTR, Phe508del, Estabilizadores da membrana plasmática, Interactoma da CFTR.

Chapter 1
General Introduction

* The information contained in this topic was published, with minor changes, as part of a minireview article entitled "**Matos AM**, Combination therapy in Phe508del CFTR: how many will be enough? *J. Lung Health Dis.* **2,** 9–16 (2018)"

1.1. Cystic Fibrosis

Cystic fibrosis (CF) is an inherited monogenic disorder affecting more than 70.000 people worldwide, with an incidence of one in every 2500 newborns among the Northern European descent population. It is a complex disease, and the types and severity of symptoms can differ widely within individuals depending on their mutations, environment and access to therapy [1,2].

1.1.1. The CFTR gene and protein

CF is caused by mutations in one single gene, the cystic fibrosis transmembrane conductance regulator (CFTR), first identified in 1989 [3]. CFTR is a 1,480-amino-acid protein that encodes a member of the ATP-binding cassette (ABC) transporter superfamily. Despite its structure similarity to other members of the ABC transporter family, CFTR is unique in its function as an chloride (Cl^-) channel [2,4]. Thus, CFTR contains the typical two transmembrane domains (TMDs) composed of six transmembrane segments that form the Cl^- translocation path, and two cytoplasmic nucleotide-binding domains (NBDs) that bind and hydrolyze ATP. In addition, CFTR contains an exclusive regulatory (R) domain that encloses multiple consensus phosphorylation sites and charged amino acids (See Figure 1.1) [2,4,5]. Upon R domain phosphorylation, ATP binding opens the CFTR channel and ATP hydrolysis closes it [6].

As a large ~165 KDa glycoprotein, biogenesis of CFTR starts with co-translationally insertion into the endoplasmic reticulum (ER) membrane and concomitantly core glycosylation. After acquiring its fully folded native conformation, CFTR follows the general route of the secretory pathway,

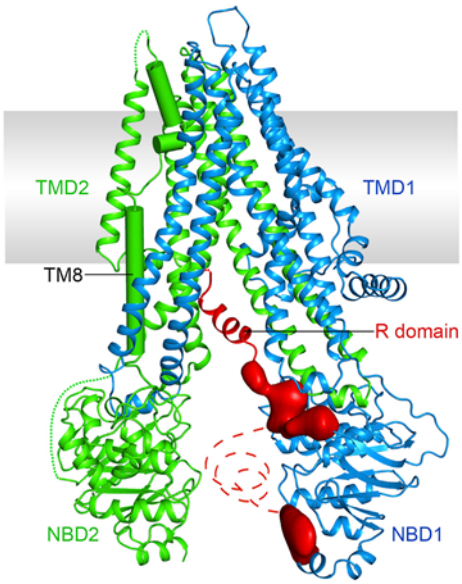

Figure 1.1 - Overall molecular structure of the human CFTR ion channel
Ribbon diagram of the overall structure of human CFTR in the dephosphorylated, ATP-Free Conformation. [Adapted from [5]]
The model shows the integral membrane glycoprotein, consisting of the six helical membrane-spanning domains TMD1 and TMD1; the nucleotide-binding domains, NBD1 and NBD2; and the single R, regulatory domain. Shown in red are unstructured regions within the R insertion of NBD1 or the R domain. Regions not resolved in the structure are shown as dashed lines for visualization purposes.

reaching the plasma membrane (PM) [7]. At the PM, its funtional location, CFTR conducts Cl^- and bicarbonate (HCO_3^-) anions down their electrochemical gradient, controlling transepithelial salt transport, fluid flow, and ion concentrations [2,4]. In addition to its role as a Cl^- channel, CFTR regulates epithelial ion transport by interfering with several other ion channels and transporters, namely the epithelial sodium channel (ENaC) [2,4,8].

1.1.2. Cystic Fibrosis pathophysiology

CF is a multisystem disorder that affects mainly children and young adults. The types and severity of symptoms in CF patients differ depending on their CFTR mutation (See below for CFTR mutation classes) [3]. The most life-threatening disease symptoms result from severe pulmonary disease. Other representative clinical symptoms include gastrointestinal problems due to pancreatic insufficiency and male infertility [9,10]. These characteristic clinical symptoms are related to tissue/organ-specific CFTR expression, which is higher in the pancreas, intestine, lungs, and reproductive tract - all mucin-secreting organs [11]. By controlling Na^+ absorption and Cl^- secretion in these tissues, CFTR and ENaC play a critical role in mucosal defense by controlling the movement of water through the epithelium and, consequently, modulating the proper volume of the airway surface liquid (ASL) and the biophysical properties of mucus [11–13]. Moreover, CFTR also plays an important role in the transcellular secretion of HCO_3^-, an alkalizing agent that plays a crucial physiological role in pH buffering [14]. Hence, the current pathophysiological model of CF disease assumes that defective CFTR function leads to fluid hyperabsorption and subsequent dehydration of the epithelial surface, resulting in abnormal thick mucus with an increased polymeric mucin concentration and altered biophysical properties [11–13]. Thus, obstruction of the airway surfaces by abnormal thick mucus initiates a complex cascade of events that leads to chronical bacterial infections and intense neutrophilic airway inflammation that culminate in pulmonary fibrosis and eventual respiratory failure [11–13].

1.1.3. CFTR Mutations and Classes

To date, over 2000 different variants of the CFTR gene have been identified, most of which cause CF [15,16]. Even though all these CF causing mutations result in defective ion conduction by epithelial cells, the molecular and cellular causes can be very different. CFTR mutations have thus been classified according to their functional defect into seven distinct classes (See Figure 1.2), with the aim of providing the scientific basis for mutation-specific corrective therapies and studies [17–20].

Class I is named “no protein” and includes mutations that affect protein production. These include mostly nonsense mutations that produce premature termination signals, thus often causing degradation of mRNA by nonsense-mediated decay. Some examples include mutation Gly542X or Arg1162X. Class II is named “no traffic” and includes mutants that fail to traffic to the cell surface due to misfolding and premature degradation by the endoplasmic reticulum quality control (ERQC) system, thus severely reducing CFTR abundance and function at the apical surface of epithelial cells. This class includes the most common CF mutation, the deletion of phenylalanine 508 (Phe508del), which occurs in at least one allele in > 85% of CF patients [15,21]. Class III is named “impaired gating”

and include CFTR mutants that, although reaching the PM, exhibit defective channel gating. Some examples include mutation Gly551Asp and pharmacologically rescued Phe508del, which exhibits a partial gating defect when it's trafficking to the PM is chemically corrected [22]. Class IV is named "decreased conductance" and includes mutants that display substantially reduced ion flow, with a resulting decrease in net transport of Cl^- and $HCO3^-$ ions. An example is Arg334Trp, a mutation in the CFTR channel pore. Class V is named "less protein" and includes CFTR mutants that lead to a major reduction in the levels of normal CFTR protein. This mutants may result from alternative splicing mutations that allows synthesis of some normal CFTR mRNA (example 3272-26A→G), promoter mutations that reduce transcription, or amino acid substitutions that cause inefficient protein maturation (example Ala455Glu). Class VI are named "less stable" and include mutations that impair the CFTR PM stability, either by increasing CFTR endocytosis or by decreasing its recycling back to the cell surface. Examples include c.120del23, which lacks the N-terminal region that has an important role in avoiding CFTR turnover and in rendering effective CFTR PM traffic [23] and chemically rescued Phe508del. Lastly, class VII are named "un-rescuable" and include mutations that impair total protein translation. These mutations cannot be pharmacologically rescued per se, and include large deletions such as the CFTRdele2, 3(21kb) mutation [17–20].

Although this classification has been crucial for the development of therapies specific to each functional mutation defect, a vast number of the identified mutations have not yet been assigned to a mutation class due to the absence of functional studies [18].

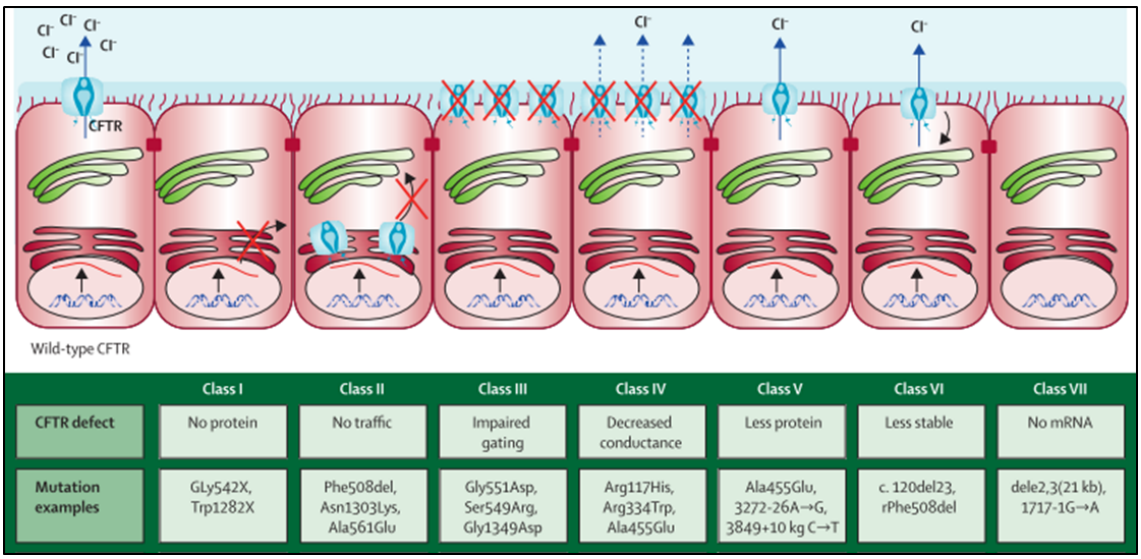

	Class I	Class II	Class III	Class IV	Class V	Class VI	Class VII
CFTR defect	No protein	No traffic	Impaired gating	Decreased conductance	Less protein	Less stable	No mRNA
Mutation examples	GLy542X, Trp1282X	Phe508del, Asn1303Lys, Ala561Glu	Gly551Asp, Ser549Arg, Gly1349Asp	Arg117His, Arg334Trp, Ala455Glu	Ala455Glu, 3272-26A→G, 3849+10 kg C→T	c. 120del23, rPhe508del	dele2,3(21 kb), 1717-1G→A

Figure 1.2 - CFTR functional mutation classes

CFTR mutations are grouped into seven classes according to their functional defect. [Adapted from [20]] Examples of mutations included in each class are shown. Different mutations can belong to more than one class, as it happens with Phe508del, included in Classes II, III and VII. rPhe508del=rescued Phe508del.

1.2. Phe508del-CFTR mutation

As above mentioned, the most common CFTR mutation worldwide consists of the deletion of three nucleotides that encode Phe508 in CFTR's polypeptide chain - Phe508del. This mutation is present in approximately 85% of all CF patients, which carry at least 1 copy of the Phe508del mutant in one of their mutated alleles [15,21].

1.2.1. Phe508del Mutation defects

Phe508del has multiple defects and is thus included in the functional mutation Classes II, III and VI [17–20]. In accordance, this mutation is first characterized by a defective protein processing, when failure to pass the various check-points of the ERQC results in considerable ER retention and premature degradation, preventing the mutant protein from trafficking to the cell surface [24,25]. Several agents were described to rescue this trafficking defect, most probably by promoting its correct folding [26–28]. Early on it was observed that the Phe508del channels are temperature-sensitive, thus making it possible to increase the protein processing and PM expression of the mutant channels at a permissive temperature of 26° C [29]. Besides this physical correction, which is difficult to translate to therapy [29], the protein conformation defect can also be targeted by stabilizing the protein native state, or enhancing its folding, using chemical chaperones [19,26–28]. Glycerol and dimethylsulfoxide (DMSO) are osmotically active molecules known to suppress protein-folding defects [26] and, accordingly, are also effective in rescuing Phe508del-CFTR cell-surface expression [30,31]. However, these chemical chaperones are nonspecific and require high concentrations and prolonged incubation to be effective. Nonetheless, as a proof of principle, these findings encouraged the search for more potent and specific compounds, latter presented as pharmacological correctors [32–34]. Indeed, when rescued by the available CFTR folding pharmacological correctors, Phe508del-CFTR is able to exit the ER, but the molecules that reach the cell surface present a partial channel function, known as a gating defect. This defect can be targeted by compounds designed to increase CFTR channel opening, named CFTR potentiators [35]. In addition, the residual or pharmacologically rescued Phe508del-CFTR present at the cell surface presents a highly decreased PM half-life. These channels show accelerated endocytosis and are quickly removed from the PM by the peripheral protein quality control (PPQC) mechanism [36–38]. At the moment there are no available molecular strategies aiming to correct this class VI defect in CF patients.

1.2.2. Pharmacological rescue of Phe508del-CFTR*

Traditionally, health care for CF patients has focused on treating the disease multi-organ symptoms, rather than targeting the underling molecular defect specific to each mutation [18,39]. This has been the goal of several CF drug discovery programs in the last decades, led both by companies and academic labs [32,39], including our own [37,40]. Below, we highlight the most recent therapies that target the molecular defects in CFTR, particularly of the Phe508del-mutant protein [15,21].

The development of pharmacological strategies to correct Phe508del-CFTR multiple functional defects has been complex, and accumulating evidence indicates that the combination of more than one type of CFTR-modulator drug will be required [41,42].

At present, there are several CFTR-modulator drug combinations and exciting new next-generation CFTR modulators under study for the clinical treatment of CF patients with the Phe508del mutation [32,43] (Figure 1.3). The latest developments will be addressed below.

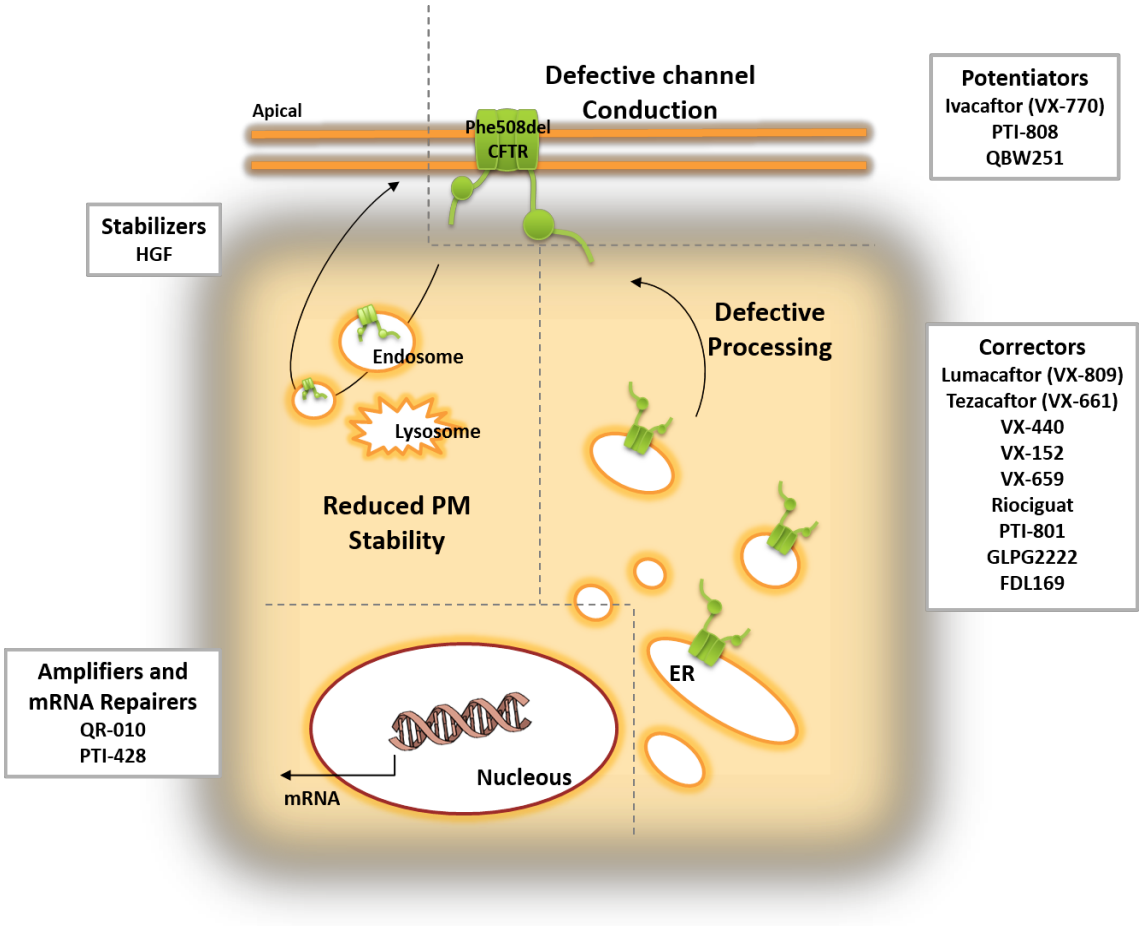

Figure 1.3 - Overview of the several molecules and strategies currently under study to rescue the multiple defects of Phe508del-CFTR. [Adapted from [214]]

1.2.2.1. Combination therapy

a. Lumacaftor plus Ivacaftor (Orkambi®)

Ivacaftor, also known as VX-770, is labeled as a CFTR potentiator, as it increases the time that activated CFTR channels remain open at the cell surface [35]. It was first introduced for the treatment of the Gly551Asp CFTR mutation, where it increased predicted mean forced expiratory volume in one second (FEV_1 [44], which in patients decreases from ~90% in infancy to ~50% by the age of 40 years-old [45]) by 10%, and was associated with less risk of pulmonary exacerbations and weight gain [35]. Since any Phe508del-CFTR protein reaching the cell surface also presents reduced channel function, the efficacy of Ivacaftor was assessed in subjects homozygous for the Phe508del mutation. In these phase II studies, the difference in the change of FEV_1 % and other spirometric parameters did not reach

statistical significance, thus, indicating that a CFTR potentiator alone is insufficient for the treatment of patients who are homozygous for the Phe508del genotype [46,47].

Lumacaftor, also known as VX-809, is an established CFTR corrector drug that has been extensively characterized. Although the correction mechanism of Lumacaftor is not fully understood, there is evidence that it promotes the proper folding of Phe508del-CFTR during its biogenesis and processing in the ER, allowing it to exit the ER and traffic to the cell surface [33,48–50]. Improvement of CFTR function to clinically meaningful levels was proposed to require a combination of Lumacaftor, to deliver CFTR channels to the PM, and Ivacaftor, to increase the proportion of time those channels are open [51]. Based on this knowledge, Lumacaftor advanced into clinical trials in patients homozygous and heterozygous for the Phe508del mutation, with the aim of evaluating its safety and efficacy alone and in combination with Ivacaftor. As assessed by a phase II study, administration of Lumacaftor alone did not provide a significant therapeutic benefit, as predicted FEV_1 % was similar between the studied groups [34]. Subsequently, the combination of Ivacaftor and Lumacaftor was explored in a series of clinical studies. In a phase II study, combination of Lumacaftor and Ivacaftor (in the higher doses administrated) significantly improved FEV_1 by a mean of 6% for patients homozygous for Phe508del-CFTR, decreased sweat chloride concentration by a mean of 8,9 to 10,3 mmol/L, and decreased pulmonary exacerbations in the treatment groups [52]. Phe508del-CFTR heterozygous patients did not have a significant improvement in FEV_1 or any other parameters [52]. Data from two phase III trials in patients homozygous for Phe508del showed that there were significant improvements in FEV_1, ranged from a mean of 2.6 to 4.0%, and that the rate of pulmonary exacerbations was 30 to 39% lower, since hospitalization or the use of intravenous antibiotics was reduced in the treatment groups [53]. While significant, these results fell below initial expectations and experimental evidence emerged to, at least partially, explain the limited improvements observed in patients. It was shown that chronic administration of Ivacaftor, as well as most other potentiators, results in a dose-dependent reversal of Lumacaftor- and Tezacaftor (another investigational corrector, see below)-mediated CFTR correction in Phe508del homozygous primary airway cell cultures [47,54]. This was due to protein destabilization and increase turnover rate, resulting in its reduced functional expression at the cell surface. A posterior study confirmed that exposure to high concentrations (>1 μM) of Ivacaftor did inhibit Lumacaftor's rescue of Phe508del-CFTR but reported that chronic exposure to low (≤100 nM), clinically relevant concentrations of the potentiator did not [55]. Thus, since combination therapy presumes an improvement of beneficial effects over the use of each drug alone, the inhibitory effect of Ivacaftor on Lumacaftor efficacy requires further evaluation, perhaps in post-treatment patient samples. In addition, it was also observed that *P. aeruginosa* reduces Phe508del-CFTR function in cells treated either with Lumacaftor alone or the with the Ivafactor/Lumacaftor combination [56,57]. Since 85% of adult CF patients are colonized with *P. aeruginosa,* this data suggests that infection with these bacteria may also partially account for a reduction in the therapeutic efficacy of these drugs in Phe508del-homozigous patients.

Nevertheless, despite its modest efficacy, the combination therapy clinical trial data supported an apparent benefit for patients. Accordingly, Ivacaftor plus Lumacaftor (commercial name: Orkambi® [58]) was approved for the clinical treatment of CF patients homozygous for the Phe508del mutation by the Food and Drug Administration (FDA) and European Medicines Agency

(EMA) [59]. This drug combination has now been used in patients since 2015, and several consequent studies of its long-term usage indicate that it does benefit CF patients, although several cases of off-target side-effects have been reported, including dyspnea (14%), diarrhea (11%), and nausea (10%) as well as serious adverse hepatobiliary reactions occurring in at least 0.5% of patients [60–62].

b. Tezacaftor plus Ivacaftor

Tezacaftor, also known as VX-661, is an investigational CFTR corrector, structurally similar to Lumacaftor, which also improves Phe508del-CFTR folding and traffic to the cell surface [63]. Tezacaftor was introduced in clinical trials as an alternative to Lumacaftor, with the advantage that it is not an inducer of CYP3A4 enzymes and, therefore, does not interfere with other medications that are frequently used in CF, particularly Ivacaftor [58,64]. The safety and efficacy of Tezacaftor monotherapy, and Tezacaftor plus Ivacaftor combination therapy was evaluated in a phase II trial in patients homozygous for Phe508del or heterozygous for Phe508del and a second Gly551Asp CFTR mutation [64]. Administration of the combined therapy resulted in a significantly decrease in sweat chloride around 6.04 mmol/L and predicted FEV_1 of 3.75% for Phe508del homozygous subjects, and 7.02 mmol/L in sweat chloride and 4.60% predicted FEV_1 for heterozygous [64]. These results supported continued clinical studies of this drug combination, since the improvements in lung function are comparable to those observed in patients treated with Lumacaftor plus Ivacaftor [53]. Results from phase III studies were similar, with values of 4.0% for predicted FEV_1 in homozygous patients, with a 35% reduction on the rate of pulmonary exacerbation in the treatment group and 6.8% for predicted FEV_1 in heterozygous patients [65,66]. In both phase II and III studies the treatment had less respiratory adverse events [65,66] when compared with previous reports from Lumacaftor trials [60–62], reveling itself to be an appealing alternative to the approved therapy.

c. Triple combinations

Last year Vertex announced the first results for the triple combination studies with Tezacaftor/Ivacaftor plus VX-440, VX-152, or VX-659, three investigational drugs that are next-generation correctors of the defective Phe508del-CFTR protein [67–70]. Data from the phase II studies showed values of mean predicted FEV_1 of 9.7% and 12.0% for the triple combination regimens with VX-152 or VX-440 respectively, in patients heterozygous for Phe508del and one minimal function mutation. In the same category of CF patients, initial data from a phase I study for the triple combination regimen of VX-659 showed an improvement in predicted FEV_1 of 9.6%. Initial data with VX-152 or VX-440 in patients homozygous for Phe508del, who were already receiving Tezacaftor and Ivacaftor, also showed an improvement in mean predicted FEV_1 of 7.3% and 9.5%. Furthermore, it was reported that all triple combinations were generally well tolerated and the majority of adverse events were mild to moderate [67].

1.2.2.2. mRNA repairers

ProQR Therapeutics is initiating clinical trials for a novel mRNA-based strategy for correction of Phe508del-CFTR mutation [32] after obtaining extremely promising *in vitro* and *in vivo* preclinical

data [71]. Their innovative compound, QR-010, is an investigational 33mer chemically modified, antisense oligoribonucleotide (AON) complementary to wt-CFTR mRNA, that was designed to repair Phe508del-CFTR transcripts. QR-010 mechanism of action is not yet fully characterized but it was postulated to involve RNAse H-mediated degradation of the mutant transcript, followed by RNA repair [72]. Treatment with inhaled QR-010 brought near complete restoration of chloride transport across the nasal mucosa of Phe508del homozygous mice. Moreover, two doses of QR-010 were able to improve CFTR-mediated saliva secretion up to 80% of the wild-type levels [71].

1.2.2.3. Proteostasis regulators

Proteostasis regulators are a novel class of CFTR correctors that act indirectly on CFTR by modulating components of the channel's interactome. One of the most promising was Cavosonstat [32], developed by Nivalis Therapeutics, Inc. Cavosonstat is a S-nitrosoglutathione reductase (GSNOR) inhibitor that increases GSNO and NO levels, which are lower in CF tissues [73]. This was postulated to promote a chaperone-dependent increase in CFTR abundance, stability and function. Unfortunately, in a February 2017 press-release, the company announced that the drug did not meet primary endpoints in a phase II trial [74]. Nonetheless, it highlighted NO signaling as a new research venue for CFTR modulators.

Another NO-related proteostasis regulator is Riociguat, the active ingredient of Adempas, an oral drug marketed by Bayer for the treatment of pulmonary hypertension. Riociguat increases the sensitivity of soluble guanylate cyclase (sGC) to NO, increasing cyclic guanosine monophosphate (cGMP) production. In addition to decreasing blood pressure, some studies report that the sGC-NO-cGMP pathway may regulate CFTR channel conductivity [75]. A phase 2 study is now underway in CF patients homozygous for the Phe508del mutation [32].

1.2.2.4. Amplifiers

Amplifiers are compounds designed to increase CFTR expression and thus increase ER protein load. In that sense, to support Phe508del-CFTR correction, they must be used in combination therapy. The starting point for the development of this CF drug class was the finding that the small-molecule HDAC7 inhibitor, SAHA1, significantly amplified Phe508del-CFTR quantity and surface expression in human bronchial epithelial cells, possibly by interfering with CFTR's proteostasis network [76]. However, the clinical applicability of HDAC inhibitors in CF treatment remains controversial. In a recent study using air-liquid interface cultures of differentiated nasal epithelia cells from CF patients, SAHA1 failed to increase CFTR transcript levels but rather inhibited mucine expression and goblet epithelial cell differentiation [77]. Nonetheless, those initial findings opened a new field in CF modulator drugs' research. Proteostasis Therapeutics, Inc., for instance, has developed a specific CFTR amplifier, PTI-428, that increases the CFTR mRNA pool, feasibly by improving mRNA stability and/or events surrounding CFTR translation. A phase II study evaluating the efficacy and safety of PTI-428 in CF patients receiving Orkambi® [58] demonstrated a mean absolute improvement in predicted FEV_1 of 5.2% in the tested group, with no significant adverse effects [78].

1.2.2.5. Additional small-molecule compounds

Proteostasis Therapeutics, Inc., developed two additional investigational compounds selectively targeting Phe508del-CFTR: PTI-801, a new-generation CFTR corrector, and PTI-808, a CFTR potentiator [32]. The company just finished the first phase I and II studies for these compounds, which showed promising results, and therefore, is now preparing new clinical studies and cohorts for the triple combination of PTI-428, PTI-801, and PTI-808, called PTI-NC-733 [78].

Galapagos/AbbVie has also developed four novel correctors currently under clinical trials [32]. Correctors GLPG2222 and GLPG2851 (C1) are additive to GLPG2737 and GLPG3221 (C2) and may be combined in therapy. GLPG2222 shares structural similarities with Lumacaftor and Tezacaftor, but was reported to produce a more efficient rescue of Phe508del-CFTR *in vitro* [79].

FDL169, a drug being developed by Flatley Discovery Lab, has been shown to increase Phe508del-CFTR cell-surface abundance with similar potency and efficacy as VX-809. However, FDL169 activity is not additive to VX-809, suggesting a similar mode of action [80]. Notwithstanding, FDL169 exhibited a higher free fraction in human serum and improved distribution in mice lungs [81], which makes it a promising alternative to Lumacaftor.

QBW251, a compound developed by Novartis Pharmaceuticals, is currently in phase II clinical trials [32]. It is described as a CFTR potentiator, similar to Ivacaftor. Preclinical data indicated that, when combined with Lumacaftor, QBW251 was more efficacious than Ivacaftor in sustaining Phe508del-CFTR membrane expression and function [82]. In an initial study in CF patients homozygous and compound-heterozygous for the Phe508del mutation, QBW251 proved to be safe and well tolerated. It promoted a significant decrease in sweat chloride and improved lung function in heterozygous patients, but, as Ivacaftor, showed no efficacy in Phe508del homozygous individuals [82]. Nevertheless, these initial results suggest QBW251 may constitute an attractive alternative to Ivacaftor in combination therapies.

Notably, several other compounds were reported to potentiate CFTR function, including the natural food components genistein, an isoflavonoid found in high concentrations in soy [83], and curcumin, a major constituent of turmeric [84]. Curcumin is able to activate CFTR channels in both ATP dependent and independent ways [84–86], whereas genistein acts through ATP-dependent CFTR gating [87]. Patch clamp studies showed additive effects of curcumin and genistein on the gating of Gly551Asp CFTR channels [88] and, importantly, a recent study showed that genistein and curcumin also enhanced forskolin-induced swelling of Ivacaftor/Lumacaftor treated intestinal organoids derived from biopsies of Phe508del homozygous patients [89]. Curcumin PKA-dependent, but ATP-independent, potentiation results from its binding to the stimulatory ICL1/ICL4-R interface to stabilize the channel open state, while PKA/ATP-dependent potentiation results from removal of inhibitory Fe^{3+} at the ICL3-R interface, which promotes dimerization of NBD1 and NBD2 [86,90–92]. These data suggest that Ivacaftor, genistein, and curcumin, in double or triple combinations, can synergize to restore CFTR-mediated fluid secretion in primary CF cells, thus supporting a possible benefit if multiple potentiators are used for treatment of CF. Still on this note, the very hydrophobic nature and low stability in water of compounds, such as curcumin, is a major drawback in their clinical application. In a very recent work,

Gonçalves et al. [93] showed that the neutral amphiphilic triblock copolymer MeOx6-THF19-MeOx6 (TBCP2) can solubilize curcumin and facilitate its penetration in Phe508del-CFTR human airway epithelial cells, enhancing curcumin potentiation of CFTR mediate Cl- selective currents in these cells. These data suggests that TBCP2 may constitute a helpful tool for the delivery of this and other highly insoluble therapeutic drugs to CF patients.

1.2.2.6. Gene Therapy

Gene therapy is a controversial subject that became a possibility for CF since the cloning of the CFTR gene [3]. In the case of CF, direct administration of the agents to the lungs *via* aerosols is an attractive option for gene therapy as pulmonary epithelium has a relative easy accessibility and reduces the risks associated with systemic delivery. Non-viral vectors seem to be the safest and most efficient gene transfer agents for this kind of therapy and, in the most promising trials, the plasmid DNA pGM169 (carrying the CFTR cDNA) combined with the cationic liposome GL67A, was the chosen formula for lung delivery [94,95]. Monthly application of the pGM169/GL67A complex in CF patients was evaluated in a phase IIb trial, where a 3,7% increase in predicted FEV_1 and stabilization of lung function was observed in the treatment group [95]. Despite the modest results, the trial offered proof of concept that non-viral gene therapy can benefit the lung function of CF patients and creates the opportunity for follow-up studies, namely combining gene therapy with the co-administration of CFTR modulator drugs.

1.2.2.7. Plasma membrane stabilizers

Although preliminary results for the triple combination therapy in patients with the Phe508del mutation look promising, there is still an unmet target for truly effective new therapies. Given the complexity of protein defects presented in Phe508del-CFTR, part of the incomplete effectiveness of the described combined therapies may derive from an inability to retain sufficient CFTR levels at the apical surface of epithelial cells. Therefore, there is a real need for molecular strategies achieving the PM retention of corrected rescued Phe508del-CFTR. Our group has investigated PPQC checkpoint in lung epithelial cells in Phe508del-CFTR exposed to VX-809. We found that the conformation of the scaffold protein Na(+)/H(+) exchange regulatory factor 1 (NHERF1, also known as SLC9A3 Regulator 1 (SLC9A3R1)) determined whether or not the PPQC recognized rescued Phe508del-CFTR at the PM [37]. Moreover, we showed that activation of the cytoskeletal regulator RAC1 promoted an interaction between the actin-binding adaptor protein ezrin and NHERF1 in a way that triggered exposure of the second (PSD-95/Drosophila disk large/Zonula occludens-1) PDZ domain of NHERF1, which interacted with rescued Phe508del-CFTR. Because binding of Phe508del-CFTR to the second PDZ of NHERF1 precluded the recruitment of ubiquitin ligase CHIP, the co-exposure of airway cells to the RAC1 activator HGF (hepatocyte growth factor) nearly tripled the functional rescue of Phe508del-CFTR by VX-809, retaining the rescued channels at the PM [96]. Since HGF signaling is determinant for lung tissue repair after acute lung injury [97], these findings open new areas of investigation worth pursuing in the development of small-molecule drugs for CF treatment.

1.3. CFTR Interactome

1.3.1. Known CFTR interactors

Until recently, relatively few proteins had been identified as CFTR interactors, involved in its processing and PM stabilization [8,98–100]. These small-scale studies reported that CFTR interactions at the apical membrane are regulated by several PDZ domain-containing proteins, which mediate protein-protein interactions between several binding partners and the amino terminal (N-) or the carboxyl terminal (C-) cytoplasmic tails of CFTR, forming three-dimensional protein complexes [98,99,101–103]. Some known PDZ scaffolding proteins that bind to the CFTR C-terminus with various affinities are: CAL (CFTR-associated ligand), NHERF1, NHERF2 (also called NHE3 kinase A regulatory protein, E3KARP), PDZ domain-containing protein in kidney 1 (PDZK1, also called CFTR-associated protein 70, Cap70; and NHERF3), PDZK2 (also called intestinal and kidney-enriched PDZ protein, IKEPP; and NHERF4), and SH3 and Ankyrin repeats containing protein 2 (Shank2, also called Cortactin-binding protein 1, CortBP1) [101,103]. These have been reported to interact with the CFTR C-terminus at the apical membrane of epithelial cells, except for CAL, which is localized primarily to Golgi, thereby suggesting that different PDZ proteins might interact with CFTR at different tissues [101,103]. In addition, the ezrin-radixin-moesin (ERM) domain within the C-terminal tails of NHERF1 and NHERF2 tether the CFTR complex to the cortical cytoskeletal elements *via* ERM protein ezrin (EZR) binding [104,105]. The interactions between CFTR, NHERF1 and EZR will be further discussed in the following section.

In a more comprehensive approach, a few studies have aimed to identify the global CFTR interactome using systematic high-throughput experimental mapping strategies [106–108]. Both these studies intended to identify the key differences between wt- and Phe508del-CFTR proteomes, although the first study focused mainly in ER-associated pathways interactors [106], while the last study integrated trafficking and PM interactors, as it was performed in rescued Phe508del-CFTR [107]. Wang et al [106] characterized an unprecedented number of CFTR-associated proteins, including robust interactions with calnexin and the cytosolic chaperone machineries Hsc-Hsp70 and 90. In particular, the authors found that changes in Hsp90 co-chaperone folding environment, specifically co-chaperones p23, FKBP8 and Aha1, markedly altered the stability and export of Phe508del-CFTR from the ER. p53, and its interacting partner FKBP8, were found to be important to prevent destabilization and degradation of Phe508del-CFTR, while Aha1 was discovered to inhibit the Phe508del-CFTR coupling to the ER export machinery [106]. By reducing Aha1 levels through siRNA, the authors rescued trafficking of Phe508del-CFTR to the cell surface and restored channel function, showing that the dynamic chaperone pool responsible by CFTR folding can be subjected to pharmacological intervention [106]. To date, the Pankow et al. work is the most complete CFTR proteomics study ever conducted [107,108]. The authors found 638 high-confidence core CFTR proteins, interacting with both Phe508del- and wt-CFTR. In addition, 208 and 62 interactors were detected specifically in Phe508del- and wt-CFTR, respectively, representing highly enriched or particular interactors [107]. Interestingly, they found that rescued Phe508del-CFTR specific interactome was larger than the wt-specific, and was characterized mainly by a gain of novel interaction partners, and an enhancement in chaperones

and protein degradation mediators from the ER quality control network. Also, protein interactors known to be involved in translation, post-translational modification, protein transport and trafficking, and endocytic recycling were altered, suggesting that large aspects of CFTR biogenesis are affected by the Phe508del mutation [107]. With both these studies it was highlighted that the differences in the interaction profiles between wt- and Phe508del-CFTR are extremely important for identifying novel CF therapeutic approaches, and stress the need for a more comprehensive knowledge of the specific CFTR interactions at the PM compartment.

1.3.2. CFTR cell surface molecular complex

Spatial and temporal assembly and disassembly of multiprotein complexes is a crucial process in cell biology. Intrinsic knowledge of these dynamic multiprotein systems can give insights into their molecular functions and aid in the design of new therapeutic approaches [101]. Accumulating evidence shows that CFTR is coupled spatially and temporally to a wide variety of interacting partners, including other ion channels, receptors, transporters, kinases, phosphatases, signaling molecules, and cytoskeletal components. These interactions were proved to be essential for the regulation of CFTR processing, localization and function within cells [8,98,99,101,102,107].

1.3.2.1. NHERF1 and EZR are essential for tethering CFTR to the PM

In secretory epithelial cells a large part of CFTR protein (~50%) is specifically localized in an immobile pool at the apical membrane, tethered to filamentous actin (F-actin) [109]. This anchoring of CFTR at the cell's apical surface involves the interaction of the channel's C-terminal domain with the PDZ adaptor NHERF1 protein, which in turn tethers CFTR to the actin cytoskeleton through the interaction with the connector protein EZR [105,110,111].

EZR is an 80/81-kDa polypeptide with known functions in cytoskeletal-related events such as: cell polarization; intracellular trafficking; cell adhesion; cell survival; cell motility; and tumor metastasis [111,112]. Members of the ERM family are structured into three functional domains: an N-terminal FERM (four point one, ERM) domain, an extended coiled-coil region and a short C-terminal domain that associates directly with F-actin (Figure 1.4A). Through the FERM domain, EZR associates with intracellular molecules such as NHERF1 [111,113,114]. These interactions are regulated through an activation process and a consequential EZR conformational change, causing the binding site for filamentous actin (F-actin) to become accessible [115–118] (Figure 1.4A). This activation process is sequential, in which EZR (and the other ERM protein family members) is recruited to membrane regions enriched in l-α-phosphatidylinositol-4,5-bisphosphate (PIP2) where it binds to this phospholipid, making available the phosphorylation of a conserved threonine residue, T567 [115–118]. Thus, this succession of events is critical for the proper activation and apical localization of EZR [118]. Several kinases have been implicated in EZR activation including: Rho-kinase (ROCK), protein kinase C (PKC) α and PKC θ, and Rho GTPase RAC1 signaling *via* AKT2 [40,119–122].

NHERF1 is a 55-kDa phosphoprotein that regulates the intracellular trafficking and signaling of membrane proteins to which it binds. Its structure contains a C-terminal EZR binding (EB) site that recognizes the EZR FERM domain (See Figure 1.4) and two tandem PDZ domains, PDZ1 and PDZ2

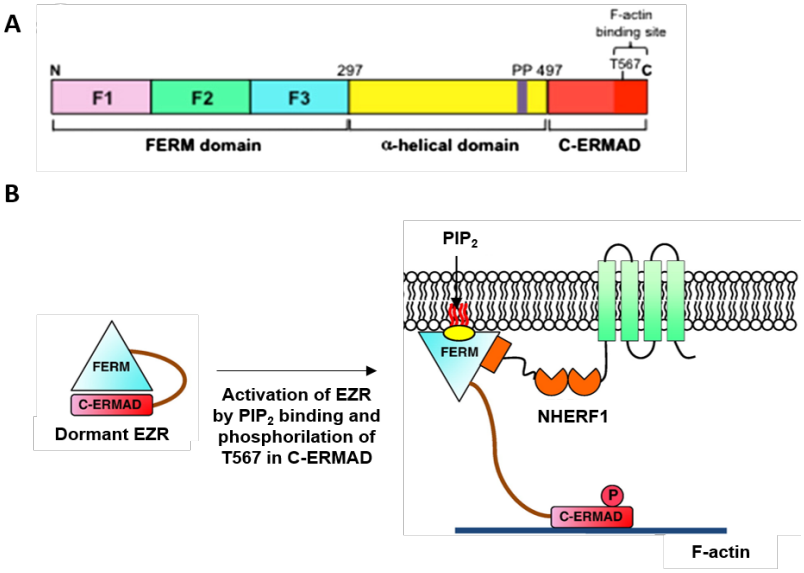

Figure 1.4 – EZR protein structure and activation process
A - EZR is composed of a ~300 residues globular FERM domain located at their N-terminus (where F1, F2 and F3 are the three subdomains of the FERM) followed by a ~200 amino acids α-helical domain that contains a coiled-coil and a proline-rich (PP) linker region, and a ~100 amino acids C-ERMAD which contains the phosphorylation site (Thr567) and the F-actin binding site. **B -** EZR exists in two states: the dormant/inactive state and the active state. EZR activation involves binding to PIP_2 and phosphorylation of a conserved threonine residue in the C-ERMAD, Thr567. This activation dissociates the FERM domain from the C-ERMAD. Upon activation, EZR functions as a cross-linker by binding to scaffolding proteins such as NHERF1. [Adapted from [246]]

[102,114]. Both PDZs have biding affinity for the consensus PDZ-binding motif located at the C-terminal domain of CFTR [110,123] (Figure 1.5A). In its native state NHERF1 is held in an autoinhibited conformation through intramolecular interactions between the PDZ2 and the C-terminal domain (Figure 1.5B) [124]. Upon activated EZR binding to the EB domain, NHERF1 undergoes significant conformational changes that are believed to regulate CFTR complex assembling, endocytic recycling, and retention at the apical PM [112,124,125].

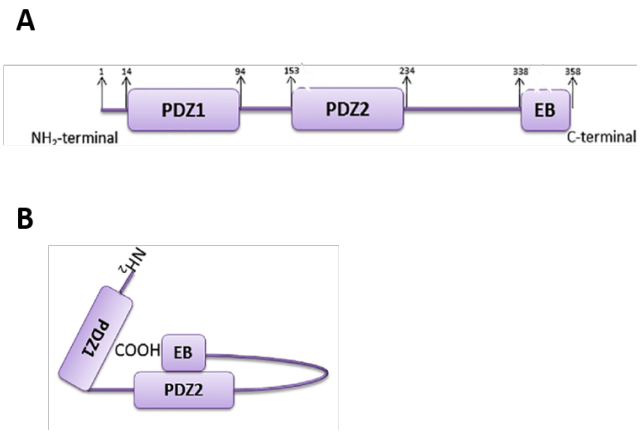

Figure 1.5 – NHERF1 structure and conformation
A – NHERF1 is composed of two modular protein-protein interaction domains, PDZ1 (residues 14-94) and PDZ2 (residues 153–234), and a C-terminal domain that contains an EB domain (residue 338-358). **B –** Head-to-tail NHERF1 conformation. This autoinhibited state is held through intramolecular interactions between PDZ2 and the C-terminal domain.

1.3.2.2. CFTR PM regulation and dynamics

The non-tethered CFTR pool (~50%) at the apical PM of polarized epithelial cells is determined by a steady-state regulation of the endocytic CFTR retrieval and the recycling/exocytic insertion of CFTR into the PM by intra-cellular vesicles [126–128]. These processes are complex and involve numerous protein interactors, including several members of the Rab and Rho subfamilies of the Ras superfamily of small GTPases [7]. In summary, CFTR endocytosis is clathrin-dependent and occurs through Rab5-positive endosomes, relying in the recognition of multiple endocytic motifs located at the C-terminus of CFTR [38,100,128–131] (Figure 1.6). CFTR internalization also relies on the interaction with the endocytic adaptor complex AP-2 and dynamin, since interfering with the binding of these proteins, as well as with Rab5 function, prevents CFTR internalization [38,100,128–131]. To maintain the functional pool of surface CFTR, the channel is continuously recycled from early endosomes back to the PM *via* Rab11/Myo5b-driven recycling vesicles, and is facilitated by Rme-1 and by NHERF1 PDZ domain interaction [38,131] (Figure 1.6). In contrast, partially unfolded PM CFTR, such as Phe508del-CFTR, is subjected to ubiquitination by the PPQC mechanism. The cytoplasmic regions of unfolded CFTR are recognized by heat shock cognate 70-kD protein (Hsc70) in concert with other co-chaperone proteins. Prolonged interaction with the Hsc70/co-chaperone complex recruits the E3 ubiquitin ligase CHIP (C terminus of Hsc70 interacting protein), culminating in accelerated endocytosis and lysosomal degradation [36].

In addition, modulation of the actin cytoskeleton has been proved essential in CFTR turnover and immobilization at the PM [40,132]. The Rho family of small GTPases are key regulators of actin cytoskeleton dynamics [132], implicated in the regulation of cell polarity and membrane trafficking through their modulation of F-actin remodeling [133,134]. Consistently, overexpression of NHERF1 was shown to stimulate the activation of endogenous RHOA and ROCK, thus leading to reorganization of the actin cytoskeleton and increased apical expression of rescued Phe508del-CFTR [135]. This increase in CFTR surface levels was promoted upon activation of both RHOA and RAC1 endogenous signaling, although, NHERF1 relies on RAC1 signaling to induce EZR mediated PM anchoring of CFTR, whereas stimulation of RHOA favors CFTR recycling to the PM *via* ROCK [40]. RAC1 acts through the stimulation of phosphatidylinositol 4-phosphate 5-kinase (PIP5K)-mediated production of PIP2 at the PM, inducing EZR active conformation [40,115–118]. These stimuli induce *de novo* polymerization of F-actin, produced by the Arp2/3 actin nucleation complex, leading to the anchoring of the CFTR/NHERF1/EZR complex at the PM [40]. In addition, several other proteins, including SNARE SYN6, CAL and GTPase TC10, a member of the CDC42 subfamily, affect the endocytic trafficking of CFTR at the PM [125,130,131,136]. Concisely, activated TC10 reduces CFTR degradation by favoring the binding of NHERF1

to the C-terminus of CFTR, thus preventing its binding to CAL, a PDZ containing protein that facilitates the trafficking of CFTR to lysosomes [130,137].

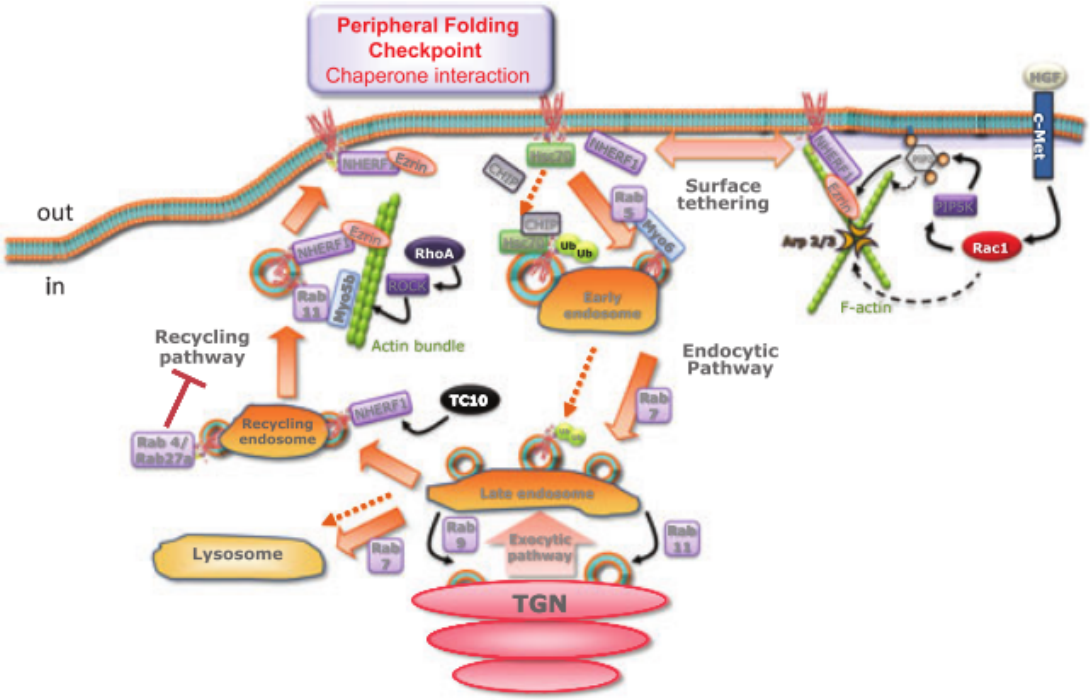

Figure 1.6 - Schematic model of CFTR membrane dynamics and the involvement of protein–protein interactions in endocytosis, recycling and lysosomal targeting of the channel. [Adapted from [7]]

Objectives

The major goal of this project is to identify novel cellular pathways and/or novel key interactors for modulation of CFTR surface retention and validate their functional significance in enhancing the pharmacological correction of Phe508del-CFTR.

To this purpose, we will:

1) Investigate the mechanism by which RAC1 signaling triggers pharmacological rescued Phe508del-CFTR retention and functional restoration at the PM.
2) Determine if HGF treatment enhances the functional correction of Phe508del-CFTR by the VX-809/VX-770 drug combination.
3) Identify the core components in Phe508del-CFTR PM molecular complex, and investigate their contribution for the CFTR cell surface stability.

Chapter 2

A molecular switch in the scaffold NHERF1 enables misfolded CFTR to evade the peripheral quality control checkpoint

Cláudia A. Loureiro, **Ana Margarida Matos**, Ângela Dias-Alves, Joana F. Pereira, Inna Uliyakina, Patrícia Barros, Margarida D. Amaral, Paulo Matos

Data included in this chapter was published in:

Loureiro CA, **Matos AM**, Dias-Alves A, Pereira JF, Uliyakina I, Barros P, et al. A molecular switch in the scaffold NHERF1 enables misfolded CFTR to evade the peripheral quality control checkpoint. Sci Signal. **8**(377):ra48 (2015).

2.1. Abstract

The peripheral protein quality control (PPQC) checkpoint removes improperly folded proteins from the plasma membrane (PM) through a mechanism involving the E3 ubiquitin ligase CHIP (carboxyl terminus of Hsc70 interacting protein). PPQC limits the efficacy of some cystic fibrosis (CF) drugs, such as VX-809, that improve trafficking to the plasma membrane of misfolded mutants of the CF transmembrane conductance regulator (CFTR), including Phe508del-CFTR, which retains partial functionality. We investigated the PPQC checkpoint in lung epithelial cells with Phe508del-CFTR that were exposed to VX-809. The conformation of the scaffold protein NHERF1 (Na+/H+ exchange regulatory factor 1) determined whether the PPQC recognized "rescued" Phe508del-CFTR (the portion that reached the cell surface in VX-809–treated cells). Activation of the cytoskeletal regulator RAC1 promoted an interaction between the actin-binding adaptor protein ezrin (EZR) and NHERF1, triggering exposure of the second PDZ domain of NHERF1, which interacted with rescued Phe508del-CFTR. Because binding of Phe508del-CFTR to the second PDZ of NHERF1 precluded the recruitment of CHIP, the co-exposure of airway cells to RAC1 activator nearly tripled the efficacy of VX-809. Interference with the NHERF1-EZR interaction prevented the increase of efficacy of VX-809 by RAC1 activation, but the actin-binding domain of EZR was not required for the increase in efficacy. Thus, rather than mainly directing anchoring of Phe508del-CFTR to the actin cytoskeleton, induction of EZR activation by RAC1 signaling triggered a conformational change in NHERF1, which was then able to bind and stabilize misfolded CFTR at the PM. These insights into the cell surface stabilization of CFTR provide new targets to improve treatment of CF.

2.2. Introduction

Several human diseases result from the absence of PM proteins due to mutation that causes these proteins to misfold [138,139]. In most cases, the defective protein is recognized by the endoplasmic reticulum (ER) quality control (ERQC) and targeted for degradation, thus preventing the accumulation of dysfunctional proteins [7,138]. However, sometimes, the defective protein retains a degree of functionality that, if allowed to evade the ERQC and reach the cell surface, could lessen the disease severity. This is the case for the CFTR protein with the Phe508del mutation, which occurs in ~85% of CF patients [140]. An intensive search in the past decades identified a small number of compounds, termed "correctors," capable of partially rescuing the trafficking of Phe508del-CFTR to the cell surface. The mechanism of action for most of these compounds is still unclear, but the most promising one, VX-809 (Lumacaftor), is thought to act as a "pharmacological chaperone" that directly interacts with Phe508del-CFTR, facilitating its folding and cellular processing [140]. However, VX-809 alone showed limited success in clinical trials [34,140,141]. CFTR functions as a chloride channel at the PM of epithelial cells, and several *in vitro* studies have shown that rescued Phe508del-CFTR channels have defective gating properties [2]. Although rescuing the gating defect of Phe508del-CFTR (and other mutants with gating defects) was made possible by "potentiator" drugs such as VX-770 (Ivacaftor, Kalydeco) [22,140,142], the combination of VX-809 and VX-770 produced only marginal clinical benefits in Phe508del-CFTR homozygous patients [141]. We and others have previously demonstrated that

correction of Phe508del-CFTR trafficking and gating may not be sufficient to rescue its functional expression at the cell surface [34,36,40,49]. Indeed, pharmacologically rescued Phe508del-CFTR channels are quickly removed from the plasma membrane by the PPQC mechanism [36]. PPQC appears to be a ubiquitous mechanism targeting misfolded proteins that reach the PM, either naturally or through pharmacological manipulation, or by incubation at folding-permissive temperatures (26 to 30°C) [36,143,144]. Okiyoneda et al. elegantly showed [36] that the cytoplasmic region of conformationally unstable Phe508del-CFTR proteins at the plasma membrane is selectively recognized by heat shock cognate 70-kD protein (Hsc70), in concert with other co-chaperone proteins. The prolonged interaction with the Hsc70/co-chaperone complex allows the recruitment of the E3 ubiquitin ligase CHIP, leading to ubiquitination of the conformationally defective Phe508del-CFTR at the PM. Ubiquitylated proteins are then rapidly endocytosed, possibly by clathrin-mediated internalization upon recruitment of ubiquitin-binding endocytic adaptors, and signaled for delivery into the degradative lysosomal compartment [36,144]. We previously demonstrated that stimulation of endogenous RAC1 signaling through treatment with hepatocyte growth factor (HGF) can potentiate the retention of rescued Phe508del-CFTR at the PM of human airway epithelial cells [40]. RAC1 is a member of the Rho family of small GTPases (guanosine triphosphatases) that are key regulators of the actin cytoskeleton remodeling [145]. By cycling through GDP (guanosine diphosphate)–bound (inactive) and GTP (guanosine 5’-triphosphate)–bound (active) conformations, these proteins function as molecular switches that transduce the activity of PM receptors into intracellular signaling. HGF, the ligand for the c-Met receptor, is a multi-functional mesenchyme-derived factor secreted by several cell types [146] . HGF appears in lung circulation under pathological conditions, such as acute lung injury, infection, and ventilator-induced lung injury, and has been implicated in lung repair and restoration of lung barrier function [146,147]. Barrier protective effects of HGF have been observed in human pulmonary endothelial cells, where HGF-induced barrier enhancement involves activation of guanine nucleotide exchange factor (GEF) Tiam1 [148,149], which facilitates exchange of GDP for GTP in the nucleotide-binding center of RAC1, leading to its activation. We showed that HGF-mediated activation of RAC1 also increased the binding of pharmacologically rescued Phe508del-CFTR to the apical actin cytoskeleton by NHERF1. NHERF1 is a scaffold protein that has two tandem PDZ domains and a C-terminal domain that interacts with the actin-binding adaptor protein EZR [109,150]. Stimulation of RAC1 induces the activation of EZR, which binds both actin and Phe508del-CFTR/NHERF1 complexes at the PM, delaying Phe508del-CFTR internalization [40]. Such enhanced cell surface retention improved nearly threefold the efficacy of corrector VX-809 in primary airway epithelial cells from patients with homozygous mutation for the Phe508del protein [40]. Unfortunately, the pleiotropic and potential pro-tumorigenic effects of continuously stimulating HGF/c-Met pathway [151] limit the therapeutic applicability of HGF in CF patients. Therefore, we investigated in further detail the mechanism by which RAC1 signaling triggers Phe508del-CFTR retention at the PM.

2.3. Results

2.3.1. Tiam1 stimulation of endogenous RAC1 signaling triggers CFTR cell surface tethering

Although HGF cellular signaling involves several pathways, we previously showed that only the RAC1 axis is a determinant for CFTR tethering at the cell surface [40]. Thus, in this study, we choose to selectively stimulate endogenous RAC1 activity. One way of achieving this is to transfect cells with an N-terminal truncated form of the RAC1-specific GDP-to-GTP exchange factor Tiam1 (C1199Tiam1) [152]. Expression of green fluorescent protein (GFP)–tagged C1199Tiam1 selectively loads endogenous RAC1 with GTP, rendering it active in the absence of upstream stimuli from receptors. This strategy enables one to study the effects of RAC1 signaling on the PPQC mechanism, avoiding potentially indirect effects of HGF on parallel signaling pathways. Analysis of the amount of active RAC1 in immortalized human bronchial epithelial cells expressing wild-type CFTR CFBE [153] was carried out using the CRIB domain pull-down assay. This assay selectively captures the pool of active, GTP-bound RAC1 in cells, and showed that expression of C1199Tiam1 strongly stimulated endogenous RAC1 activation (Figure 2.1A). Using surface protein biotinylation assay, we found that Tiam1 overexpression led to about a threefold increase in CFTR abundance at the cell surface (Figure 2.1B), similar to that which we described for HGF treatment [40]. Consistently, treatment of these cells with a RAC1-specific inhibitor, either NSC23766 or EHT 1864, suppressed this Tiam1-induced increase in CFTR. In addition, because cell lysis was performed under non-denaturing conditions, the blots containing the CFTR surface pool were further probed for the presence of co-captured actin. This revealed that the amount of actin co-isolated with the surface pool was directly proportional to the amount of CFTR at the plasma membrane (Figure 2.1B). This observation is consistent with our previous findings that RAC1 signaling induces the activation of EZR, which binds both actin and CFTR/NHERF1 complexes at the plasma membrane, anchoring CFTR to the actin cytoskeleton and retaining it at the cell surface [40] (Figure 2.1C).

As with HGF stimulation [40], expression of Tiam1 also significantly stimulated CFTR-mediated ion transport in bronchial epithelial cells expressing Phe508del-CFTR (Phe508del-CFTR CFBE) [153], as determined by iodide efflux (Figure 2.1D). Moreover, the levels of the fully-glycosylated form of Phe508del-CFTR detected by Western blot (WB) were also increased in the presence of GFP-C1199Tiam1, but not those of the more abundant immature form of the mutant protein (the faster migrating, core-glycosylated, ER-associated) (Figure 2.1E). Notably, these effects were abrogated by co-treatment with a RAC1 inhibitor, either NSC23766 or EHT 1864. Because RAC1 signaling affects only the surface tethering of CFTR and not its processing or trafficking [40], these observations were in agreement with a scenario where favoring the anchoring of Phe508del-CFTR that reaches the cell surface would allow the mutant protein to evade the PPQC, despite its abnormal folding.

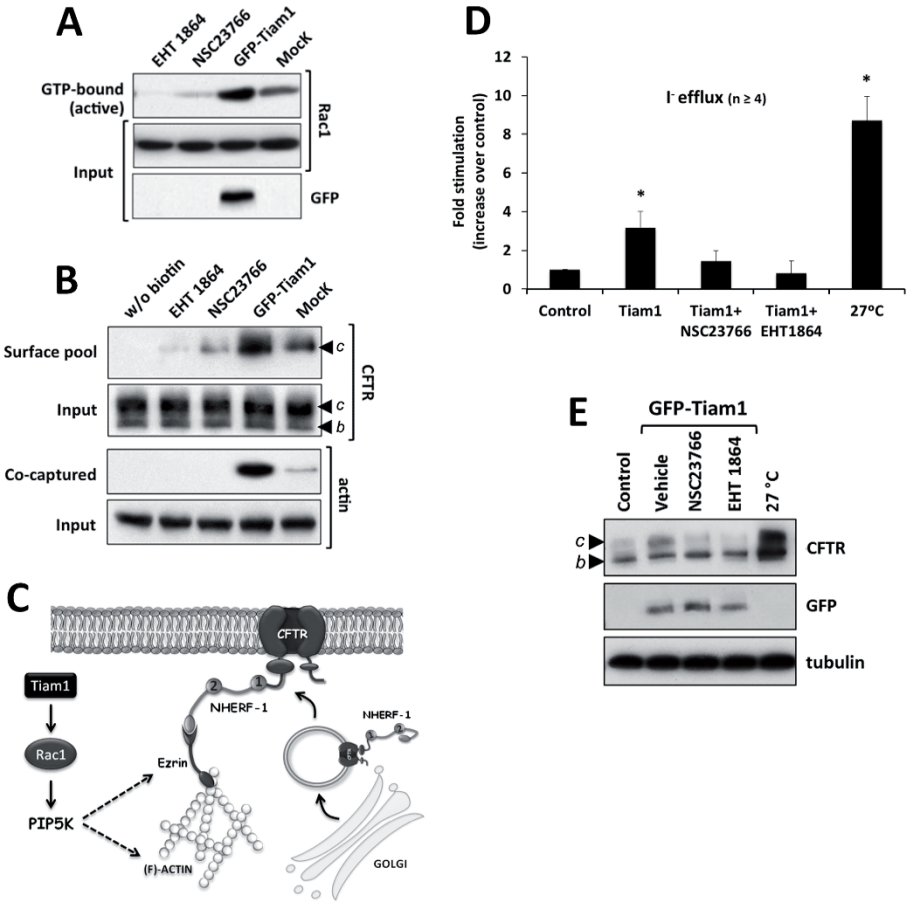

Figure 2.1 - Correlation of CFTR cell surface levels with Tiam1-mediated activation of endogenous RAC1 signaling

A- CRIB-domain pull-down assay for active (GTP-bound) RAC1 molecules in wild-type CFTR CFBE cells either treated with RAC1 inhibitor (NSC23766 or EHT 1864) or transfected with GFP-C1199Tiam1 or mock-transfected. **B-** Surface biotinylation assay in wild-type CFTR CFBE cells treated and transfected as in (A). Bottom, co-capture of actin with CFTR. *b*, immature, core-glycosylated CFTR; *c*, mature, fully-glycosylated CFTR. **C-** Schematic diagram of the mechanism we propose mediates the effects shown in (A) and (B). **D-** Iodide efflux from CFBE cells expressing Phe508del-CFTR and either mock-transfected (control) or transfected with GFP-C1199Tiam1 and treated either with the indicated RAC1 inhibitors or an equal volume of PBS (vehicle). A second sample of control cells grown for 24 hours at 27°C was included for comparison. **E-** Western blot of the steady-state abundance of Phe508del-CFTR in CFBE cells treated as in (D). *b*, immature, core-glycosylated F508del-CFTR; *c*, mature, fully-glycosylated Phe508del-CFTR. Blots are representative of at least 4 independent assays. Data are means ± SEM. **p*<0.05, compared to control (ANOVA followed by Tukey's test). [CRIB-domain pull-down assay, cell surface biotinylation, WB and iodide efflux performed by Cláudia Loureiro, construct production by Patrícia Barros and schematic diagram designed by Paulo Matos, included with permission]

2.3.2. Stimulation of RAC1 signaling prevents temperature-dependent turnover of mature Phe508del-CFTR

The amount of Phe508del-CFTR that manages to escape the ER at 37°C is minimal. Thus, to test our hypothesis that Tiam1-induced tethering of Phe508del-CFTR to the actin cytoskeleton participates in its evasion from the PPQC, we first enriched the intracellular amount of post-Golgi, fully glycosylated Phe508del-CFTR. For this, we pre-incubated Phe508del-CFTR CFBE cells at 27°C, a well-known experimental maneuver that rescues Phe508del-CFTR processing and surface expression

[29] by relaxing the ERQC [49]. After 24 hours at 27°C the cells were moved to 37°C and the abundance of fully glycosylated Phe508del-CFTR, rescued by the low-temperature treatment, was monitored by WB for the following 4 hours to analyze the kinetics of its decay at physiological temperatures. As previously described [36], the amount of mature Phe508del-CFTR was reduced in control cells to less than 50% within 4 hours (Figure 2.2A and B). This observation is likely due to the activation of the PPQC that accelerates endocytosis and degradation of Phe508del-CFTR at the PM [36]. Remarkably, when C1199Tiam1-expressing cells were moved to 37°C, the abundance of fully glycosylated Phe508del-CFTR remained mostly unchanged within the same time frame (Figure 2.2A). Conversely, when basal RAC1 signaling was inhibited by treatment with 10 µM EHT 1864 before switching cells to 37°C, the turnover of rescued Phe508del-CFTR was considerably accelerated, reducing its post-Golgi abundance to roughly 20% of that in control cells after 4 hours (Figure 2.2A). Consistent with a PPQC-specific effect, the kinetics of immature Phe508del-CFTR decay remained unchanged upon manipulation of RAC1 signaling (Figure 2.2A and B).

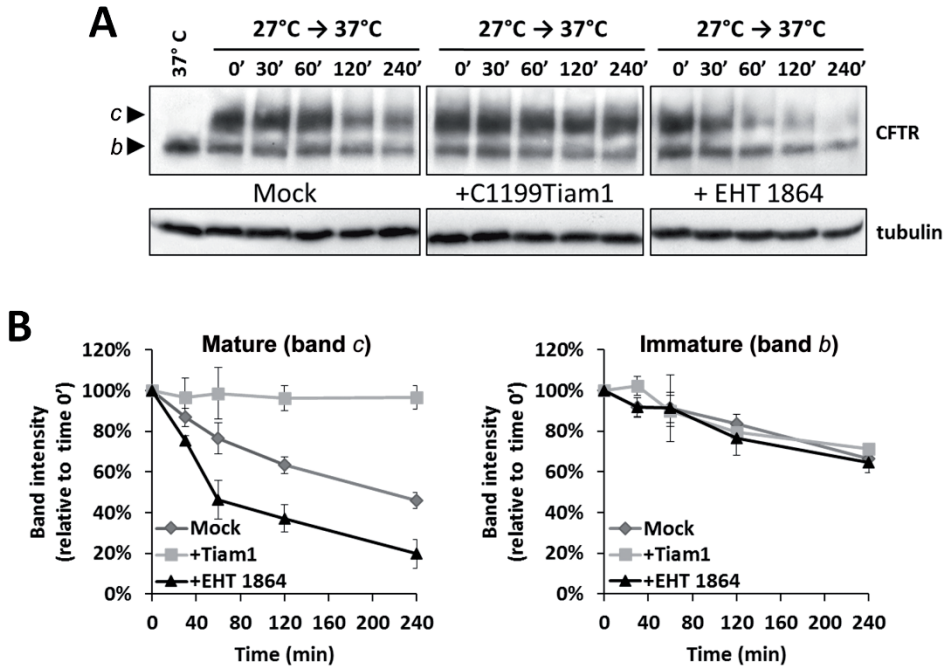

Figure 2.2 - Kinetics of temperature-rescued Phe508del-CFTR degradation upon re-incubation at 37°C
A- Temperature switch assay in CFBE cells expressing Phe508del-CFTR transfected with GFP-C1199Tiam1 or treated with EHT 1864 compared with control (mock) cells, grown at 27°C for 24 hours then 37°C for the indicated time. **B-** Quantification of mature (*c*, left) and immature (*b*, right) Phe508del-CFTR band intensities at the different time points, normalized to the intensity at time 0 min (100%). Data are means ± SEM from 3 independent experiments. [Temperature switch assay performed by Cláudia Loureiro and included with permission]

2.3.3. Stimulation of F-actin anchoring impedes CHIP-mediated Phe508del-CFTR ubiquitination

We recently developed novel parental CFBE cell-based models [153] that express previously described constructs of either wild-type or Phe508del human CFTR, bearing both a N-terminus-fused

mCherry tag and a Flag epitope tag located at the 4th extracellular loop, under the control of a tetracycline-inducible (Tet-ON) promoter [154]. The trafficking and functional behavior of these double-tagged proteins was equivalent to their untagged counterparts [154] with the advantage that their expression can be switched on or off by adding or removing doxycycline (Dox) from the culture medium. Thus, to investigate potential variations in the composition of PPQC-associated Phe508del-CFTR complexes at the PM, we first incubated cells at 27°C for 12 to 24 hours in the presence of Dox (0.5 µg/mL). This incubation revealed a clearly detectable abundance of complex-glycosylated mCherry-Flag-Phe508del-CFTR (mChF-Phe508del-CFTR) in post-Golgi compartments by WB (Figure 2.3A) and at the PM by staining for the Flag tag in non-permeabilized cells (Figure 2.3B). Cells were then maintained at 27°C for additional 8 to 12 hours in the absence of Dox. At 27°C, the PPQC was inefficient, allowing the accumulation of fully-glycosylate Phe508del-CFTR, but most immature, core-glycosylated protein was depleted by the ER-associated degradation (ERAD) machinery after 8 hours of Dox removal (Figure 2.3A and B). This strategy allowed us to considerably enrich lysates in post-Golgi complex-glycosylated proteins without resorting to the conventional cycloheximide (CHX) chase [36], which interferes with the whole cell proteome and can thus perturb PPQC. Immunoprecipitation of mChF Phe508del-CFTR from cells incubated as above, after in vivo cross-linking by 0.1 mM dithiobis succinimidyl propionate (DSP), revealed that C1199Tiam1 expression caused a significant decrease in the abundance of co-captured CHIP E3-Ub-ligase, with a concomitant decrease in the amount of ubiquitinated CFTR, whereas treatment with the RAC1 inhibitor EHT 1864 produced the opposite result increasing both CHIP co-precipitation and the amount of immunoprecipitated Ub-mChF-Phe508del-CFTR (Figure 2.3C and D). No change was observed in the amount of co-precipitated Hsc70 chaperone in the correspondent samples (Figure 2.3C and D).

2.3.4. Interaction of rescued Phe508del-CFTR with the second PDZ domain of NHERF1 precludes CHIP recruitment

The results described above indicated that the effects of RAC1 signaling on the PPQC of rescued Phe508del-CFTR involved the inhibition of CHIP recruitment independently of Hsc70 displacement. This suggested an event related to the formation of a CFTR/NHERF1/EZR/actin complex. Interaction with NHERF1 is required for CFTR localization at the apical PM [109,155,156]. The first PDZ domain of NHERF1 (PDZ1) can readily interact with CFTR, but its second PDZ domain (PDZ2) is blocked from binding to CFTR by an intramolecular interaction with the NHERF1 C-terminus [150] that is only released in the presence of active EZR [157]. Because we previously showed that the conformational opening of NHERF1 through EZR activation participates in Phe508del-CFTR surface retention [40], here we constructed a deletion mutant of NHERF1 (NHERF1-Δ1) wherein the PDZ1 domain was replaced by GFP (Figure 2.4A). Thus, binding of CFTR to NHERF1-Δ1 can occur only through interaction with NHERF1 PDZ2. Immunoprecipitation of mChF-Phe508del-CFTR, after induction and DSP cross-linking as above, revealed that NHERF1-Δ1 overexpression led to a significant decrease in the amount of co-captured CHIP, in comparison to mock-transfected cells (Figure 2.4B).

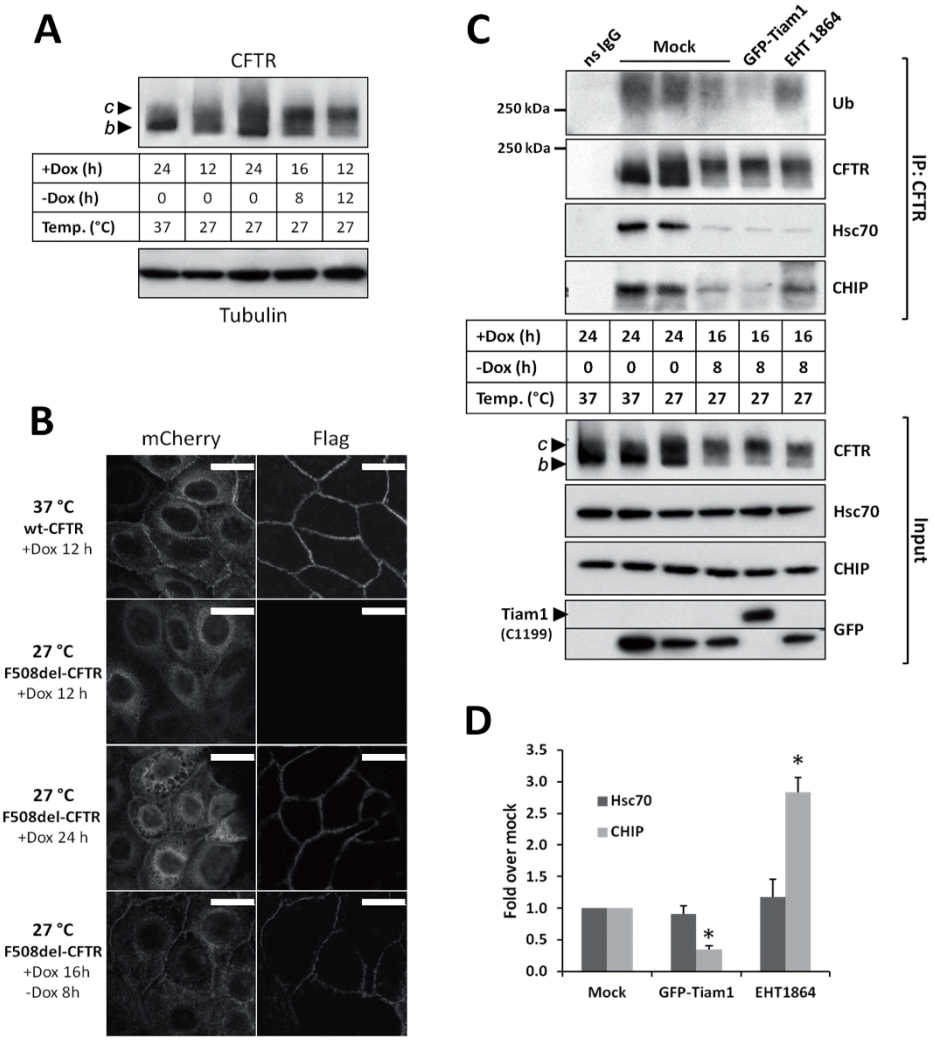

Figure 2.3 – Analysis of post-Golgi CFTR complex composition using the inducible CFBEmChF cell model
A- Western blotting for mCherry-Flag-Phe508del-CFTR in CFBEmChF cells induced with doxycycline at 27°C, for the indicated periods [+Dox (h)], to enable part of it to escape the ERQC and mature (band *c*). To enable ERAD of immature Phe508del-CFTR (band *b*) after production of the mature form (band *c*), Dox was withdrawn for 8 to 12 hours [-Dox (h)]. **B-** Confocal images of immunofluorescent staining of non-permeabilized CFBEmChF cells treated as in (A) detecting the intracellular distribution of Dox-induced mCherry-Flag-Phe508del-CFTR (mCherry) and its amount at the cell surface using the extracellular Flag-tag (detected with anti-Flag followed by an Alexa488-conjugated secondary antibody). Scale bars: 25 µM. **C-** Immunoprecipitation of mCherry-Flag-F508del-CFTR s from DSP-crosslinked CFBEmChF cells incubated either at control conditions or at the conditions [determined in (A) to produce the higher amounts of band *c* with nearly absent band *b*] and either mock-transfected or transfected with GFP-C1199Tiam1 or pretreated with the RAC1 inhibitor EHT 1864. **D-** Quantification of Hsc70 and CHIP co-precipitating with mCherry-Flag-F508del-CFTR in (C) from 5 independent assays. Data are means ± SEM**.** ***p*<0.05 , compared to mock (ANOVA followed by *t* test). [WB, co-immunoprecipitation and confocal images aquired by Cláudia Loureiro and Paulo Matos, included with permission]

We also overexpressed a second NHERF1 mutant (NHERF1-Δ1,2), which because of the ablation of both PDZ domains (Figure 2.4A) competes with endogenous NHERF1 for EZR binding. Conversely, this resulted in increased amounts of CHIP that co-precipitated with mChF-Phe508del-CFTR (Figure 2.4B), suggesting that EZR-mediated opening of PDZ2 in NHERF1 and the subsequent binding of CFTR precludes the recruitment of CHIP to Phe508del-CFTR proteins residing at the cell surface. To further investigate this hypothesis, we constructed a truncated mutant of EZR (ezrin-ΔCt) in which the C-

terminal actin-binding domain was replaced by GFP (Figure 2.4A). This mutant causes actin-independent opening of the PDZ2 in NHERF1 [150]. Consistent with our hypothesis, its overexpression

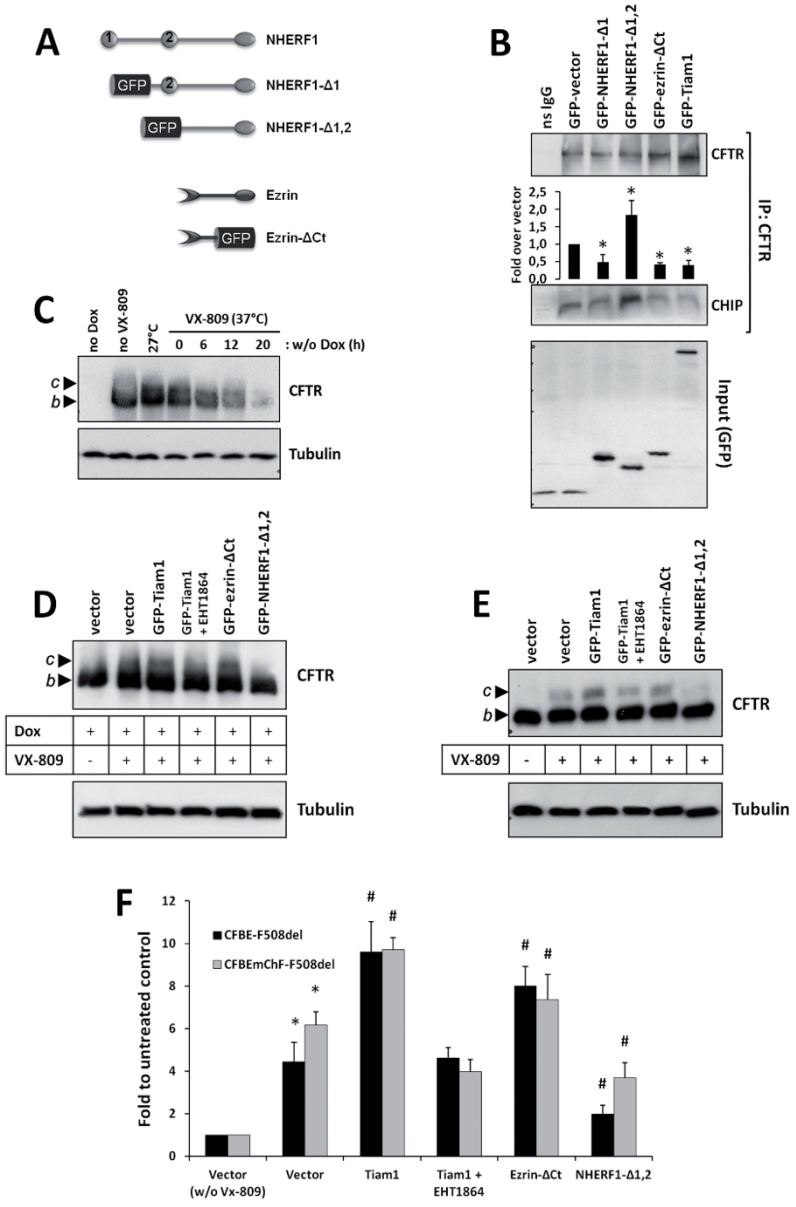

Figure 2.4 - Post-Golgi Phe508del-CFTR binding to NHERF1 PDZ2 averts CHIP recruitment
A- Schematic representation of the truncated constructs of NHERF1 and EZR. "1" and "2" indicate the location of PDZ1 and PDZ2 domains, respectively. **B-** Abundance of the E3 ubiquitin-ligase CHIP that co-precipitated with mCherry-Flag-Phe508del-CFTR from DSP-crosslinked CFBEmChF cells incubated for 16 hours in the presence of Dox, followed by 8 hours of Dox withdrawal and either mock-transfected or transfected with the indicated GFP-tagged C1199Tiam1, NHERF1 or EZR mutants. **C-** CFTR blotting in CFBEmChF cells incubated for 24 hours at either 27°C (where indicated) or at 37°C without or with 3 μM of VX-809, were exposed to 0.1 μg/mL Dox for 16 hours, followed by 6-20 hours of Dox withdrawal [w/o Dox (h)] to enable ERAD of immature Phe508del-CFTR (band *b*). **D, E-** Western blotting for CFTR in either CFBE-mChF cells expressing Dox-induced mCherry-Flag-Phe508del-CFTR (D) or CFBE cells expressing Phe508del-CFTR (E) and the indicated constructs, then treated for 24 hours with VX-809 (3 μM), the last 4 hours of which was also in the presence of of EHT 1864 (50 μM) where indicated. **F-** Quantification of fully-glycosylated Phe508del-CFTR band intensities (band *c*) in 3 independent assays as in (D) (grey bars) and as in (E) (black bars). Data are means ± SEM. # $p<0.05$ compared to VX-809-treated cells; *$p<0.05$ compared to untreated cells (ANOVA followed by Tukey's tests). [Co-mmunoprecipitation performed by Cláudia Loureiro and Ângela Alves. Mutants constructed by Joana Pereira and Ângela Alves. Data included with permission of the mentioned authors]

also led to a significant reduction in the amount of CHIP that co-precipitated with Phe508del-CFTR (Figure 2.4B).

2.3.5. Availability of the NHERF1 PDZ2 enhances VX-809-mediated rescue of Phe508del-CFTR abundance at the cell surface

Because we previously demonstrated that RAC1-mediated retention of Phe508del-CFTR at the PM greatly enhanced the efficacy of investigational protein trafficking "correctors" such as VX-809, we used our inducible system to test whether CHIP displacement by CFTR binding to the PDZ2 of NHERF1 also participated in this effect. As expected, treatment with VX-809 promoted the rescue of mChF-Phe508del-CFTR, clearly increasing the abundance of its post-Golgi, fully glycosylated form (Figure 2.4C). However, in contrast to low-temperature exposure, the VX-809 treatment somehow interfered with the turnover of the immature protein, because the core-glycosylated form of mChF-Phe508del-CFTR remained detectable even 20 hours after the withdrawal of Dox (Figure 2.4C). A similar stabilization of the immature form of Phe508del-CFTR by VX-809 has also been observed in pulse-chase experiments using BHK (baby hamster kidney) cells constitutively expressing an untagged human Phe508del-CFTR protein [158], thus excluding potential effects specific to these cellular models. Moreover, upon expression of the ezrin-ΔCt truncation mutant in either mChF-Phe508del-CFTR or Phe508del-CFTR CFBE cells, we observed a clear enhancement of VX-809-induced abundance of post-Golgi Phe508del-CFTR, which was comparable to that induced by the activation of endogenous RAC1 signaling through C1199-Tiam1 (Figure 2.4D to F). Conversely, expression of the NHERF1-Δ1,2 mutant produced the opposite effect, reducing the amount of Phe508del-CFTR rescued to the cell surface by VX-809 to an even lower abundance than that induced by co-treatment with the EHT 1864 RAC1 inhibitor (Figure 2.4D to F).

2.3.6. Retention of functional Phe508del-CFTR at the plasma membrane can occur in the absence of actin cytoskeleton anchoring

We and others have shown that the immobilization of Phe508del-CFTR at the PM through the anchoring of the CFTR protein to the actin cytoskeleton, is required to achieve the best restoration of CFTR-mediated ion transport [40,109,123,150,159]. Because the ezrin-ΔCt mutant does not bind the actin cytoskeleton, we asked whether using this mutant to retain Phe508del-CFTR at the PM would still enhance the functional restoration achieved by VX-809, despite the lack of actin anchoring and CFTR immobilization. To test this, we measured CFTR activity through iodide influx using the well-established halide-sensitive YFP (HS-YFP) functional assay (Figure 2.5A) [159–161]. Consistent with increased abundance of functional CFTR at the PM, we observed that the iodide influx rate was stimulated nearly 7 fold by CFP-ezrin-ΔCt expression in VX-809-treated Phe508del-CFTR CFBE cells, compared to CFP expression alone (Figure 2.5B and C). Confirming CFTR-specificity, co-treatment with the CFTR 172 inhibitor (inh172) blocked the effect of ezrin-ΔCt expression. Moreover, the iodide

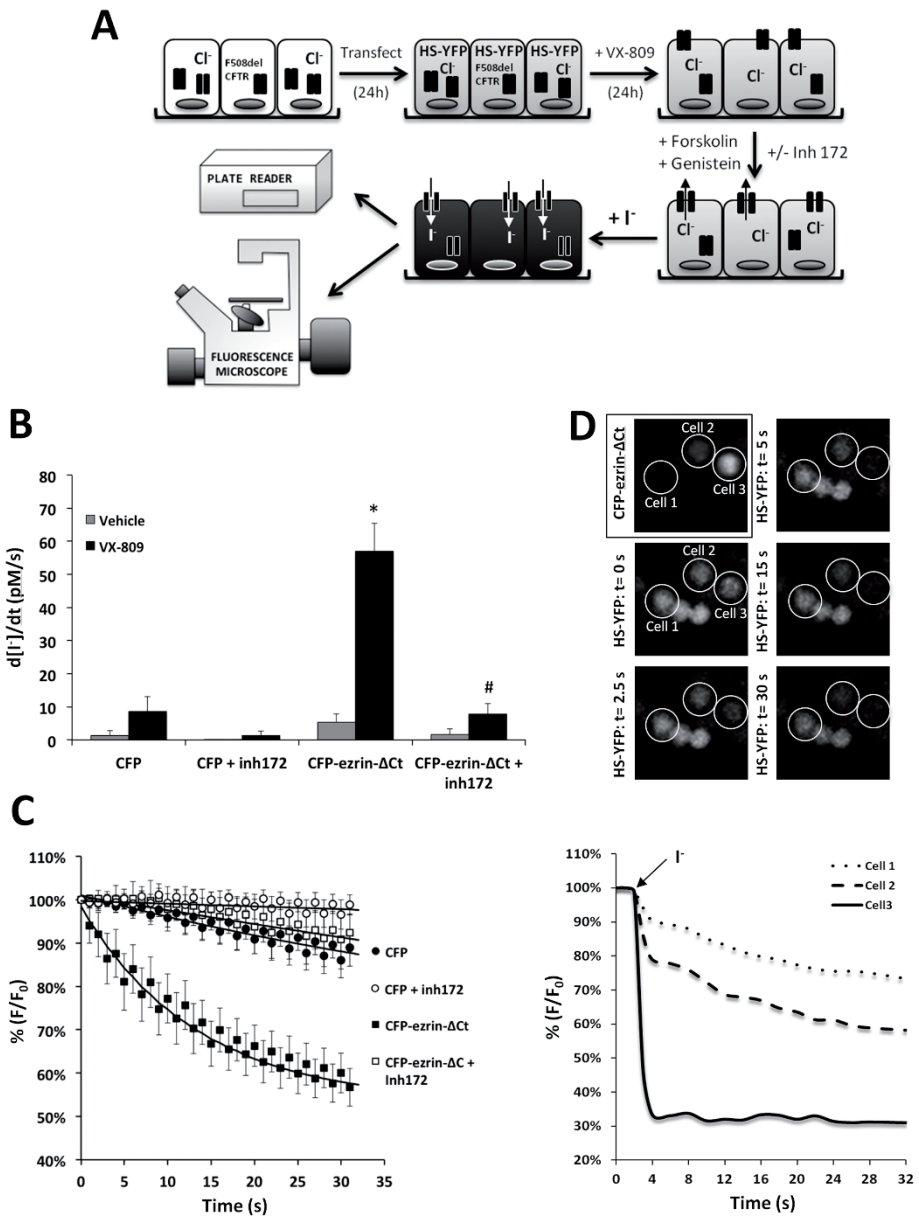

Figure 2.5 - Retention of VX-809-rescued Phe508del-CFTR at the plasma membrane through expression of ezrin-ΔCt potentiates the functional restoration of CFTR despite the lack of actin cytoskeleton anchoring
A- Schematic representation of the iodide influx assay in CFBE Phe508del-CFTR cells co-transfected with the halide sensitive YFP protein (HS-YFP) and either CFP or CFP-ezrin-ΔCt. After CFTR stimulation with forskolin and genistein, with or without CFTR inhibitor 172, fluorescence decay was measured after addition of iodide to the external solution. **B-** Summary of iodide influx rates in cells transfected as in (A) alone or also treated with VX-809. **C-** Traces of iodide-induced HS-YFP fluorescence decay in VX-809-treated cells transfected and stimulated as above ($n \geq 15$ wells, triplicates of 5 independent assays). Lines are double exponential curve fittings. **D-** Representative time-lapse images of HS-YFP quenching by iodide in cells expressing different amounts of CFP-ezrin-ΔCt. Full-time traces for each cell are shown in the bottom graph. Data are means ± SEM. ∗p<0.05 relative to CFP; #p<0.05 relative to CFP-ezrin-ΔCt. [Schematic diagram designed by Paulo Matos, included with permission].

influx observed in cells expressing ezrin-ΔCt that were treated only with vehicle was not significantly induced (Figure 2.5B). This indicates that ezrin-ΔCt acts specifically at the PM, synergizing with VX-809 to produce a dramatic functional stabilization of rescued Phe508del-CFTR at the cell surface. In addition, using time-lapse fluorescence microscopy, we established that the rate of HS-YFP

quenching by iodide was directly proportional to the amount of ezrin-ΔCt expressed in individual cells. Because ezrin-ΔCt does not bind to actin [150], these results further indicate that in the stabilization of rescued Phe508del-CFTR at the PM, actin cytoskeleton anchoring is not essential but rather consequential to the opening of the PDZ2 in NHERF1.

3.1. Discussion

Phe508del-CFTR proteins are targeted for degradation by the PPQC, once rescued to the PM by either low temperature and corrector compounds [36]. We previously demonstrated that stimulation of endogenous RAC1 signaling overcomes the PPQC, retaining rescued Phe508del-CFTR at the PM and boosting the functional restoration achieved by VX-809 from ~10% to over 25% of wild-type CFTR function in primary airway epithelial cells from Phe508del/Phe508del patients [40]. Here, we characterized the molecular mechanism behind this effect. We demonstrate that besides promoting CFTR anchoring to actin, RAC1 also induces the opening of NHERF1 PDZ2 by EZR, which precludes the recruitment of CHIP in a way that does not depend on the Hsc70 chaperone. This is an important observation because mutant CFTR matures inefficiently and there is evidence that even the mature wild-type protein may require chaperones to stabilize its conformation and function [162,163]. Hence, it was proposed that the decreased stability of post-Golgi Phe508del-CFTR results from a prolonged interaction with multiple chaperones thus triggering the PPQC [36]. Notably, our results indicate that it is possible to prevent Phe508del-CFTR turnover at the PM without losing chaperone-mediated conformational integrity. Our data show that the binding of CHIP to rescued Phe508del proteins can be avoided by inducing CFTR to switch its interaction from NHERF1-PDZ1 to the NHERF1-PDZ2 domain. Moreover, using a C-terminus truncated mutant of EZR, incapable of binding to actin, we demonstrated that this PDZ switch does not require the physical anchoring of the channel to the actin cytoskeleton, suggesting that actin anchoring is a consequence rather than the cause of CFTR surface stabilization. This is another very important finding in the way that it opens a brand new field of therapeutic possibilities in CF. The fact that this PDZ switch causes a conformational change in the Phe508del-CFTR/NHERF1 complex that either prevents CHIP from binding or causes its displacement offers clear new targets for pharmacological intervention. To further assess the potential impact of our findings, we investigated whether they also applied to Phe508del-CFTR proteins rescued by the investigational drug VX-809. The latter, administered in combination with VX-770, has recently passed phase III clinical trials, representing the most promising therapeutic option for Phe508del-CFTR carriers to date [140]. We showed that, as happens with active Tiam1, expression of ezrin-ΔCt in CFBE cells increases the steady-state, post-Golgi abundance of both low temperature- and VX-809-rescued Phe508del-CFTR. In contrast, sequestering endogenous EZR through overexpression of the NHERF1-Δ1,2 mutant produces the opposite effect, in agreement with an accelerated turnover of rescued proteins. These data demonstrate that the manipulations that determined the absence of CHIP in temperature-rescued Phe508del complexes, clearly translate to increased abundance of VX-809-rescued Phe508del-CFTR. Indeed, these effects were functionally validated and shown to significantly enhance VX-809 functional restoration of Phe508del-CFTR in epithelial cells. It is currently known that VX-809 rescued Phe508del-CFTR remains thermodynamically unstable because

its abundance can be increased up to 5-fold by co-incubation at low temperatures [164]. Nevertheless, VX-809 administration can increase, albeit modestly [63], the PM stability of low temperature-rescued Phe508del-CFTR possibly through post-Golgi conformational events that increase the protein's affinity to NHERF1 [165]. The mechanism characterized here explains how this stabilization is achieved by inducing the NHERF1 PDZ switch and CHIP displacement through endogenous signaling. NHERF1 is a scaffold for many surface proteins. These include the NHE3 antiporter and the β1-3 adrenoceptors [158,166] involved in CF, but also several membrane receptors known to have altered surface stability under different conditions, namely in several types of cancer [167]. Thus, the NHERF1 PDZ switch mechanism described here may also have impact in our understanding of the pathophysiology of other diseases and reveal a set of highly attractive new targets for rational drug design.

4.1. Materials and Methods

4.1.1. Plasmid constructs

All NHERF1 (Δ1: a.a. 150-358; Δ1,2: a.a. 230-358) and EZR (ΔCt: a.a. 1-310) deletion mutants were generated by PCR using, respectively, SacI (5') and BamHI (3') or XhoI (5') and EcoRI (3') degenerate primers. Amplicons were cloned into pCR2.1 TOPO-TA vector (Life Technologies) and subcloned into pEGFP or pECFP (Clontech). pEGFP-C1199Tiam1 was generated by direct subcloning from pCDNA3.1-HA-C1199Tiam1, a kind gift from John Collard (Netherlands Cancer Institute, Netherlands). All constructs were verified by automated sequencing. The YFP-H148Q/I152L halide sensitive construct was a generous gift from Peter Haggie (UCSF School of Medicine, USA).

4.1.2. Cell culture and transfection

CFBE41o- cells stably expressing wt- or Phe508del-CFTR were a gift from JP Clancy, University of Alabama USA [153]. CFBE41o- cells stably transduced with lentivirus encoding mCherry-Flag-tagged (CFBEmChF cells) wt- or Phe508del-CFTR under the Tet-ON promoter, were generated by ADV Bioscience LLC, Birmingham, AL, USA as described before [154]. Expression of CFTR constructs was induced by incubation with 0.1 to 0.5 μg/mL doxycycline (Dox, Sigma-Aldrich) as indicated. All cells were grown as described [153,154,168] at 37°C under 5% CO_2, in minimal essential medium (MEM) supplemented with L-glutamine, Earle's salts, 10% (v/v) FBS and penicillin/streptomycin (all from Life Technologies). Cells were transfected with LipofectAMINE 2000 (Life Technologies) using a DNA:LipofectAMINE ratio of 1:3 (μg:μl) and analyzed 24-48 hours later. Constructs were supplemented with empty vector when required. Cells were treated, for the indicated periods, with the described concentrations of NSC23766 (Merck4Biosciences-Calbiochem) EHT 1864 (Santa Cruz Biotechnology) or with VX-809 (Selleck Chemicals) in 1% FBS supplemented medium.

4.1.3. Temperature switch assays

Phe508del-CFTR CFBE cells were transfected with either pEGFP-vector or pEGFP-C1199Tiam1 using the conditions above. After 6 hours at 37°C the medium was replaced and cells were incubated

at 27°C for 24 hours, the last four of which with or without the addition of EHT 1864 (50 μM), and then placed at 37°C for 30 to 240 min prior to direct lysis in Laemmli sample buffer. Lysates were analyzed by immunoblotting as described below.

4.1.4. Immunofluorescence and confocal microscopy

CFBEmChF cells grown on coverslips were induced with 0.5 μg/mL Dox and treated as indicated. Cells were rinsed on ice with cold PBS supplemented with $CaCl_2$ (0.9 mM) and $MgCl_2$ (0.5 mM) and incubated with mouse anti-Flag (1:500, Sigma-Aldrich) in PBS supplemented with 1% bovine serum albumin for 1 hour at 4°C. Cells were then fixed with 4% formaldehyde, washed with PBS and incubated with anti-mouse AlexaFluor488 secondary antibody for 1hour (1:500, Life Technologies) for 30 min, followed by thorough washing in PBS and DAPI staining of nuclei. Images were recorded on a Leica TCS-SPE confocal microscope.

4.1.5. Co-immunoprecipitation and immunoblotting

CFBEmChF cells were transfected and treated as indicated. To rescue Phe508del-CFTR trafficking, cells were incubated at 27°C for 12-24 hours, in the presence of 0.5 μg/mL of Dox. To isolate complex-glycosylated Phe508del-CFTR cells were maintained for additional 8-12 hours in the absence of Dox to minimize the expression of core-glycosylated form in the ER. To detect the weak CFTR interaction with chaperones, cells were washed in PBS and incubated with 0.1 mM dithiobis [succinimidyl propionate] (DSP, Life Technologies) in PBS for 30 min at room temperature. Cells were lysed in Nonidet P-40 (NP-40) buffer (50 mM Tris-HCl pH 7.5, 1% (v/v) NP-40, 100 mM NaCl, 10% (v/v) glycerol, 10 mM $MgCl_2$, supplemented with protease inhibitors), lysates pre-cleared and incubated O/N at 4°C with mouse anti-CFTR clone 570 (CFF), followed by incubation with protein G-agarose (Life Technologies) for 1 hour at 4°C. Immunoprecipitates were washed 4 times with NP-40 buffer and eluted in 2x Laemmli sample buffer. Samples were analyzed by immunoblotting (WB) as previously described [40]. Additional antibodies used for WB were: mouse anti-CFTR clone 596 (CFF), rabbit anti-GFP ab290 (Abcam), mouse anti-Myc clone 9E10, mouse anti-α-Tubulin clone B-5-1-2, mouse anti-Flag clone M2 (Sigma-Aldrich), mouse anti-Rac1 clone 23A8 (Millipore), rat anti-Hsc70 (StressGen) and rabbit anti-ubiquitin clone 10H4L21 (Life Technologies).

4.1.6. Surface protein biotinylation and CRIB pull-down

Cell surface proteins were labeled on ice with EZ-Link Sulfo-NHS-SS-biotin (Life Technologies) in non-permeabilizing conditions and captured with streptavidin-agarose beads (Life Technologies). Captured proteins were analyzed by WB as above. GTP-RAC1 CRIB-pull-down assays were performed as previously described [40,169]. Briefly, cells were washed in cold PBS, and lysed on ice in a non-denaturing buffer (50 mM Tris-HCl, pH 7.5, 1% (v/v) NP-40, 100 mM NaCl, 10% (v/v) glycerol, 10 mM $MgCl_2$, and protease inhibitor mixture (Sigma-Aldrich). The lysate was then incubated for 1 hour at 4 °C with a biotinylated CRIB-domain peptide pre-coupled to streptavidin-agarose beads (Sigma-Aldrich). The CRIB domain (CDC42/RAC1 Interactive Binding) of the CDC42/RAC1 effector protein, p21 activated kinase 1 (PAK1), binds specifically to the GTP-bound form of RAC1 proteins allowing the selective capture and quantitation of the active pool of RAC1 molecules inside the cells. Precipitates were washed three times with excess lysis buffer, eluted in Laemmli sample buffer and analyzed by WB.

4.1.7. Iodide efflux

CFTR-mediated iodide efflux was measured at room temperature using the cAMP agonist forskolin (10 µM) and the CFTR potentiator genistein (50 µM) (both from Sigma-Aldrich) as described previously (10).

4.1.8. Halide-sensitive YFP-based functional assay

CFTR activity was determined in cells stably expressing Phe508del-CFTR transiently transfected with the previously described [159–161] halide-sensitive yellow fluorescent protein (HS-YFP-H148Q/I152L), and either CFP or CFP-ezrin-ΔCt. Cells were plated in either 8-well chamber slides or 96-well microplates and transfected with LipofectAMINE 2000, as described [40]. After 24 hours, the culture medium was replaced and cells were treated, or not, with 3 µM of VX-809 for another 24 hours. Cells were washed with PBS and incubated for 30 min in PBS containing compounds for CFTR stimulation/inhibition (forskolin 10 µM, genistein 10 µM, and CFTR-inh172 25 µM). Cells were then transferred either to a microplate reader (Tecan® Infinite M200) (excitation: 505nm and emission: 535nm) or to a Leica TCS-SPE confocal microscope for time-lapse analysis. Each well was assayed individually for iodide influx by recording fluorescence continuously (500 ms/point) for 2 s (baseline) and then for 30 s after the rapid (<1 s) addition of isomolar PBS in which 137 mM Cl^- was replaced by I^- (final NaI concentration in the well: 100 mM). Assays were performed at room temperature. After background subtraction, cell fluorescence recordings were normalized for the initial average value measured before addition of I^-.

4.1.9. Statistical Analysis

Quantitative results are shown as means ± SEM of *n* observations. To compare sets of data, we used either ANOVA or two tailed Student's *t* tests, and considered significant differences when *p* values < 0.05. In the halide-sensitive YFP-based functional assay, the signal decay caused by YFP fluorescence quenching was fitted to a one- or two-phase exponential decay function to derive the maximal slope that corresponds to initial influx of I^- into the cells [159,161]. Maximal slopes were converted into rates of variation of the intracellular I^- concentration (in µM/s) using the equation $d[I^-]/dt = K_d\,[d(F/F_0)/dt]$, where K_d is the affinity constant of YFP for I^- [159,161], and F/F_0 is the ratio of the cell fluorescence at a given time versus the initial fluorescence.

Chapter 3

Prolonged co-treatment with HGF sustains epithelial integrity and improves pharmacological rescue of Phe508del-CFTR

Ana Margarida Matos, Andreia Gomes-Duarte, Márcia Faria, Patrícia Barros, Peter Jordan, Margarida D. Amaral, and Paulo Matos

Data included in this chapter was published in:

Matos AM, Gomes-Duarte A, Faria M, Barros P, Jordan P, Amaral MD, et al. Prolonged co-treatment with HGF sustains epithelial integrity and improves pharmacological rescue of Phe508del-CFTR. *Sci. Rep.* **8,** 13026 (2018)

3.1. Abstract

Cystic fibrosis (CF), the most common inherited disease in Caucasians, is caused by mutations in the CFTR chloride channel, the most frequent of which is Phe508del. Phe508del causes not only intracellular retention and premature degradation of the mutant CFTR protein, but also defective channel gating and decreased half-life when experimentally rescued to the plasma membrane (PM). Despite recent successes in the functional rescue of several CFTR mutations with small-molecule drugs, the folding-corrector/gating-potentiator drug combinations approved for Phe508del-CFTR homozygous patients have shown only modest benefit. Several factors have been shown to contribute to this outcome, including an unexpected intensification of corrector-rescued Phe508del-CFTR PM instability after persistent co-treatment with potentiator drugs. We have previously shown that acute co-treatment with hepatocyte growth factor (HGF) can significantly enhance the chemical correction of Phe508del-CFTR. HGF coaxes the anchoring of rescued channels to the actin cytoskeleton *via* induction of RAC1 GTPase signaling. Here, we demonstrate that a prolonged, 15-day HGF treatment also significantly improves the functional rescue of Phe508del-CFTR by the VX-809 corrector/VX-770 potentiator combination, in polarized bronchial epithelial monolayers. Importantly, we found that HGF treatment also prevented VX-770-mediated destabilization of rescued Phe508del-CFTR and enabled further potentiation of the rescued channels. Most strikingly, prolonged HGF treatment prevented previously unrecognized epithelial dedifferentiation effects of sustained exposure to VX-809. This was observed in epithelium-like monolayers from both lung and intestinal origin, representing the two systems most affected by adverse symptoms in patients treated with VX-809 or the VX-809/VX-770 combination. Taken together, our findings strongly suggest that co-administration of HGF with corrector/potentiator drugs could be beneficial for CF patients.

3.2. Introduction

Mutations in the CFTR gene cause cystic fibrosis (CF), the most common inherited disease in Caucasians [2]. They can alter the synthesis, processing, function, and half-life of CFTR, the main chloride channel expressed apically at the plasma membrane (PM) of epithelial cells [170]. Respiratory failure, derived from severe airway obstruction, inflammation, and recurrent infections, is the most prevalent mortality cause in CF [170]. Although CF is still incurable (mean survival of ~40 years), the last decade brought remarkable progress towards personalized CF treatments, with the development of small-molecule drugs targeting frequent CFTR mutations [171,172]. The proof-of-principle was Ivacaftor (VX-770), a potentiator drug that relieved CF symptoms in patients bearing mutations (e.g., Gly551Asp) that impair CFTR channel activity (4–8% of patients) [173]. Soon after, Lumacaftor (VX-809), a pharmacological chaperone, in combination with VX-770, was approved by the Food and Drug Administration (FDA) and European Medicines Agency (EMA) [59] for patients homozygous for the most common mutation – Phe508del (~40% of patients), which impairs CFTR folding and trafficking [174]. In phase II trials, the VX-809/VX-770 combination (at the higher administered doses) significantly improved the percentage predicted forced expiratory volume in one second (FEV_1) by a mean of 6% in patients homozygous for Phe508del-CFTR, decreased sweat chloride concentration by ~10

mmol/L, and decreased pulmonary exacerbations in the treatment groups [52]. Data from subsequent phase III trials revealed improvements in predicted FEV_1 ranging from 2.6–4.0% and a clear, 30–39% decrease in the rate of pulmonary exacerbations, significantly reducing hospitalization and the use of intravenous antibiotics in the treatment groups [53]. The VX-809/VX-770 drug combination has now been used in patients since 2015, and several subsequent studies of its long-term usage indicate that it does benefit CF patients, although several cases of off-target side-effects have been reported, the most frequent being respiratory and gastrointestinal manifestations [60–62]. Despite the reported benefits, the results from these studies fell below initial expectations and experimental evidence emerged to, at least partially, explain the limited clinical improvements observed in patients. For instance, it was shown that persistent exposure to potentiator drugs, particularly VX-770, results in a dose-dependent reversal of VX-809-mediated CFTR correction in Phe508del-CFTR homozygous primary airway cell cultures [47,54]. This was due to destabilization and increased turnover of the rescued protein, resulting in its reduced functional expression at the cell surface. A posterior study, however, argued that at clinically relevant concentrations (below 1 µM), continuous exposure to VX-770 does not inhibit the rescue of Phe508del-CFTR by VX-809 [55]. In addition, it was also observed that *Pseudomonas aeruginosa* reduces Phe508del-CFTR function in cells treated either with VX-809 alone or with the VX-809/VX-770 combination [56,57]. Since 85% of adult CF patients are colonized with *P. aeruginosa*, these data suggest that infection with these bacteria may also contribute to a reduction in the therapeutic efficacy of these drugs.

Importantly, we and others showed that the intrinsically reduced stability of rescued Phe508del-CFTR at the cells' PM (less than 10% that of wt-CFTR) [36,175] – due to its deficient anchoring to the actin cytoskeleton and targeting by the peripheral protein quality control - could be a major obstacle to its pharmacological correction [36,37,40,131]. However, we showed that acute treatment with hepatocyte growth factor (HGF) can increase Phe508del-CFTR stability and retention at the PM [40]. HGF acts *via* RAC1 GTPase to promote the PDZ-mediated interaction of Phe508del-CFTR with NHERF1 and ezrin adaptor protein, favouring the channel's anchoring to the actin cytoskeleton [37,40]. Notably, co-treatment with HGF enhanced over 3-fold the functional restoration efficacy of chemical correctors such as corr-4a (C4) and C3, by preventing internalization of rescued Phe508del-CFTR from the PM [40]. Here, we investigated whether HGF treatment would enhance the functional correction of Phe508del-CFTR by the VX-809/VX-770 drug combination. For this, we used *in vitro* epithelium-like cellular models to determine what would be the cellular and functional consequences of a prolonged, phase II trial duration-consistent, combined treatment with VX-809/VX-770 and HGF. We found that prolonged co-administration of HGF significantly increased the Phe508del-CFTR functional rescue by VX-809/VX-770 in bronchial polarized monolayers, also preventing VX-770-mediated destabilization of PM-rescued channels. Intriguingly, we show that prolonged co-treatment with HGF strengthens the integrity of bronchial and intestinal epithelium-like cellular cultures, suppressing yet unreported cellular dedifferentiation effects of continued exposure to VX-809, which may relate to the drug's adverse effects. Our data strongly suggests that HGF co-administration might be beneficial for CF patients, particularly in the initial weeks of treatment, and in patients with severe lung disease, who suffered from more frequent and pronounced adverse drug effects.

3.3. Results

3.3.1. HGF enhances functional rescue of Phe508del-CFTR by acute VX-809/VX-770 co-treatment

We previously demonstrated that the functional correction of Phe508del-CFTR by corrector C4 in CFBE cells can be enhanced up to 3-fold by co-treatment with HGF [40]. Thus, we asked if HGF treatment would also enhance Phe508del-CFTR functional rescue when co-administered with the VX-809/VX-770 drug combination. To address this question we used the well-established halide-sensitive YFP (HS-YFP) functional assay [37,159,160]. Briefly, CFBE cells co-expressing Phe508del-CFTR and the halide-sensitive YFP-F46L/H148Q/I152L mutant [159] (HS-YFP) were incubated in duplicates for 48 hours with either DMSO, 10 µM of C4, or 3 µM VX-809. One of each replicate was co-treated with 50 ng/mL of HGF for the last 24 hours. One additional replicate was added for the VX-809/HGF treatment, which was incubated with 25 µM of CFTR inhibitor 172 (inh172), 15 min prior to the assay. Cells were then stimulated for 30 min in PBS with 5 µM forskolin (Fsk), and either 20 µM genistein (Gen) or 10 µM VX-770. Analysis of HS-YFP fluorescence decay showed that HGF enhanced the functional response of C4-rescued Phe508del-CFTR by ~2.2-fold in this assay (Figure 3.1A and B), in agreement with our previous findings using other methods [40]. Importantly, we also observed an equivalent increase (~2.5-fold) in CFTR function with VX-809/HGF co-treatment, versus VX-809 treatment alone, upon acute stimulation with Fsk and VX-770. Moreover, confirming a CFTR-specific response, co-treatment with inh172 reversed this effect (Figure 3.1B). Next, we tested whether the effect of HGF co-treatment was sustained in polarized CFBE cells.

CFBE-Phe508del/HS-YFP cells were polarized in transwell, 0.4 µm PET filter inserts (24-well size), until they reached a transepithelial electrical resistance (TEER) of ≥600 Ω. Cells, in duplicate or triplicate filters, were treated with DMSO or 3 µM VX-809 for 48 hours. Two of the VX-809 replicates were co-treated with 50 ng/mL of HGF for the last 24 hours. One of these replicates was additionally incubated for 15 min with 25 µM of inh172 prior to the iodide influx assay. TEER was monitored for all conditions and no significant variations were observed over time (Figure 3.2A). To measure fluorescence decay after CFTR stimulation we developed an in-house setup (see Methods and Figure 3.2B) that forms a chamber on top of a glass slide. The setup can be positioned on the confocal microscope stage and loaded with transwell inserts containing CFBE-Phe508del/HS-YFP polarized cells. This places the polarized cells within the focal length of a 10× objective (Figure 3.2B), allowing live imaging acquisition. Thus, XZ confocal fluorescence images were collected continuously after the rapid (≤1 s) apical addition of iodide (I^-) together with 5 µM Fsk, with or without 10 µM VX-770, and with or without 25 µM of inh172, as indicated (Figure 3.2C). Calculation of initial iodide influx rates from the fluorescence decay curves (Figure 3.2D) clearly showed that HGF co-treatment significantly increased the Phe508del-CFTR functional rescue by the combination of VX-809-mediated correction and VX-770 acute potentiation. Moreover, consistent with the results from non-polarized cells, this functional increase was 2.9-fold higher than with VX-809/VX-770 treatment alone and was completely suppressed by the presence of inh172 (Figure 3.2D). Western blot (WB) analysis from these filters showed that HGF treatment produced a small increase in rescued Phe508del-CFTR mature C band steady-state levels (Figure 3.3A), but this was not sufficient to justify the roughly 3-fold increase in CFTR-dependent ion transport (Figure 3.2D). We, therefore, immunostained replicate

filters to detect the localization of CFTR (Figure 3.3B). We found that, more than enhancing the overall levels of CFTR in these cells, HGF promoted the accumulation of 2-times more rescued Phe508del-CFTR at the apical membrane (Figure 3.3D), shifting to ~2.6-fold the ratio of CFTR apical/basolateral distribution (Figure 3.3D). These data were confirmed by conventional cell surface protein biotinylation assays, where HGF produced a 1.4-fold increase in the total levels of VX-809-rescued band C but a 3.3 fold increment in the levels of CFTR at the PM (Figure 3.3E). Both results are consistent with the enhancement of the channel's anchoring and retention at the cell surface that we previously described for HGF co-treatment in C4-corrected CFBE-Phe508del cells [40].

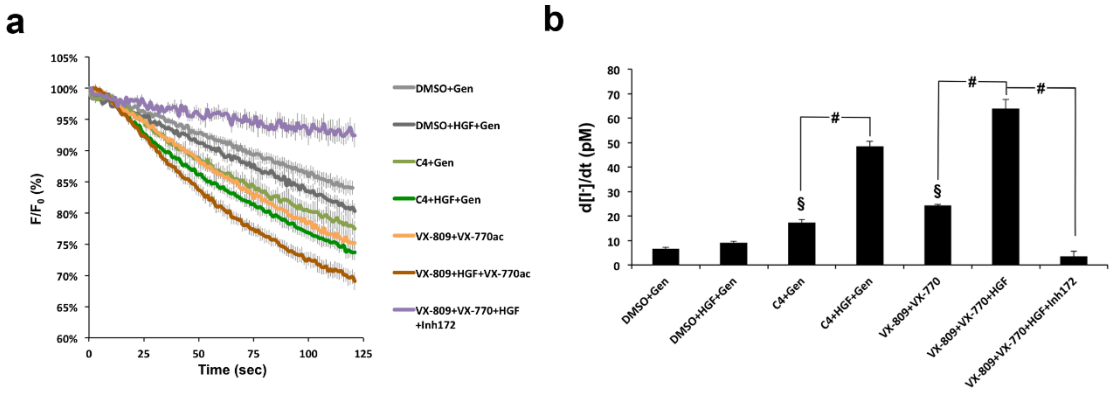

Figure 3.1 - HGF treatment improves functional rescue of Phe508del-CFTR by chemical correctors
A- Fluorescence decay curves of the iodide influx assay. CFBE-Phe508del cells stably expressing the YFP-halide sensor were treated, as indicated, for 48 hours with 10 µM corr-4a (C4) or 3 µM VX-809, in the presence or absence of 50 ng/ml of HGF for the last 24 hours. Cells were then stimulated with 5 µM forskolin (Fsk) and either 20 µM genistein (Gen) or 10 µM VX-770, in the presence or absence of 25 µM CFTR inhibitor 172 (inh172). Fluorescence was recorded continuously in a microplate reader, first for 10 s (baseline) and then for 110 s after the rapid (≤1 s) addition of isomolar PBS, in which Cl^- was replaced by I^-. Fluorescence (F) was plotted over time as percentage of fluorescence at time 0 (F_0). Data are means ± SEM of three independent assays. **B-** Iodide influx rates calculated by fitting the curves to the exponential decay function to derive the maximal slope that corresponds to initial influx of I^- into the cells [159]. Data are means ± SEM of three independent assays. §$p <$ 0.01 relative to DMSO; #$p < 0.001$.

3.3.2. Prolonged co-treatment with HGF sustains enhanced Phe508del-CFTR functional rescue by VX-809/VX-770 drug combination

The hyperactivity of the HGF/c-MET pathway has been observed in numerous neoplasms, including non-small-cell lung carcinomas [176]. Prolonged or continuous activity of the c-MET receptor by mutation, gene amplification, or altered signaling properties, leads to excessive cell proliferation and is related to the development and progression [177].

Thus, we used WB to analyze the levels of Ki-67 protein in the lysates of polarized CFBE-Phe508del cells, treated as above. Ki-67 is commonly and reliably used as a pro-proliferative marker

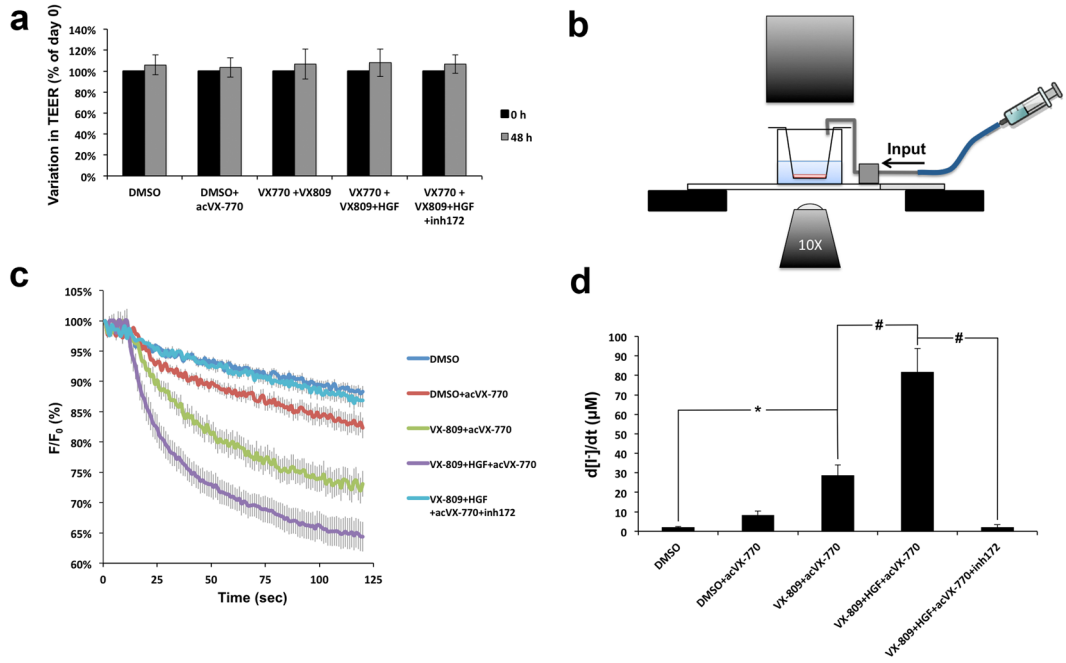

Figure 3.2 - HGF treatment improves functional rescue of Phe508del-CFTR by VX-809/VX-770 in polarized CFBE cells
A- Variation in TEER of polarized CFBE-Phe508del/HS-YFP cells treated for 48 hours as indicated. **B-** Schematic representation of the in-house setup used to record HS-YFP fluorescence decay in polarized cells. **C-** Fluorescence decay curves of the iodide influx assay in polarized CFBE-Phe508del/HS-YFP cells, treated for 48 hours with either DMSO or 3 μM of VX-809 in the presence or absence of HGF for the last 24 hours, as indicated, and stimulated acutely with 10 μM of VX-770 (acVX-770). Fluorescence (F) was plotted over time as percentage of fluorescence at time 0 (F_0). Data are means ± SEM of three independent assays. **D-** Iodide influx rates calculated as in Figure 3.1B. Data are means ± SEM of three independent assays. *$p < 0.01$; #$p < 0.001$. [Schematic diagram in b designed by Paulo Matos, included with permission]

for human cells and tumors [178]. It is present during all active phases of the cell cycle, being markedly increased in proliferating cell populations but only residual or absent in resting (non-dividing) cells [179]. Here, we observed no significant change in Ki-67 abundance in polarized CFBE-Phe508del cells after 24 h of HGF treatment (Figure 3.3A). Therefore, we decided to analyzed the effects of a more prolonged treatment with HGF, both regarding its enhancement of VX-809/VX-770 action and its effect on the differentiation and proliferation of polarized CFBE epithelia. We chose to extend our treatment for a period of 15 days, since this would be within the time frame of a phase II trial [52]. Moreover, we also considered previous studies reporting that the prolonged exposure to VX-770 concentrations above 1 μM inhibited the functional rescue of Phe508del-CFTR by VX-809 [47,55]. Thus, CFBE-Phe508del cells were polarized in filter inserts to a minimum TEER value of 600 Ω and exposed, for 15 days, to either DMSO (control), DMSO + 50 ng/ml HGF, 3 μM VX-809, 0.5 μM VX-770, 3 μM VX-809 + 0.5 μM VX-770, or 3 μM VX-809 + 0.5 μM VX-770 + 50 ng/ml HGF. TEER was monitored at days 3, 7, 11, and 15, and the culture medium replaced by fresh medium containing the same compound combinations. A clear decrease in relative TEER values (normalized to day 0) was observed from day 3 onwards in cells treated with VX-809 alone, and in cells treated with VX-809/VX-770 after day 7, when compared to DMSO (Figure 3.4A). Notably, co-treatment with HGF prevented relative TEER decrease in CFBE cells treated either with VX-809 alone or in combination with VX-770 (Figure 3.4A). WB analysis of these cells showed a significant ~1.5-fold increase in CFTR C band levels in cells treated with HGF alone (DMSO+HGF), compared to DMSO, consistent with an enhanced apical

retention of the residual Phe508del-CFTR rescued by prolonged exposure to low DMSO concentrations (Figure 3.4B).

Prolonged VX-809 treatment produced a significant ~2.5-fold increase in mature C band levels, compared to DMSO. Co-treatment with VX-809 and VX-770 also produced a significant increase in C band abundance, though slightly lower (~2.1-fold) than with VX-809 alone (Figure 3.4B).

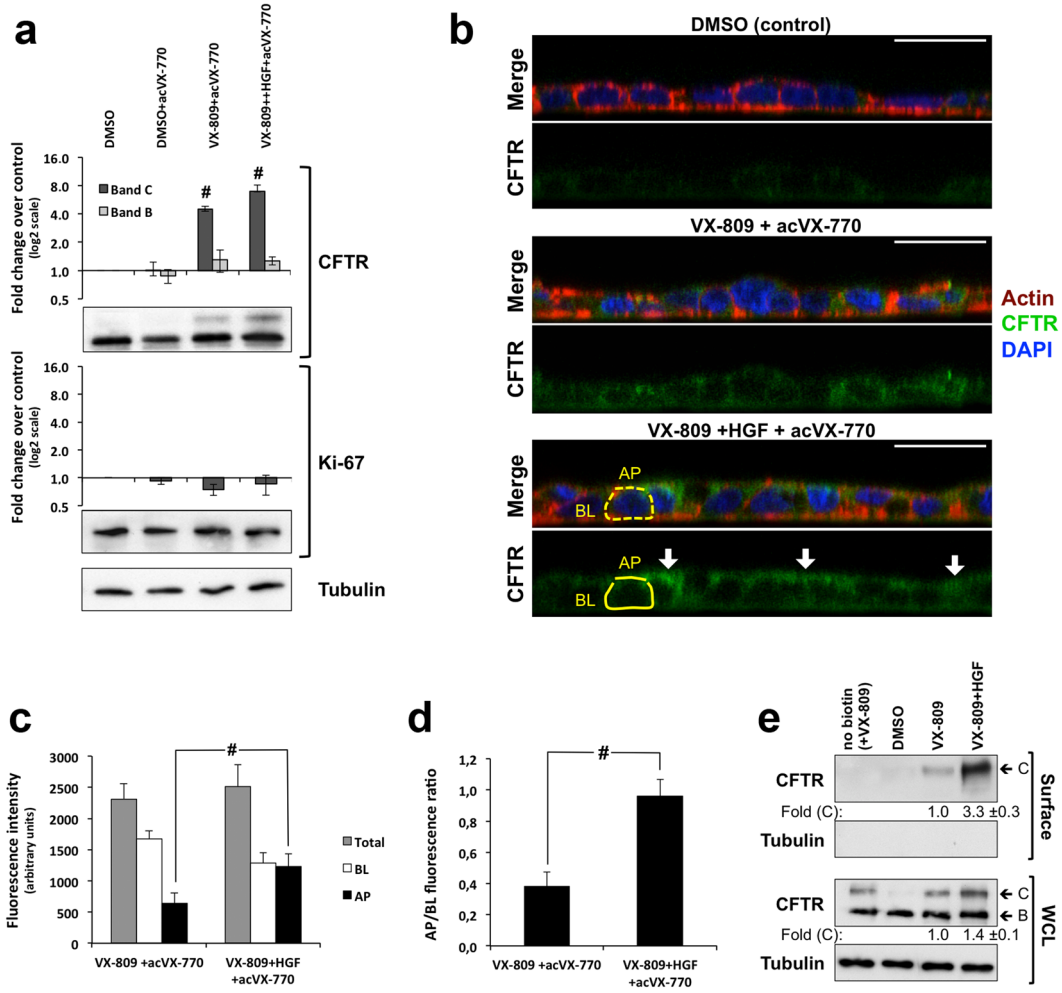

Figure 3.3 - HGF treatment promotes apical localization of VX-809-rescued Phe508del-CFTR in polarized CFBE cells
A- WB analysis of whole cell lysates from polarized CFBE cells treated for 48 hours with either DMSO or 3 µM of VX-809 in the presence or absence of HGF for the last 24 hours, as indicated, and stimulated acutely with 10 µM of VX-770 (acVX-770). Shown are representative images of CFTR and Ki-67 immunoblots together with bar plots of band intensity quantification, normalized to DMSO (means ± SEM), from three independent assays. Tubulin was used as a loading normalizer in band intensity quantification. **B-** Immunofluorescence staining of polarized CFBE-Phe508del cells treated as in (A), were stained with anti-CFTR/Alexa 488, phalloidin- TRITC and DAPI, and analyzed by confocal microscopy. Shown are overlay images (upper images) as well as isolated CFTR-staining (green channel) representative of the indicated treatment conditions. Yellow trace lines exemplify the method used for CFTR signal quantification. Actin signal was used as a guide to define the apical (AP) and basolateral (BL) membrane regions (dotted lines) that were used to quantify CFTR signal intensity (solid lines). AP, BL and Total (BL + AP) signal intensities in cells treated or not with HGF and VX-809/acVX-770 are plotted in (**C**) and the ratio between AP and BL signal intensities in (**D**). Data indicates mean ± SEM of signals from at least 30 cells analyzed in each of the three independent experiments. White arrows indicate apical shift in CFTR localization upon HGF treatment. White horizontal bar represents 10 µm. #$p < 0.001$
E- Conventional cell surface protein biotinylation assays of CFBE cells treated as in (A). Fold change in total (WCL) and PM (Surface)-rescued Phe508del-CFTR band C levels were quantified by WB densitometry and are indicated below the respective panels. [Confocal images acquired and analyzed together with Paulo Matos]

Importantly, the effect of HGF was additive to the prolonged treatment with VX-809 alone (from ~2.5 to ~3.4-fold, over DMSO) and, remarkably, it appears to protect VX-809-rescued Phe508del-CFTR from the destabilization caused by VX-770 co-treatment, allowing for C band levels ~3.7-fold over DMSO-treated cells (Figure 3.4B). No significant variations in B band levels were observed between treatments.

Next, we tested the double and triple 15-day treatments in the CFBE cell line co-expressing Phe508del-CFTR and the HS-YFP sensor. As before, fluorescence decay in these cells was measured after CFTR stimulation with 5 µM Fsk. Treatment with the VX-809/VX-770 combination produced a significant ~3.6-fold increase in iodide influx over DMSO treated cells (Figure 3.4C and D), although in absolute values this activity was roughly 2.5 times lower than that achieved by 48 hours of VX-809 treatment followed by acute 10 µM VX-770 potentiation (see Figure 3.2D). Consistent with its impact

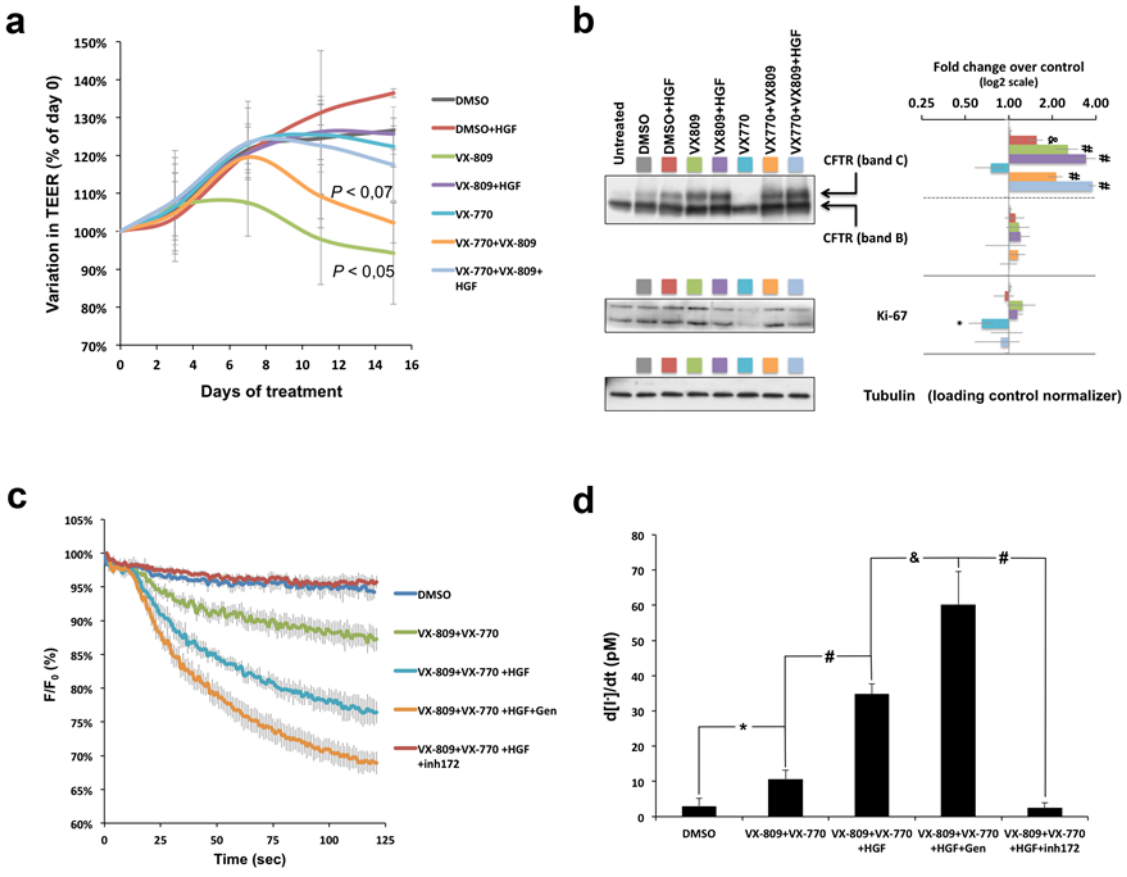

Figure 3.4 - Prolonged HGF treatment improves functional rescue of Phe508del-CFTR by the VX-809/VX-770 combination without stimulating proliferation of polarized CFBE cells.
A- Variation in transepithelial electrical resistance (TEER) of polarized CFBE-Phe508del cells treated for 15 days with DMSO, HGF (50 ng/ml), VX-809 (3 µM), VX-770 (0.5 µM) alone or in the indicated combinations. Conditions leading to significant or near-significant TEER variations are indicated. **B-** WB analysis of whole cell lysates from polarized CFBE-Phe508del cells treated as in (A). Shown are representative images of CFTR and Ki-67 immunoblots together with bar plots of band intensity quantification, normalized to DMSO (means ± SEM) from three independent assays. Tubulin was used as loading normalizer in band intensity quantification. **C-** Fluorescence decay curves of iodide influx assays in polarized CFBE-Phe508del/HS-YFP cells treated as in (A) with the indicated drug combinations, and stimulated with 5 µM Fsk alone or together with 20 µM of Gen in the presence or absence of 25 µM of inh172, as indicated. Fluorescence (F) was plotted over time as percentage of fluorescence at time 0 (F_0). Data are means ± SEM of 3 independent assays. **D-** Iodide influx rates calculated as in Figure 1B. Data are means ± SEM of 3 independent assays. *$p < 0.05$, &$p < 0.005$, and #$p < 0.001$. [WB performed jointly with Márcia Faria and images acquired jointly with Paulo Matos; included with permission]

on the apical retention of rescued CFTR, co-treatment with HGF more than tripled (~3.3-fold) the effect of the VX-drugs alone (Figure 3.4D), a result that was reverted by the presence of 25 µM inh172. Notably, this effect of HGF co-treatment was increased by ~1.7-fold when 20 µM Gen and 5 µM Fsk were added acutely (Figure 3.4C and D), consistent with further potentiation of apically rescued CFTR.

Remarkably, prolonged treatment with HGF, alone or in combination with the VX-drugs, did not increase the steady-state levels of Ki-67, which indicates no change in the proliferative behavior of these cells (Figure 3.4B). Of note, there was a small (1.5-fold) but significant decrease in the levels of Ki-67 upon prolonged exposure to VX-770 alone.

3.3.3. Co-treatment with HGF prevents depolarization of CFBE epithelium-like monolayers after prolonged exposure to VX-809

The decrease in TEER observed in polarized monolayers exposed to VX-809 for more than 3 to 7 days (see Figure 3.4A) led us to use WB to analyze the effects of the prolonged treatment on epithelial integrity and differentiation markers (Figure 3.5A). While E-cadherin levels showed no significant variations, a significant ~2-fold decrease in Zonula Occludens-1 (ZO-1) steady-state abundance was detected in both conditions where cells were treated with VX-809 (Figure 3.5A).

Once again, co-treatment with HGF seemed to revert this effect in both cases, bringing ZO-1 levels back to those observed in DMSO control cells. In fact, incubation with HGF alone produced a small (~1.5-fold) but significant increase in ZO-1 levels, which might be compensating for VX-809-induced ZO-1 downregulation. These effects were also observed through confocal microscopy after ZO-1 immunostaining (Figure 3.5B). Moreover, we could confirm that treatment with HGF alone stimulated ZO-1 localization to sub-apical, focal cell-cell contacts, consistent with an enhancement of tight-junction (TJ) maturation. This observation, together with the clear morphologic improvement in cell polarity (as seen through phalloidin staining of the actin cytoskeleton - Figure 3.5B) and the increase in relative TEER (Figure 3.4A), is indicative that the prolonged HGF treatment of bronchial epithelial cells has a pro-differentiation effect. In contrast, treatment with VX-809 alone led to a clear loss of ZO-1 at TJ sites that, based on the actin cytoskeleton morphology, was accompanied by a loss of cellular polarity (Figure 3.5B) consistent with the pronounced decrease in TEER observed after 15 days of treatment (Figure 3.4A). Combination of VX-809 and VX-770 had a similar effect on ZO-1 levels and distribution at day 15, albeit with a lower impact on cellular morphology and TEER levels relatively to VX-809 alone (Figures 3.4A and 3.5B, respectively), possibly related to the observed delay in TEER decline induced by VX-770 co-treatment (Figure 3.4A). Importantly, co-incubation with HGF clearly reverted VX-809-induced CFBE depolarization, particularly in the triple treatment combination, where the cellular phenotype closely resembled that of DMSO-treated cells (Figure 3.5B). We also analyzed the steady-state levels of cytokeratin 8 (CK8) and 18 (CK18) after the 15-day treatment. Interestingly, we found that whereas the prolonged treatment with VX-809 significantly decreased the steady-state abundance of CK18, either alone or in combination with VX-770 (Figure 3.5A), CK8 levels increased in response to both VX-809 and VX-770. Moreover, the combination of the two drugs had an additive effect, increasing CK8 levels ~2.3-fold over DMSO-treated cells (Figure

3.5A). Importantly, co-treatment with HGF returned CK8/CK18 expression near to control levels, even in the presence of the VX-809/VX-770 combination (Figure 3.5A, C and D).

3.3.4. HGF treatment prevents depolarization of colorectal epithelial cells after prolonged exposure to VX-809/VX-770 treatment

Several cases of off-target effects have been reported for VX-809/VX-770 combination treatment, most of which result in pulmonary and gastrointestinal complications [180]. Given the observed effects in the polarization of bronchial epithelial cells, we questioned the consequence of a prolonged treatment with the VX-drugs, alone and in combination with HGF, on the polarity and expression of epithelial differentiation markers in cells from gastrointestinal origin.

The human intestinal Caco-2 cell line has been extensively used over the last decades as a model of the intestinal epithelium, namely to study the regulation and function of wild-type CFTR, which they express endogenously and in high levels (see Figure 3.6A) [181–185]. Originally obtained from a human colon adenocarcinoma, these cells undergo a process of spontaneous differentiation in culture that leads to the formation of a cell monolayer, resembling a simple columnar epithelium (Figure 3.6A), which exhibits several morphological and functional characteristics of mature enterocytes [185,186]. Thus, as before, we polarized Caco-2 cells in filter inserts to a TEER of ~600 Ω and exposed them for 15 days to either DMSO (control), DMSO + 50 ng/ml HGF, 3 µM VX-809, 0.5 µM VX-770, 3 µM VX-809 + 0.5 µM VX-770, or 3 µM VX-809 + 0.5 µM VX-770 + 50 ng/ml HGF. As for CFBE cells, TEER was monitored at days 3, 7, 11, and 15, and the cell medium was replaced by fresh medium containing the same compound combinations.

A significant decreased in relative TEER (normalized to day 0) was observed from day 3 onwards in cells treated with VX-809, either alone or in combination with VX-770, when compared to DMSO-treated cells (Figure 3.6B). Notably, in both situations, co-treatment with HGF obviated the decrease in relative TEER (Figure 3.6B). Moreover, treatment with HGF alone seemed to promote Caco-2 differentiation, significantly increasing TEER values when compared to control cells. WB analysis, after prolonged treatment, showed that HGF alone promoted a ~2-fold increase in ZO-1 and E-cadherin levels, two markers of epithelial differentiation (Figure 3.6C). In contrast, prolonged exposure to VX-809, alone or in combination with VX-770, led to a nearly 2-fold decrease in the steady-state abundance of ZO-1, similar to the observed with CFBE cells. In both cases, co-incubation with HGF reverted ZO-1 decrease by the VX-drugs (Figure 3.6C). Consistently, immunostaining of

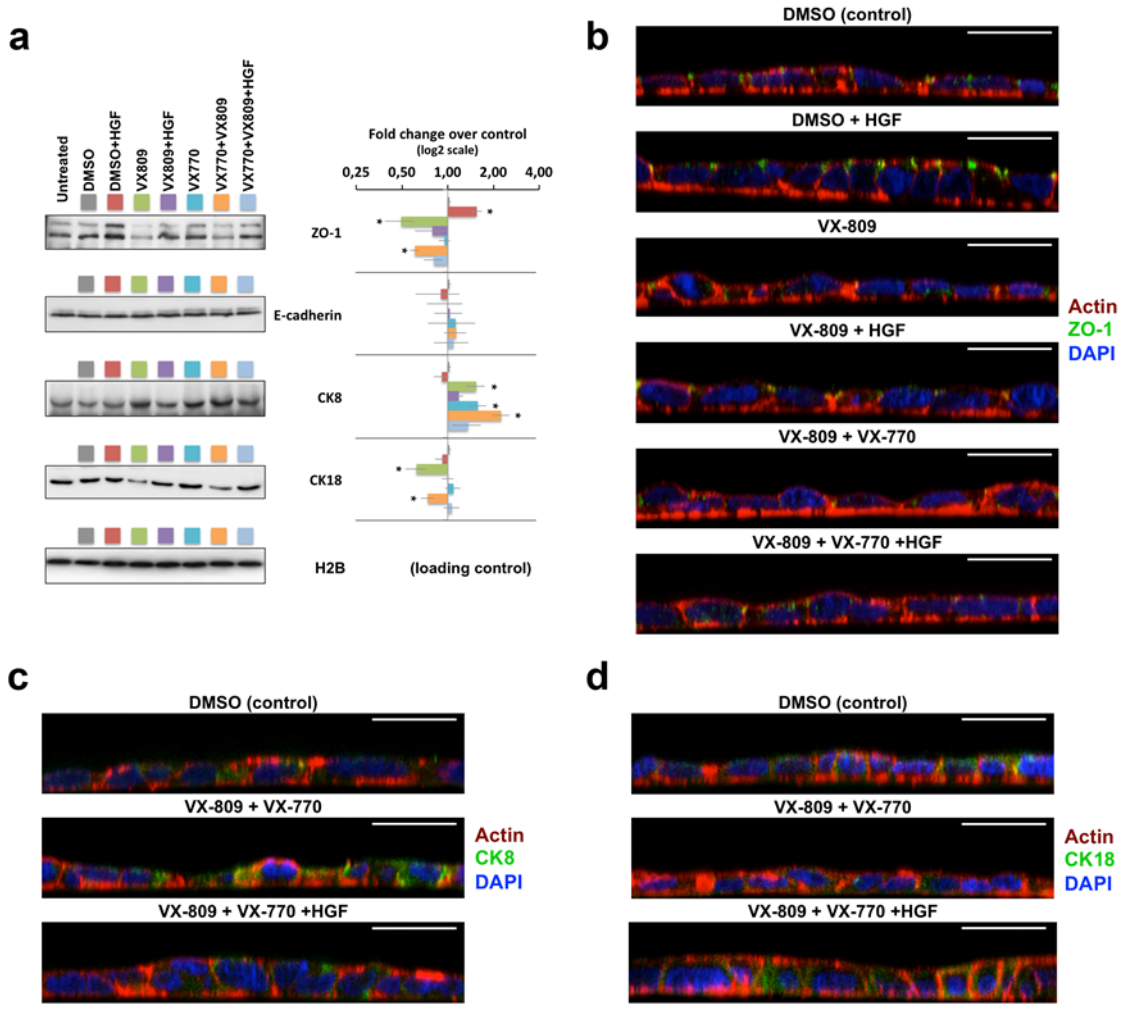

Figure 3.5 - HGF co-treatment prevents dedifferentiation of polarized CFBE cells after prolonged exposure to VX-809
Polarized CFBE-Phe508del cells were treated for 15 days with DMSO, HGF (50 ng/ml), VX-809 (3 µM), or VX-770 (0.5 µM), alone or in the indicated combinations. **A-** WB analysis of whole cell lysates. Shown are representative images of immunoblots for ZO-1, E-cadherin, CK8, and CK18 together with bar plots of band intensity quantification, normalized to DMSO (means ± SEM) from three independent assays. Histone H2B was used as loading normalizer in band intensity quantification. **B-D-** Immunofluorescence staining of polarized CFBE-Phe508del cells, treated as in (A), were stained with phalloidin-TRITC, DAPI, and either anti-ZO-1/Alexa 488 (**B**), anti-CK8/Alexa 488 (**C**), or anti-CK18/Alexa 488 (**D**), and analyzed by confocal microscopy. Shown are overlay images representative of the indicated treatment conditions. White horizontal bars represent 10 µm. *$p < 0.05$. [Images acquired jointly with Paulo Matos]

Caco-2 cells showed that prolonged exposure to VX-drugs results in a clear dedifferentiation of epithelial-like morphology, with abrogation of ZO-1 expression and localization, leading to an apparent loss of TJs integrity (Figure 3.6D). Moreover, in contrast to what was observed in CFBE cells, prolonged treatment of Caco-2 cells with either VX-809 or VX-770 alone, resulted in a clear (>1.6-fold) decrease of E-cadherin steady-state levels, producing in a nearly 3-fold decrease when both drugs were combined (Figure 3.6C). This effect on E-cadherin was also readily seen by confocal microscopy after immunostaining of Caco-2 cells (Figure 3.6E). Notably, co-treatment with HGF prevented E-cadherin downregulation by the VX-drug combination (Figure 3.6C), restoring TEER values (Figure 3.6B), E-cadherin localization to cell-cell contacts, and polarized epithelium morphology (Figure 3.6E). Interestingly, Caco-2 cells did not show any significant variation in CK8

expression in response to the different treatments (Figure 3.6C). In addition, while a small decrease in CK18 levels was observed upon prolonged exposure to VX-770 (not statistically significant), HGF treatment produced a significant ~1.6-fold increase in CK18 expression, which was sustained in the presence of both VX-drugs (Figure 3.6C). This effect was also clearly observed in immunostained cells (Figure 3.6F).

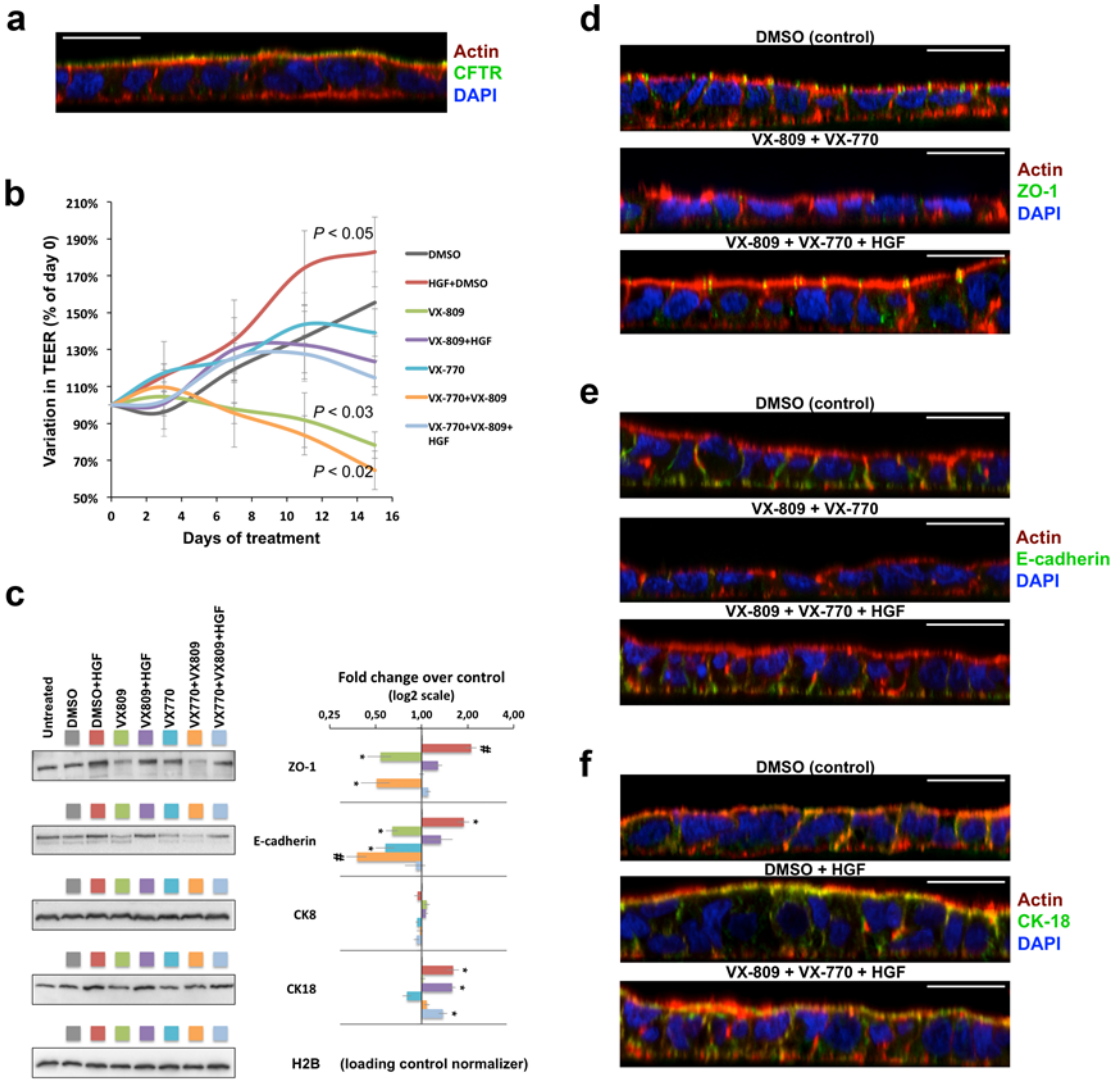

Figure 3.6 - HGF co-treatment prevents dedifferentiation of polarized Caco-2 cells after prolonged exposure to the VX-809/VX-770 drug combination

A- Caco-2 colorectal cells were polarized to a TEER above 600 Ω, stained with phalloidin-TRITC, DAPI, and anti-CFTR/Alexa 488, and analyzed by confocal microscopy. **B-** Variation in TEER of polarized Caco-2 colorectal cells treated for 15 days with DMSO, HGF (50 ng/ml), VX-809 (3 µM), or VX-770 (0.5 µM), alone or in the indicated combinations. Conditions leading to significant TEER variations are indicated. **C-** WB analysis of whole cell lysates from polarized Caco-2 cells treated as in (B). Shown are representative images of immunoblots for ZO-1, E-cadherin, CK8, and CK18 together with bar plots of band intensity quantification, normalized to DMSO (means ± SEM) from three independent assays. Histone H2B was used as loading normalizer in band intensity quantification. **D-F**- Immunofluorescence staining of polarized Caco-2 cells, treated as in (B), with phalloidin-TRITC, DAPI, and either anti-ZO-1/Alexa 488 (**D**), anti-E-cadherin/Alexa 488 (**E**), or anti-CK18/Alexa 488 (**F**) and analyzed by confocal microscopy. Shown are overlay images representative of the indicated treatment conditions. White horizontal bars represent 10 µm. *$p < 0.05$; #$p < 0.01$. [Images and WB performed by Andreia Gomes-Duarte and acquired jointly with Paulo Matos; included with permission]

3.3.5. HGF and the VX-809/VX-770 combination have opposite effects in Ki-67 expression in Caco-2 cells

Analysis of Ki-67 steady-state abundance in polarized Caco-2 cells revealed that whereas stand-alone exposure to HGF significantly increased the levels of this pro-proliferative marker (~1.6-fold), incubation with the VX-770 had the opposite effect, resulting in a ~1.8-fold decrease in Ki-67 expression (Figure 3.7). Significantly, the triple combination (VX-809/VX-770/HGF) generated Ki-67 levels close to those of DMSO-treated cells, consistent with a reversal of VX-770- induced Ki-67 downregulation by HGF co-treatment (Figure 3.7).

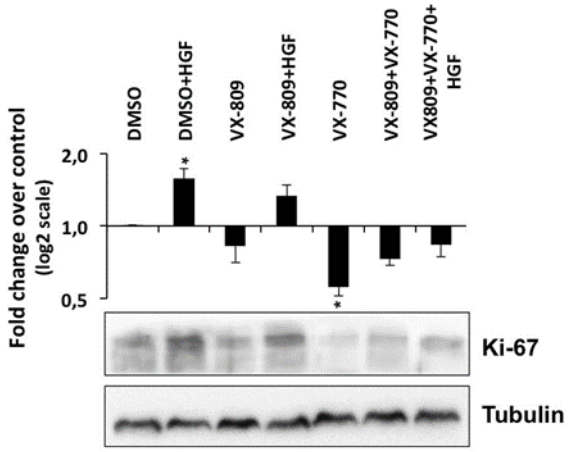

Figure 3.7 - Prolonged HGF and VX-770 treatments have opposite effects on Ki-67 levels in polarized Caco-2 cells
Polarized Caco-2 colorectal cells were treated for 15 days with DMSO, HGF (50 ng/ml), VX-809 (3 µM), or VX-770 (0.5 µM), alone or in the indicated combinations. Shown are representative WB images of whole cell lysates probed with anti-Ki-67 and anti-Tubulin antibodies. Bar plot shows quantification of Ki-67 band intensity, normalized to DMSO (means ± SEM) from three independent assays. Tubulin was used as loading normalizer in band intensity quantification. [WB performed by Andreia Gomes-Duarte and included with permission]

3.4. Discussion

In this study we investigated three major questions: (1) whether HGF treatment would enhance the functional correction of Phe508del-CFTR by the VX-809/VX-770 drug combination; (2) whether the effect would be sustained in polarized, epithelium-like bronchial cell monolayers; and (3) what would be the cellular and functional consequences of a phase II trial duration-consistent, 15-day long combined treatment with VX-809/VX-770 and HGF.

We found, similar to what we had previously shown for corrector C4 [160], that 24 hours of co-treatment with HGF increased by roughly 3-fold the functional correction of Phe508del-CFTR that can be achieved in CFBE cells by treatment for 48 hours with VX-809 followed by acute potentiation with VX-770. Significantly, this result was consistently observed in both polarized and non-polarized cells. Moreover, we found evidence that HGF treatment also significantly enhanced the apical accumulation of VX-809-rescued Phe508del-CFTR in polarized CFBE cells, not by varying the total abundance of the protein but by increasing the ratio of its apical/basolateral distribution, indicating an enhanced retention of the rescued channels at the cell's apical membrane. This is consistent with

our previous findings that HGF treatment stimulates the anchoring of apical CFTR to the actin cytoskeleton *via* stimulation of RAC1-mediated PIP2 production and the formation of a CFTR/NHERF1/EZR/F-actin macromolecular complex [160]. Importantly, we found that the effect of HGF treatment was still observable after prolonged, 15-day co-treatment with HGF, VX-809 and 0.5 µM VX-770. Notably, prolonged exposure to this low VX-770 concentration still decreased VX-809-mediated rescue of Phe508del-CFTR. This is consistent with previous findings that sustained exposure to VX-770, even at concentrations below 1 µM, can interfere with Phe508del-CFTR cell surface stability, promoting its PM removal, accelerating its internalization and markedly increasing its turnover rate [47,55]. Also of note, we show here that HGF can protect VX-809-rescued Phe508del-CFTR from VX-770 induced destabilization. This is in agreement with our previous findings that HGF treatment prevents the internalization of rescued Phe508del-CFTR by promoting its anchoring to the sub-apical cytoskeleton [37,40], and with our current observation that HFG exposure leads to the apical accumulation of VX809/VX770-rescued CFTR. Moreover, whereas the functional output of VX-809-rescued Phe508del-CFTR after prolonged treatment with 0.5 µM VX-770 was considerably lower than that achieved by acute potentiation with 10 µM of the drug, co-treatment with HGF more than compensated for this decrease, reaching levels of CFTR-mediated ion transport 30% higher than those of the acute treatment. In addition, this effect was nearly doubled by acute co-stimulation with genistein, which is consistent with previous reports that VX-809-rescued CFTR channels at the apical membrane are poorly potentiated by therapeutic range VX-770 concentrations [55], making them receptive to further potentiation [47,55]. Consistently, a recent study showed that potentiators, such as genistein and curcumin, additively enhanced forskolin-induced swelling of VX-809/VX-770-treated intestinal organoids derived from biopsies of Phe508del homozygous patients [89]. Together with our results, these data suggest that genistein and/or curcumin could be used in combination with HGF to synergistically increase CFTR-mediated chloride secretion in the treatment of CF.

The VX-809/VX-770 combination has now been used in patients since 2015, and several cases of off-target side-effects have been reported [180]. These adverse effects can manifest in up to 40% of treated patients, with the vast majority (~80%) being pulmonary but with some patients (~24%) also manifesting gastrointestinal symptoms, including diarrhea and nausea [62]. Our findings, suggest that these manifestations may, at least partially, be related to a previously unreported epithelial dedifferentiation effect resulting from prolonged exposure to VX-809. This is of particular interest since we show that HGF treatment was highly effective in preventing VX-809-induced dedifferentiation of bronchial and colorectal epithelium-like monolayers. In polarized bronchial epithelia cells we demonstrated that HGF restored ZO-1 levels, TJ localization and TEER values. It is interesting to note that VX-770 also had a partially protective effect on VX-809-induced dedifferentiation of CFBE cells, delaying TEER reduction by 3 days when compared to VX-809 stand-alone treatment. This protective effect of VX-770 may relate to its impact on Ki-67 levels. We observed that prolonged exposure to VX-770 alone nearly depleted Ki-67 levels in CFBE cells. Absence of Ki-67 is associated with resting cells that have entered a 'quiescent' state due to the absence of extrinsic pro-proliferative signals [187–189]. Our results indicate that prolonged exposure to low concentrations of VX-770 may somehow mimic this state, partially desensitizing bronchial epithelial cells from depolarization by VX-809.

HGF also prevented VX-809-induced dedifferentiation of colorectal Caco-2 polarized cells. For this cell type, however, although prolonged treatment with VX-770 also significantly decreased Ki-67 abundance, it was not sufficient to constrain the depolarizing effect of VX-809 when used in combination. In fact, the VX-drug combination produced the most pronounced TEER decrease in Caco-2 cells, which by the end of the treatment reached below 65% of the initial value (corresponding to TEER values under 400 Ω). This may relate to our observation that stand-alone treatment with either drug produced a significant decrease of E-cadherin steady-state levels, which was additive, reaching nearly 3-fold when both drugs were combined. Indeed, decreased expression of E-cadherin and ZO-1 adhesion molecules are well known markers of colorectal cell dedifferentiation and strongly correlate with epithelial-mesenchymal transition (EMT) in colorectal cancers [190–192]. Importantly, despite inducing a small but significant increase in Ki-67 levels when used alone, prolonged treatment with HGF had a marked pro-differentiation effect on polarized colorectal cell monolayers; it stimulated ZO-1 and E-cadherin expression, promoted their localization to cell-cell contacts, prevented their downregulation by VX-drugs, and restored TEER values and epithelial morphology. Moreover, the opposite effects of HGF and VX-drugs on Ki-67 expression apparently compensate for each other, producing a net result of Ki-67 levels close to those of control cells.

We also monitored the levels of Cytokeratins 8 and 18 (CK8/18). These intermediate filament components are typically co-expressed as the primary keratin pair in simple epithelial cells, but tissue-specific variations in their expression are often associated with cancer-related cellular dedifferentiation and EMT [193,194]. In lung cancers, for instance, increased CK8 expression is correlated with increased invasiveness of tumor cells *in vitro* and *in vivo* [193]. In contrast, the role of CK18 upregulation is less clear having been described associated with lung cancer progression [195] as well as with better differentiation and decreased tumor malignancy [196]. Here we found that the dedifferentiation of CFBE cells induced by prolonged exposure to VX-809 associated with a significant increase in CK8 levels and a decrease in CK18 expression. Interestingly, whereas prolonged exposure to VX-770 alone also increased CK8 abundance, being additive with VX-809 in the combination treatment, it did not, however, decrease the levels of CK18. Rather, co-treatment with VX-770 reduced the downregulation of CK18 by VX-809, which considering that the co-treatment delayed TEER decrease in CFBE cells, is consistent with the reported effect of CK18 in preventing dedifferentiation of lung epithelial cells [196]. Again, co-treatment with HGF attenuated the variations in CK8/18 levels induced by the VX-drugs, consistent with its effect in restoring epithelial morphology. Notably, in colorectal Caco-2 cells, neither VX-809 nor VX-770, alone or in combination, induced significant variations in CK8/18 levels. Loss of CK8 expression has been associated with hyper-proliferation of colorectal cells [197,198], but despite elevating Ki-67 levels, prolonged HGF treatment produced no significant change in CK8 levels in polarized Caco-2 cells. However, HGF significantly up-regulated CK18 levels. Upregulation of CK18 levels has been associated with promotion of enterocytic differentiation of Caco-2 cells *via* Notch signaling [198], and this is consistent with previous reports showing that exposure to HGF accelerates Caco-2 cell differentiation by stimulating the metabolic and structural events accompanying this process [199].

In summary, we found that, as expected, HGF treatment also significantly enhanced the functional rescue of Phe508del-CFTR by acute treatment with the VX-809/VX-770 drug combination. Moreover, we further demonstrated this enhancement was sustained in polarized bronchial epithelial monolayers after prolonged, 15-day HGF co-treatment with VX-809 and low, therapeutic-compatible VX-770 doses, reaching functional rescue levels higher than those achieved by acute potentiation with high VX-770 concentrations. Importantly, we found that HGF treatment also prevented VX-770-mediated destabilization of recued Phe508de-CFTR and enabled further potentiation of the rescued channels by genistein, indicating that HGF co-treatment would also favor previously suggested combination therapies using multiple correctors [89]. Most striking, we observed that rather than promoting cell scattering and proliferation, a well-known effect of HGF on polarized MDCK cells [200], prolonged HGF treatment of polarized airway cells actually prevented the previously unrecognized epithelial dedifferentiation effects of prolonged exposure to VX-809. While the physiologic relevance of these observations cannot be fully ascertained through the use of in vitro models, they strongly suggest that there may be a potential gain in addressing *in vivo* and *ex vivo* (in patient-derived tissues) the effects of adding HGF to current combinational drug therapies. Moreover, while polarized CFBE and Caco-2 monolayers do not fully recapitulate the properties of differentiated epithelia in vivo, these models have been extensively used to study the mechanisms of CF disease and, in the case of CFBE cells, for the development and characterization of several CFTR modulator drugs [47,48,54,55,201], where they have been shown to respond similarly to primary airway cells [40,48,201]. Thus, our findings of unreported potentially dedifferentiative effects of prolonged exposure to VX-809 in these cells, highlight the importance of using more extended treatment periods while assessing the cellular effects of new CF-modulator drugs in pre-clinical studies. It should be metioned that a next-generation CFTR corrector, VX-661 (Tezacaftor), in combination with VX-770, has proven to be equally effective and better tolerated than VX-809 in clinical trials [64,66,202], and recently received FDA approval for the treatment of patients, aged 12 years and older, homozygous for the Phe508del mutation or having at least one CFTR mutation that is responsive to the drug combination, based on in vitro data and/or clinical evidence [203]. However, it should be noted that the destabilizing effect of long exposure to VX-770 therapeutic-range concentrations on VX-661-rescued Phe508del-CFTR channels was even more pronounced than that observed for VX-809 [54]. This suggests that, if supported by further in vivo studies, the potentially protective effect of HGF co-treatment against VX-770-induced destabilization of apically rescued Phe508del-CFTR could also be beneficial for VX-661-treated patients. More so, in the case of patients with severe lung disease (predicted FEV_1 < 40%), that were not included in the initial VX-661/VX-770 trials [64,66,202] but for which recent clinical data, following treatment with VX-809/VX-770, revealed a considerably higher frequency and severity of therapy-related respiratory adverse events (particularly in the first weeks of treatment) and lessened clinical benefit [60,204,205]. Supportive of a potential application of HGF in the CF setting, several studies in animal models have provided strong evidence that HGF administration potently mitigates the effects of acute and chronic lung injuries caused by oxidative stress and inflammation [147]. Encouragingly, some of these studies have also shown that HGF had a protective activity when given either simultaneously with or after prolonged lung-damaging stimuli, suggesting that HGF pro-

regenerative action is effective during both the initiation and the progressive phases of lung disease [206].

Taken together, our findings emphasise the critical importance of assessing the cellular effects of prolonged exposure to investigational CF drugs in pre-clinical studies and provide compelling evidence for the potential benefit of including HGF in CF combination therapies, alerting the scientific community for the need and relevance of further *in vivo* studies with this physiological factor in the CF context. Supporting the plausibility of such studies, the intravenous/systemic administration of recombinant HGF protein has been well tolerated in phase I/II clinical trials for liver regeneration [207] and it is currently under trial for its regenerative effects in several other conditions [208,209].

3.5. Materials and Methods

3.5.1. Cell culture, polarization and treatment

CFBE41o- cells stably expressing Phe508del-CFTR (Phe508del-CFBE cells) (a kind gift from JP Clancy, University of Alabama USA) were maintained in minimal essential medium (MEM) supplemented with L-glutamine, Earle's salts, 10% (v/v) fetal bovine serum (FBS) and penicillin/streptomycin, whereas Caco-2 cells were maintained in RPMI supplemented with 10% (v/v) FBS (all reagents were from Life Technologies Invitrogen Corporation). All cell lines were cultured at 37°C under 5% CO_2 and regularly checked for the absence of mycoplasm infection. Phe508del-CFBE cells stably co-expressing the YFP-H148Q/I152L halide sensor (Phe508del/HS-YFP CFBE cells) were generated by transfection with LipofectAMINE 2000 followed by 3-week selection with 0.4 mg/ml hygromycin B (both from Thermo Scientific). Fluorescent cells were then sorted (FACSAriaIII, BD Biosciences) and expanded maintaining selective pressure with 0.4 mg/ml hygromycin B.

Cell monolayers were polarized in transwell, collagen IV coated, porous (0.4 µm) PET filter inserts (Ø 6.4mm, from Falcon – Thermo Fisher Scientific), in medium supplemented with 2.5% FBS, until they reached a TEER above 600 Ω, as measured with a Chopstick Electrode (STX2 from WPI®). Cells were then treated for the indicated periods, with DMSO (Sigma-Aldrich) or the described concentrations of recombinant human HGF (Santa Cruz Biotechnology), corr4a (CF Foundation modulator library), VX-809, VX-770 (both Selleck Chemicals), CFTRinh-172 (CFFT USA), forskolin or genistein (both from Sigma-Aldrich). All stock solutions were made 10^3 times concentrated, dissolved in DMSO.

3.5.2. Fluorescent Iodide Influx Assay/Halide-sensitive YFP-based functional assay

CFTR activity was determined using Phe508del/HS-YFP CFBE cells seeded in 8-well chamber slides or 96-well microplates, or yet polarized in transwell filter inserts, as described above. Cells were treated with the indicated compound concentrations for the described time periods. Cells were washed with PBS and incubated for 30 min in PBS containing compounds for CFTR stimulation/inhibition (forskolin, VX-770, genistein and CFTR-inh172) at the indicated concentrations. Non-polarized cells were then transferred either to a microplate reader (Tecan® Infinite M200)

(excitation: 505 nm and emission: 535 nm) or to a Leica TCS-SPE confocal microscope for time-lapse analysis. Each well was assayed individually for iodide influx by recording fluorescence continuously (500 ms/point) for 10 s (baseline) and then for 110 s after the rapid (<1 s) addition of isomolar PBS in which 137 mM Cl^- was replaced by I^- (PBSI, final NaI concentration in the well: 100 mM). Assays were performed at room temperature. After background subtraction, cell fluorescence recordings were normalized for the initial average value measured before addition of I^-.

For polarized cells in transwell filter inserts, we developed an in-house setup to assess HS-YFP fluorescence decay by confocal microscopy. Briefly, a Ø 16 mm x 17 mm-high x 1mm-thick polypropylene ring was sealed on top of a glass slide to form a PBS-containing chamber (Figure 3.2B), which can be positioned on the confocal microscope stage. This setup allows the transwell inserts, containing Phe508del/HS-YFP CFBE polarized cells, to be placed inside the slide chamber within the focal length of a 10x objective. The apical side medium is replaced by 100 µl PBS, and the insert secured to the chamber through a Ø 0.5 mm steel tubing clamp that also allows the addition of I^- and CFTR stimulators to the apical side of the polarized cell layer (Figure 3.2B). XZ fluorescence images were collected continuously with a 3 Airy pinhole at 500 ms intervals, first for 10 s (baseline), and then for 110 s after the rapid (≤1 s) apical pumping of 350 µl of PBSI, containing 5 µM Fsk with or without 10 µM VX-770, and with 25 µM of inh172 for some experimental conditions. Quantification of fluorescence decay was performed on at least 20 individual cells per filter, using ImageJ (NIH) as previously described [37].

3.5.3. Immunoblotting, immunofluorescence and confocal microscopy

Samples were analyzed by WB as previously described [37,40]. Additional antibodies used for WB were: mouse anti-CFTR clone 596 (obtained through the UNC CFTR antibody distribution program sponsored by CFFT), mouse anti-α-Tubulin clone B-5-1-2 (Sigma-Aldrich), mouse-anti-E-cadherin (Transduction Laboratories), mouse-anti-CK18 (Millipore), rabbit-anti-ZO-1, rabbit-anti-CK8, rabbit-anti-Ki-67 and rabbit-anti-H2B (all from Santa Cruz Biotechnology). Primary antibodies were detected using secondary, peroxidase-conjugated antibodies (BioRad) followed by ECL. For densitometric analysis of WB bands, x-rays films were digitalized and images analyzed with ImageJ software (NIH).
For immunofluorescence analysis, cells grown on filters were fixed with 4% formaldehyde, washed with PBS (Sigma-Aldrich), permeabilized with 0.2% Triton X-100 (Sigma-Aldrich), and incubated for 1 hour with the indicated primary antibodies. Cells were then thoroughly washed with PBS and incubated for 30 min with AlexaFluor488-conjugated secondary antibody (Life Technologies Invitrogen Corporation). Actin was stained using phalloidin-TRITC (Jackson ImmunoResearch Laboratories), followed by thorough washing in PBS and DAPI staining of nuclei. Filters were mounted on microscope slides with Vectashield (Vector Laboratories), covered with coverslips and sealed. Images were recorded on a Leica TCS-SPE confocal microscope and assembled into figures with Adobe Photoshop software.

3.5.4. Statistical Analysis

Quantitative results are shown as means ± SEM of at least three independent observations. To compare sets of data, we used either ANOVA or two tailed Student's *t* tests, and considered significant differences when *p* values < 0.05. In the halide-sensitive YFP-based functional assay, the signal decay caused by YFP fluorescence quenching was fitted to an exponential decay function to derive the maximal slope that corresponds to initial influx of I^- into the cells [37,159]. Maximal slopes were converted into rates of variation of the intracellular I^- concentration (in pM/s) using the equation $d[I^-]/dt = K_d\,[d(F/F_0)/dt]$, where K*d* is the affinity constant of YFP for I^- [37,159], and F/F_0 is the ratio of the cell fluorescence at a given time versus the initial fluorescence.

Chapter 4

Plasma membrane-specific interactome analysis reveals Calpain 1 as a druggable modulator of rescued Phe508del-CFTR cell surface stability

Ana Margarida Matos, Francisco Pinto, Patrícia Barros, Margarida D. Amaral, Rainer Pepperkok and Paulo Matos

Data included in this chapter is under manuscript preparation.

4.1. Abstract

Cystic Fibrosis (CF) is a devastating genetic disease that is caused by mutations in CFTR (CF transmembrane conductance regulator), a chloride (Cl^-) channel normally expressed at the surface of epithelial cells. The most frequent mutation, the deletion of a phenylalanine residue at position 508 (Phe508del), causes the protein to misfold and be prematurely degraded. Low temperature or pharmacological "correctors" can partly rescue Phe508del-CFTR processing defect and enhance the channel traffic to the cell surface. Nevertheless, the rescued channels show an accelerated endocytosis rate and are quickly removed from the PM by the peripheral protein quality control (PPQC) mechanism. We previously showed that rescued Phe508del-CFTR can be retained at the cell surface by stimulating signaling pathways that tether both actin and CFTR-Na+/H+-exchange regulatory factor isoform-1 (NHERF1) complexes, anchoring the mutant channel to the actin cytoskeleton and preventing its endocytosis. Thus, protein interactions at the cell apical membrane are thought to be major determinants of CFTR retention and stability. At this moment, although it has been recognized that the different Phe508del and wt-CFTR protein interactions may contribute to the defects observed in the mutated channels, there are no studies identifying the specific PM CFTR interactome. Based on this knowledge, here we used a proteomic approach to isolate the core components of wt and low temperature/VX-809 rescued Phe508del-CFTR cell surface macromolecular complexes. This allow us to identify exclusive PM interactions between rescued Phe508del-CFTR, NHERF1 and ezrin (EZR). Furthermore, we identified CAPN1 as a key contributor for the decreased Phe508del-CFTR actin anchoring and PM stability. In that sense, our results propose that modulation of CAPN1 PM activity can be a new field in CF therapeutic research, since CAPN1 downregulation and chemical inhibition dramatically improved the functional rescue of Phe508del-CFTR in bronchial epithelial cells.

4.2. Introduction

The cystic fibrosis transmembrane conductance regulator (CFTR) is a multi-spanning cAMP-regulated chloride channel primarily localized to the apical membrane of polarized epithelial cells [3]. Mutations in the CFTR gene cause a complex inherited disorder, called Cystic fibrosis (CF) [3,210]. The most common CFTR mutation is the deletion of phenylalanine 508 (Phe508del), with approximately 85% of all CF patients having at least 1 copy of the Phe508del mutant [15,21]. This mutation is mainly characterized by protein misfolding and premature degradation by the endoplasmic reticulum (ER) quality control (ERQC), preventing the mutant protein from trafficking to the cell surface [7,25,211]. Although Phe508del ER retention is not complete, the very small proportion of channels that reach the cell surface possess only partial activity [211–213] and show a severely decreased PM half-life, due to accelerated endocytosis and lysosomal degradation [131,175].

At the moment there are several investigational drugs that intend to target the molecular defects in Phe508del [140,214,215], the most well-known and commercial approved being a combination of "corrector" VX-809 and "potentiator" VX770 (Orkambi® [58]). VX-809 is an extensively characterized

pharmacological chaperone that promotes folding of Phe508del-CFTR during its biogenesis and processing in the ER [33,48–50], while VX-770 increases the time that activated rescued CFTR channels remain open at the cell surface [35]. Though beneficial, results from clinical trials of the folding corrector/gating potentiator combination therapies available for the Phe508del patients have shown only modest efficacy in restoring Phe508del-CFTR function [34,52,53,64,66,216]. Given the complexity of Phe508del-CFTR protein defects, part of the incomplete effectiveness of the existing combination therapies may derive from an inability to retain sufficient CFTR levels at the apical surface of epithelial cells. Indeed, we and others have showed that the PM stability of chemical chaperone-rescued Phe508del-CFTR is still dramatically inferior to that of wt-CFTR, due to its targeting by the peripheral protein quality control (PPQC) and its deficient anchoring to the actin cytoskeleton [37,40,131]. Notwithstanding, there are no current offered therapies that target the Phe508del-CFTR PM decreased stability.

Previously we demonstrated that the anchoring of rescued channels to the actin cytoskeleton can be improved by promoting the PDZ-mediated interaction of Phe508del-CFTR with the Na^+/H^+ exchange regulatory factor-1 (NHERF1) and the actin-binding adaptor protein ezrin [37,40]. The mechanism behind this PM stabilization lies on a conformational change in NHERF1, triggered by ezrin activation through RAC1 signaling, which is then able to bind and stabilize misfolded CFTR at the PM [37]. This strongly indicated that the type of protein interactions that wt- and rescued Phe508del-CFTR establish at the cell surface can be a major determinant of CFTR stabilization and retention at the cell's PM.

Over the last years a growing number of proteins have been reported to interact with PM CFTR, possibly participating in the assembly of large macromolecular complexes [99,101]. Most interactions occur through the terminal N-terminus, R-domain or C-terminal tail of CFTR, either directly or mediated through various PDZ domain-containing proteins [8,98,101]. These dynamic interactions impact on channel function, as well as on its processing and localization within cells [99,101]. Furthermore it has been established that mutated and non-mutated CFTR proteins show considerable differences in their whole cell interactome, and that this differential protein interactions may contribute to the defects observed in Phe508del-CFTR processing and function [107]. Hence, although several CFTR interactor partners are known [99,107,217], there is no study describing specifically what is CFTR's particular interactome at the PM, what differs between wt- and pharmacologically rescued Phe508del-CFTR, and how this differences could contribute to the defective function and stability of the rescued channels.

Here we propose to clarify these questions, identifying the core components of the CFTR PM molecular complexes in airway cells expressing wt- and Phe508del-CFTR. For this we developed an immunoprecipitation method that selectively captures the CFTR-containing macromolecular complexes at the PM. Our data revealed significant differences between the interactors of wt and pharmacological rescued Phe508del-CFTR at the PM and allowed us to identified CAPN1 protease as a key player in the Phe508del-CFTR reduced actin anchoring and PM stability, thus contributing for the decreased cell surface retention of the rescued mutated channel. Importantly, downregulation of CAPN1 activity dramatically improved the functional rescue of Phe508del-CFTR by VX-809 in bronchial epithelial cells.

4.3. Results

4.3.1. CFTR assembles different membrane protein-protein interactions between wt-CFTR and corrector rescued Phe508del-CFTR

CFTR is primarily localized to the apical membrane of epithelial cells, where it is known to interact with several proteins, potentially participating in a vast network of macromolecular complexes [99,101]. Although several CFTR interactor partners are known [99,107,217], there is no study describing the specific CFTR interactome at the PM. Based on previous findings [37,40], we hypothesized that CFTR protein interactions at the PM may be a major determinant for its stabilization and retention. Accordingly, we asked if wt-CFTR and rescued Phe508del-CFTR have different membrane protein interactors, and if these differentially associated proteins could be contributing to the deficient cell surface stability of rescued Phe508del-CFTR. To answer this question we develop an

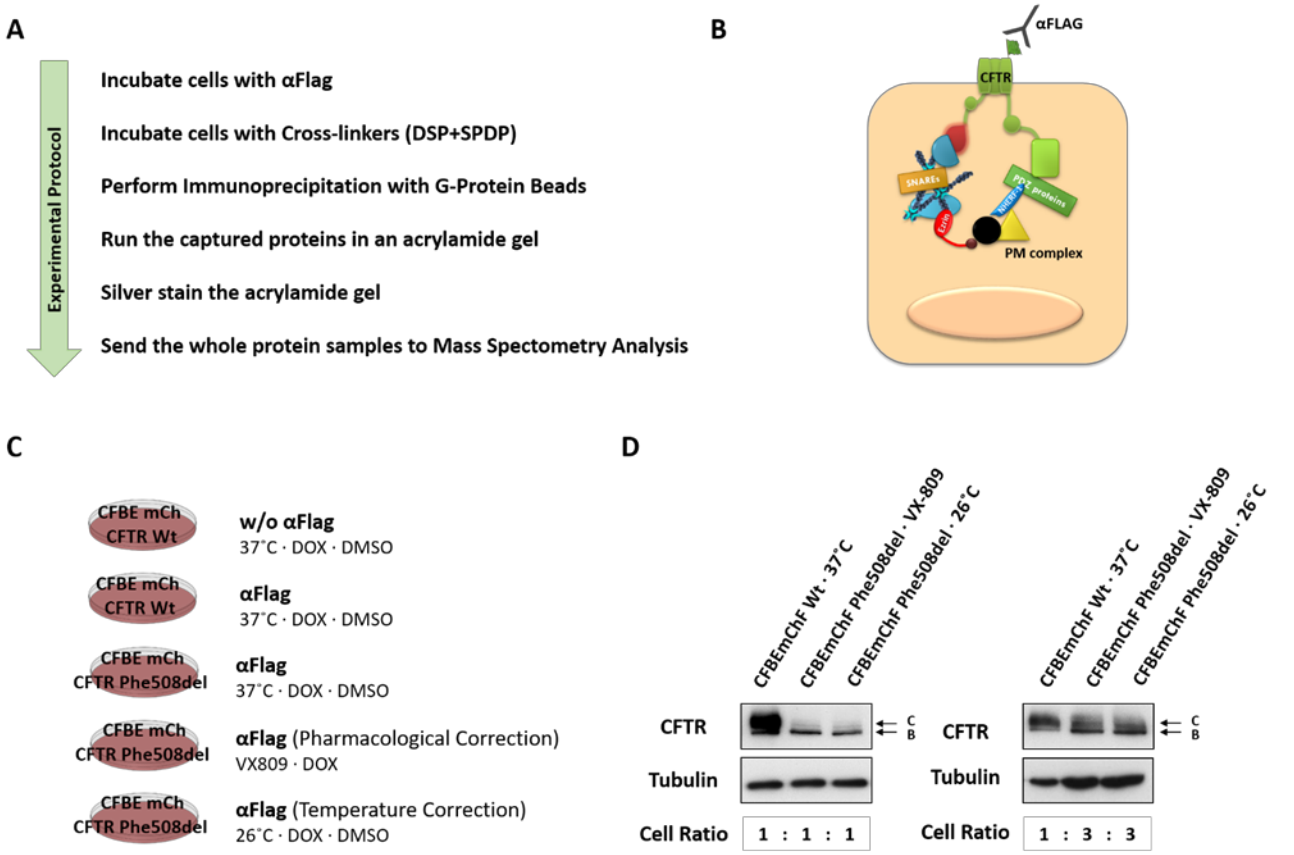

Figure 4.1 - Precipitation of CFTR membrane association complex Assay
A- Summary of the protocol used for the precipitation of CFTR membrane association complex. CFTR containing complexes at the PM were selectively immunolabeled on ice using an antibody specifically recognizing the extracellular Flag-tag. Following crosslink and lysis, these complexes were immunoprecipitated according to the indicated steps. **B-** Schematic representation of the immunoprecipitated crosslinked CFTR membrane association complex. **C-** Schematic representation of the used experimental conditions. CFBEmChF-CFTR-Wt cells were incubated at 37˚C while CFBEmChF-CFTR-Phe508del cells were incubated in three different conditions: at 37˚C; at 26˚C for lower temperature CFTR correction; and with VX-809 for pharmacological correction. We included a CFBEmChF-CFTR-Wt condition for a no Flag-antibody control. CFTR expression in all cells was induced by incubation with 1 µg/mL Dox for 48 hours. **D-** Western Blot of CFBEmChF-CFTR-Wt cells and CFBEmChF-CFTR-Phe508del, cultured in the same conditions, except for the cell quantity, which mas modified by using three times more CFBEmChF-CFTR-Phe508del on the two right panels. Arrows indicate immature (band B) and fully glycosylated (band C) CFTR. [Immunoprecipitation performed jointly with Patrícia Barros]

immunoprecipitation (IP) protocol that allows us to biochemically capture PM-selective interactomes of wt-CFTR and rescued Phe508del-CFTR. Briefly, using a cell line model (CFBEmChF [168]) stably expressing a CFTR protein that has a Flag epitope tag inserted at the 4th extracellular loop, we were able to exclusively label CFTR proteins at the PM by incubating the cells at 4°C with the M2 anti-Flag antibody (Merck), without permeabilizing them. We then used DSP (short spacer, Thermo Scientific) and SPDP (long spacer, Thermo Scientific) crosslinkers to reversibly bind, at 4°C, both the antibody (extracellularly), and the intracellular proteins associated with CFTR at the PM (see Figure 4.1A and 4.1B). The same procedure was applied in parallel to CFBEmChF cells expressing either Flag-tagged wt-CFTR or Phe508del-CFTR, rescued either by low temperature (26˚C) or by VX-809 treatment (see Figure 4.1C and Methods section for further details).

As part of the optimization process, we scaled up the amount of cells in the Phe508del-CFTR experiments so that the total amount of rescued CFTR (band C) immunoprecipitated was roughly equivalent to that of wt-CFTR (Figure 4.1D). To control the experiment for background IP contaminants we used, for wt-CFTR, cell extracts incubated with G-protein agarose beads but without the anti-Flag antibody. For Phe508del-CFTR IPs, lysates from cells incubated at 37°C (that have none to residual levels of band C at the PM) were considered the most reliable control for proteins co-IPed with artificially rescued Phe508del-CFTR (Figure 4.1C). The recovered proteins were first analyzed by SDS-PAGE followed by MS-compatible [218] silver staining (Figure 4.2).

Noticeably, a particular band profile was observed for each condition, suggestive of different co-precipitate compositions (Figure 4.2). These profiles were reproducible between experimental replicates, and therefore, the whole samples of three individual assays were sent to mass spectrometry analysis.

4.3.2. Bioinformatic analysis of MS data highlighted a candidate interactor potentially involved in the PM destabilization of rescued Phe508del-CFTR

Qualitative nanoLC MS/MS analysis of our samples generated a set of data in which each MS spectra protein hit was characterized by a protein confidence score (PCS) given by the SCIEX proprietary ProteinPilot™ Software. For PCS higher that 1.3, the confidence in the identification of that particular peptide is equal or higher than 95%. Given that all the experiments were performed in triplicate, we created an algorithm to generate a combined confidence score (CCS), producing five additional integrated confidence levels for the proteins detected among the different replicates: level 5 proteins are detected with PCS ≥ 1.3 in more than one replicate and not in the controls; level 4 proteins are detected in one replicate with a PCS ≥ 1.3 and not in the controls; level 3 proteins are detected in more replicates than in controls, and with an average PCS higher than their respective controls; level 2 proteins are detected in one replicate with a PCS ≤ 1.3, and not in the controls; and level 1 are proteins detected in the same number of replicates and controls, with an average PCS higher than the corresponding controls.

Altogether, we found 519 wt-CFTR PM putative interactors and 691 and 664 PM Phe508del-CFTR putative protein interactors, respectively rescued by pharmacological and low temperature (Figure 4.2B). Notably, most proteins from both Phe508del-rescued conditions overlap, sharing a total of 557 protein interactors (Figure 4.2B). Interestingly, ~40% (356 proteins, see Figure 4.2C) of

the identified proteins are common between all datasets, possibly representing the core PM CFTR interactome. For downstream analyses, a high confidence level was considered for proteins with a CCS of 4 or 5, and a medium confidence level was considered to include proteins with a CCS greater than 1. This approach restricted the list of putative interactors interfering with CFTR stability to 61 high confidence proteins in wt-CFTR, whereas the number of high confidence proteins in complex with rescued Phe508del-CFTR was considerably larger, comprising 240 in pharmacological rescued and 257 in low temperature rescued Phe508del-CFTR (Figure 4.2D). By crossing our results with the Pankow et al. [107] whole CFTR interactome dataset we observe that 10 (~16%) of our detected wt-CFTR proteins and 45 (~27%) of the rescued Phe508del-CFTR associated proteins were also identified by Pankow and colleagues (Figure 4.2E).

Because our previous data [37] suggested to look for proteins that differentially interacted with NHERF1-bound wt- and rescued Phe508del-CFTR at the PM, we extracted known physical protein interactions from curated human interactome databases (see Methods) to build an integrated network of CFTR interactors. In addition, since an overlap of over 80% was observed for both low temperature and VX-809-rescued Phe508del-CFTR PM interactors and both treatments produce rescued proteins that have an equally decreased half-life at the PM [36], we postulated that it would be highly likely that whatever molecules are interfering with the protein's surface stability these would be present at the PM in complex with CFTR rescued by either approach. Thus, when building the protein network for rescued Phe508del-CFTR, we took this hypothesis in consideration and intersected the groups of high-confidence proteins in both datasets, excluding those that also co-precipitated with wt-CFTR. Thus, from the 156 putative interactors interfering with CFTR stability (Figure 4.2C and D), 140 formed a connected network with 539 interactions, which besides CFTR also included ezrin (EZR) and NHERF1 (Supplementary Figure S4.1). This means that available interatomic data supports the close relationship between most of the proteins here detected to be specifically interacting with CFTR at the PM, both upon VX-809 and low temperature treatment. Knowing that the CFTR/NHERF1/EZR complex is essential for CFTR PM stabilization [37,40], we further restricted this network to proteins annotated as direct interactors of either CFTR, EZR or NHERF1, thus, generating a subnetwork of 22 proteins (Figure 4.3). This group of proteins was selected as the core of putative candidates involved in destabilizing rescued Phe508del-CFTR-containig complexes at the PM.

Gene ontology-based functional annotation analysis of these 22 hit proteins using DAVID (Database for Annotation, Visualization and Integrated Discovery at "https://david.ncifcrf.gov/") revealed that, as expected, all 22 proteins are known to participate in macromolecular protein complexes. Interestingly, 52% of these proteins are annotated as being localized at the membrane and 64% at the cytosol (Supplementary Table S4.1). Both subcellular localizations are expected for such a large and dynamic protein complex, as both the amino (N) and carboxyl (C) terminal tails of CFTR are inside the cytoplasm and mediate its interaction with large clusters of PDZ adaptor and structurally/functionally related proteins [99,101].

To infer the potential relevance of each of these 22 proteins to the assembling of the CFTR-EZR-NHERF1-containing PM complexes, we devised a scoring formula that measures the contribution of each node to the establishment of molecular bridges between these three proteins. Bridges involving more proteins are given a lower weight in the final score (see Methods). This analysis,

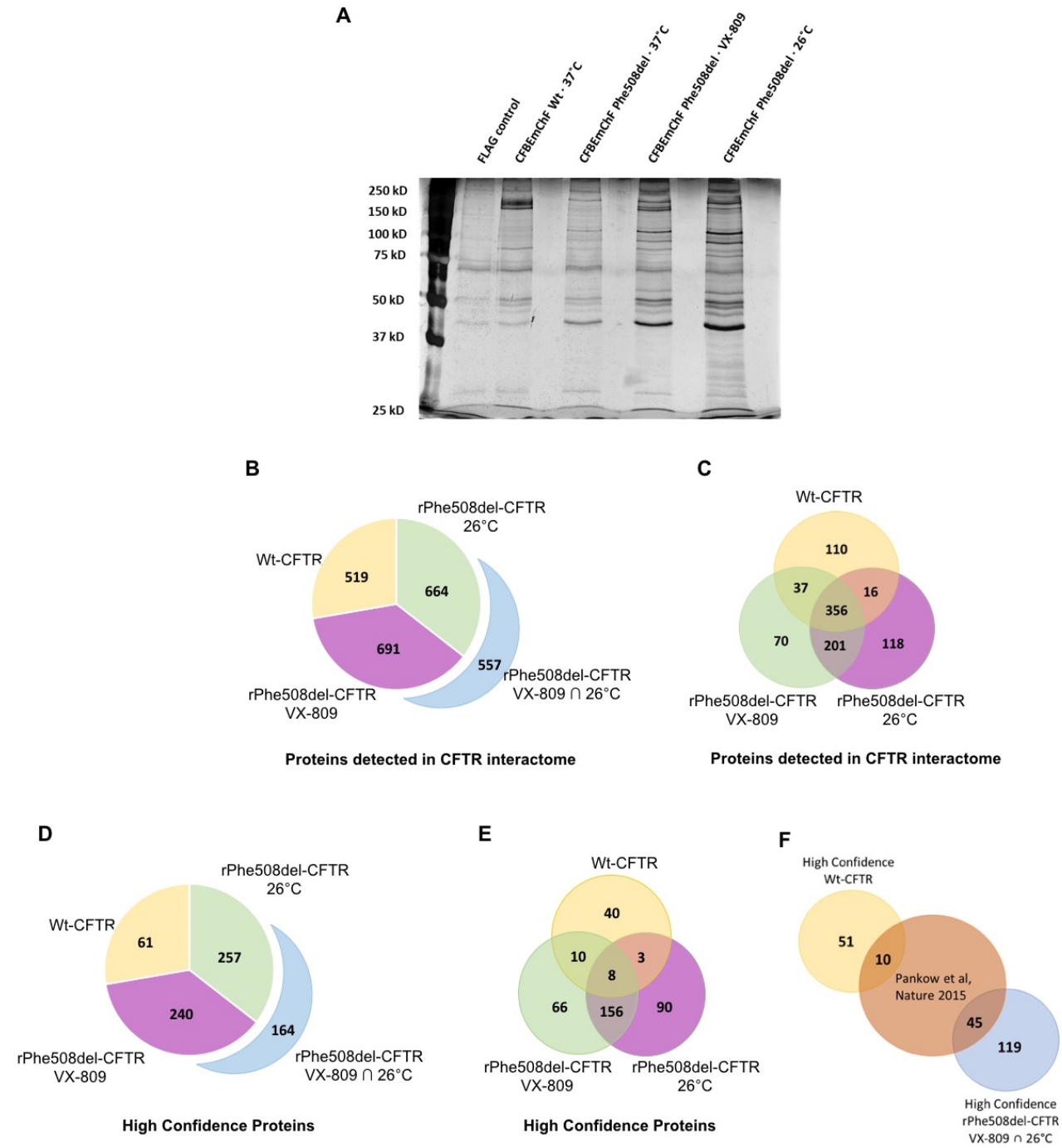

Figure 4.2 – Proteins detected in CFTR Interactome

A- Representative band profile of the PM CFTR co-precipitates. PM-CFTR co-immunoprecipitates from each experimental condition were de-crosslinked with 100 mM DTT, separated on a 9% (w/v) SDS-PAGE gel, and silver stained. Note that, while there are a few common bands, particular band patterns are observable for each experimental condition. **B-** Graph representing the number of CFTR interactors detected by Qualitative nanoLC MS/MS analysis in Wt-CFTR (Yellow) and Phe508del-CFTR, rescued either by pharmacological rescued with VX-809 (Green), or by low temperature at 26° C (Purple). In blue is the number of proteins in common between the rescued conditions. **C-** Venn diagram of the CFTR interactors represented in B. **D-** Graph representing the number of CFTR interactors detected with a high confidence score (CCS of 4 or 5) in Wt-CFTR and Phe508del-CFTR, rescued either by pharmacological rescued with VX-809, or by low temperature at 26° C, and their common proteins. **E-** Venn diagram of proteins detected with a high confidence score represented in D. **F-** Venn diagram with the intersection of the whole CFTR interactome data set detected by Pankow and colleagues [107] and our high confidence PM CFTR interactors in Wt-CFTR and rescued Phe508del-CFTR. [Bioinformatic analysis performed by Francisco Pinto, included with permission]

depicted in Figure 4.3 by the size of node boxes, identified the proteins YWHAZ (14-3-3 zeta), CAPN1 (Calcium-Activated Neutral Proteinase 1, catalytic subunit) and IPO5 (Importin 5) as the more relevant in the context of interactions with rescued Phe508del-CFTR at the PM. IPO5 is a direct interactor of CFTR and EZR, while YWHAZ and CAPN1 interact directly with EZR and NHERF1. YWHAZ reaches a higher score because it interacts with five CFTR direct neighbors. CAPN1 can form a complex with its small regulatory subunit CAPNS1. Remarkably, the CAPN1-CAPNS1 complex interacts directly with CFTR, EZR and NHERF1.

This protein list was also intersected with the druggable proteome at the ChEMBL database to identify the most likely druggable hits. This intersection highlighted one particular candidate: CAPN1.

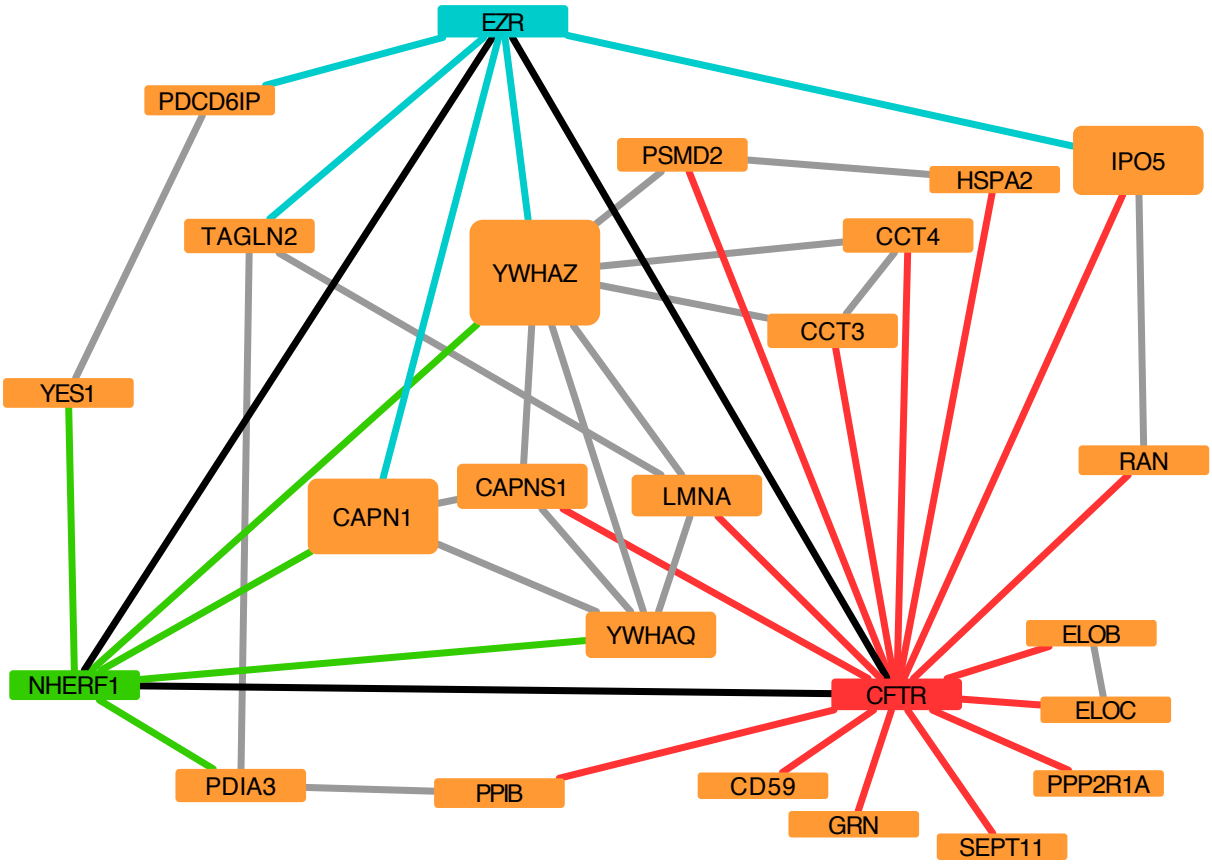

Figure 4.3 - Subnetwork of 22 proteins with direct interactions to CFTR, EZR or NHERF1
Schematic representation of the 22 proteins network with direct interactions to CFTR, EZR or NHERF1 that were detected with high confidence interacting with rescued Phe508del-CFTR at the PM, both through the action of VX-809 or low temperature. The size of orange nodes represents a visual score of putative relevance of the protein to the formation of the CFTR-EZR-NHERF1 complex. [Bioinformatic analysis performed by Francisco Pinto, included with permission]

4.3.3. Calpain 1 is a strong candidate for selective interaction with rescued Phe508del-CFTR

CAPN1, Calpain 1, was identified with a high confidence score (See Methods), as a druggable target by the ChEMBL database, and as highly relevant for the formation of the surface CFTR-EZR-NHERF1 complex by our bridging score. Calpain 1 belongs to a group of calcium-sensitive cysteine proteases that are ubiquitously expressed in human cells and associated with subcellular organelles such as the cytoskeletal actin filaments, vesicles, and the PM [219]. Furthermore, Calpain 1 inhibition was shown to promote the partial rescue of Phe508del-CFTR in peripheral blood mononuclear cells (PBMC) from CF patients [220].

To assess the robustness/directness of the interaction between PM-CFTR and Calpain 1 we performed the same IP protocol, but in the absence of crosslinking agents. To that purpose, we used a protein-specific antibody to detect its presence in the co-precipitates through Western blot (WB). We confirmed that Calpain 1 co-precipitates with rescued Phe508del-CFTR but not with wt-CFTR, even in the absence of crosslinking agents, proving the strength of this interaction (Figure 4.4). In contrast, Tubulin, which was consistently absent from the isolated CFTR-containing PM-associated complexes, was also absent from the un-crosslinked co-precipitates, confirming the specificity of CAPN1 detection (Figure 4.4). We, therefore, decided to proceed with the study of Calpain 1 effect on the PM stability of rescued Phe508del-CFTR.

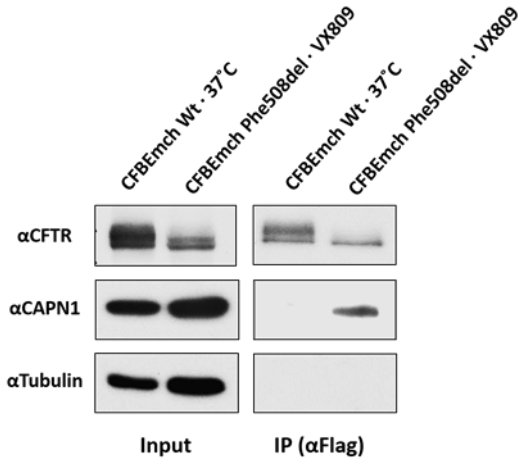

Figure 4.4 - Validation of hit proteins putatively destabilizing rescued Phe508del-CFTR at the PM
Western blot analysis of proteins co-immunoprecipitating with α-Flag-tagged wt- or Phe508del-CFTR at the cell surface, the latter rescued to the PM by 48 hours incubation with 3 μM VX-809.

4.3.4. Calpain 1 downregulation increases the PM abundance and function of VX-809-rescued Phe508del-CFTR

Using a specific siRNA (sc-29885, Santa Cruz) we were able to downregulate Calpain 1 expression in CFBEmChF cells to approximately 32% of its normal levels (Figure 4.5A). We then assessed the effect of Calpain 1 downregulation on the PM abundance of VX-809-rescued Phe508del-CFTR. For this we performed a cell surface protein immunolabelling assay that allows the selective labelling of CFTR proteins at the PM ([168] and see Methods). Briefly, Phe508del-CFTR PM expression

was rescued by VX-809 treatment (48 hours at 37˚C) in CFBEmChF cells transfected with either siCAPN1 or siLuc (used as control). The cells were then placed at 4˚C to arrest endocytic traffic and, without permeabilization, CFTR proteins at the cell surface were labelled with M2 anti-Flag antibody followed by detection with an Alexa488-conjugated secondary antibody. Confocal images selectively capturing the cell's surface plane clearly show that CAPN1 downregulation increased PM expression of rescued Phe508del-CFTR, when compared to siLuc control (Figure 4.5B). Quantification of membrane (Alexa 488) CFTR signals (Figure 4.5C) revealed that this increase is statistically significant, corresponding to a 3-fold increment in the PM abundance of VX-809-rescued Phe508del-CFTR (from 7 to 21% of wt-CFTR signal). Quantification of total CFTR (signal from CFTR's N-terminal mCherry tag) signals showed that Calpain 1 downregulation also slightly increased, albeit not significantly, the overall abundance of Phe508del-CFTR in these cells. Nevertheless, by calculating the ratio of surface/total CFTR signals, a significant >2-fold increase in CFTR abundance at the PM was still observed in CAPN1 depleted cells (Figure 4.5C). These results were further confirmed using a surface protein biotinylation assay where proteins at the cell surface are labelled with non-permeable EZ-Link-Sulfo-NHS-SS-Biotin and captured with streptavidin-agarose beads (Figure 4.5D). WB analysis of biotin precipitates from CFBEmChF cells treated as before confirmed an increase in rescued Phe508del-CFTR abundance at the cell surface upon Calpain 1 downregulation, compared to control cells (siLuc). Moreover, detection of Glucose transporter 1 (Glut-1), an integral membrane protein transporter of glucose of mammalian cells, in these samples showed no noticeable variations in the abundance of this transporter at the cell surface, indicating a specific effect of Calpain 1 downregulation in increasing rescued Phe508del-CFTR PM levels (Figure 4.5D). Next, we evaluated how Calpain 1 downregulation impacted the functional rescue of Phe508del-CFTR by the VX-809 corrector. For this we used the previously described iodide influx assay, based in the halide-sensitive yellow fluorescent protein (YFP) (HS-YFP) [159–161]. Briefly, CFBE cells co-expressing Phe508del-CFTR and the HS-YFP F46L/H148Q/I152L mutant [159] were transfected with either siCAPN1 or siLuc and incubated with VX-809 for 48 h (Figure 4.5E,F). Cells were then stimulated for 30 min in PBS with 5 µM forskolin (Fsk) and 20 µM genistein (Gen) to induce CFTR activity. Next, a HS-YFP fluorescence baseline was recorded for 5 seconds, and its decay followed continuously (at 0.5 s intervals) after the rapid (< 1 s) addition of iodide (Figure 4.5E). Curves were fitted to an exponential decay function to derive the initial rates of iodide influx, which, as previously described [37], are directly proportional to the extent of chloride effluxed from these cells *via* CFTR. Consistent with the observed > 2-fold increase in PM abundance of VX-809-rescued Phe508del-CFTR, Calpain 1 downregulation increased by 2.5-fold the iodide influx rate in these cells, which was completely dependent on CFTR activity since the effect was abolished upon co-treatment with the CFTR-specific inhibitor 172 (Figure 4.5F). Together, these results strongly suggest that Calpain 1 might play an important role in regulating the overall PM stability of pharmacologically rescued Phe508del-CFTR at the PM of bronchial epithelial cells.

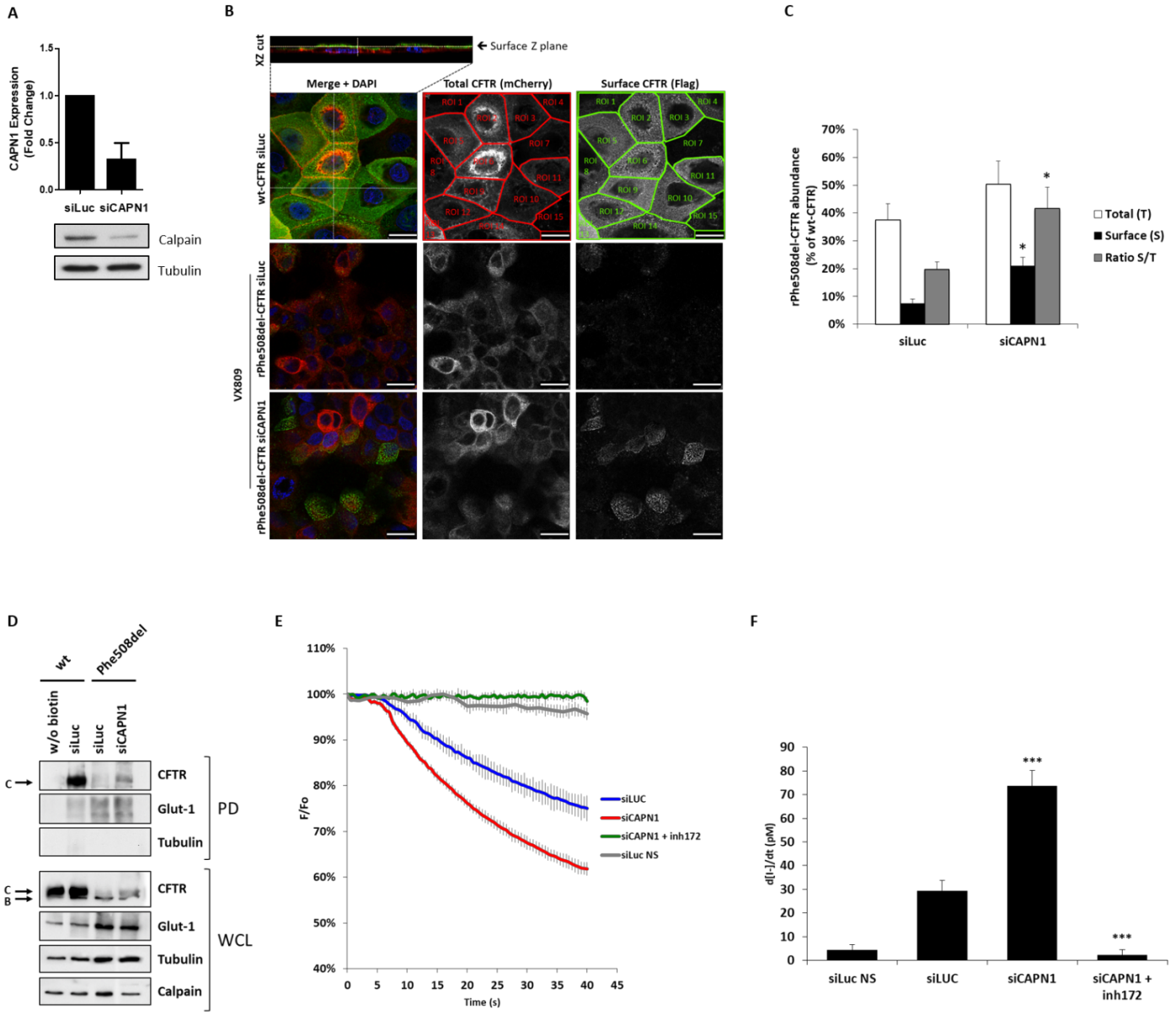

Figure 4.5 – Calpain 1 downregulation outcome on rescued PM Phe508del-CFTR abundance and function

A- Assessment of Calpain 1 siRNA-mediated knockdown efficiency (*n*=7). Data is shown as fold change relative to siLuc (control). **B-** Confocal images of Dox-induced-CFBEmChF-Wt or Phe508del cells, transfected with either siLuc or siCAPN1. Phe508del-CFTR was rescued to the PM by 48h incubation with 3 µM VX-809 at 37°C. Images are tripled labelled unpermeabilized cells, where mCherry fluorescence is proportional to the total amount of CFTR, AlexaFluor488 fluorescence is proportional to the amount of CFTR present at the cell surface, and nuclei were stained with DAPI. A 0.2 µm Z-stack of 1 Airy confocal images were acquired (top left insert) to select the best XY plane to analyze the CFTR protein at the cell surface. ImageJ software (NIH) was used to delimitate each single cell as individual ROIs (Regions Of Interest) so as to allow measurement of mcherry (red lined lattice) and AlexaFluor488 (green lined lattice) fluorescence signal intensities **C-** Analysis of single-cell fluorescence signals in three independent experiments. Data is presented as total (T), surface (S), or S/T ratio of rescued Phe508del-CFTR abundance, expressed as percentage of Wt-CFTR values. **D-** WB analysis of biotinylated cell surface proteins (biotin pull-down - PD) and whole cell lysates (WCL), treated as in (B). **E-** Traces of iodide-induced HS-YFP fluorescence decay of CFBE Phe508del-cells treated with 3 µM VX-809 for 48h, transfected with either siLuc or siCAPN1, and co-treated or not with 25 µM of inh172 for 15 min prior to stimulation for 30 min in PBS with Fsk and Gen, in the presence or absence of inh172, followed by continuous fluorescence recording and addition of Iodide (100 mM). **F-** Summary of iodide influx rates calculated by fitting the iodide assay results to exponential decay curves. All shown data represent means ± SEM.: **p* < 0.01; ****p* < 0.0001; rPhe508del-CFTR=rescued Phe508del-CFTR; PD=pull-down; WCL=whole cell lysate [Images acquired jointly with Paulo Matos]

4.3.5. Knockdown of Calpain 1 improves the PM stability of rescued Phe508del-CFTR through enhanced EZR binding

To determine whether CAPN1 downregulation improved rescued-Phe508del-CFTR stability at the cell surface we coupled the surface CFTR immunolabelling assay to a previously described surface thermal destabilization assay ([37] and see Methods). Briefly, VX-809 rescued Phe508del-CFTR (48 h) was stabilized at the surface by incubation of the cells at 30˚C. Cells were then moved for 4 hours to 37˚C (thermal shift - TS) which destabilizes rescued CFTR at the cell surface causing its internalization, unless the additional experimental conditions lead to the retention of the rescued channel at the PM [36,143]. CFTR at the cell surface was immunolabelled and analyzed as before (Figure 4.6A). Fluorescence signal quantification revealed that upon TS to 37°C, rescued-Phe508del-CFTR in siLuc-transfected cells was destabilized and removed from the PM, reducing the protein surface abundance by ~60% (Figure 4.6B). In contrast, downregulation of Calpain 1 clearly increased the surface stability of the rescued channels since ~80% of the protein remained at the plasma membrane after 4 hours at 37° (Figure 4.6B). The immunolabeling results were again confirmed by cell surface protein biotinylation (Figure 4.6C), which also showed that Glut-1 PM abundance was not influenced by CAPN1 knockdown, again supporting a CFTR-specific PM retention effect (Figure 4.6C).

We have previously shown that the critical step to stabilize Phe508del-CFTR at the PM is the opening of NHERF1 PDZ2 domain by the binding of activated EZR [37]. Since interaction with Calpain 1 was shown to cause the proteolytic inactivation of EZR [219,221,222] we hypothesised that by downregulating Calpain 1 we could be enhancing Phe508del-CFTR anchoring by promoting CFTR-NHERF1-EZR interaction. To test this hypothesis we immunoprecipitated PM-rescued Phe508del-CFTR in the thermal destabilization assay conditions used above and analyzed the levels of co-precipitating EZR and NHERF1 (Figure 4.6D). Notably, while the levels of co-precipitated NHERF1 were equivalent between control (siLuc) and siCAPN1 transfected cells, the amount of EZR co-precipitating with PM Phe508del-CFTR upon Calpain 1 downregulation increased to levels near those found in wt-CFTR expressing cells (Figure 4.6D). These results are in accordance with our hypothesis, and show that CAPN1 binding negatively influences the formation of Phe508del-CFTR/NHERF1/EZR anchoring complex leading to a diminished stability of the pharmacological corrected channels.

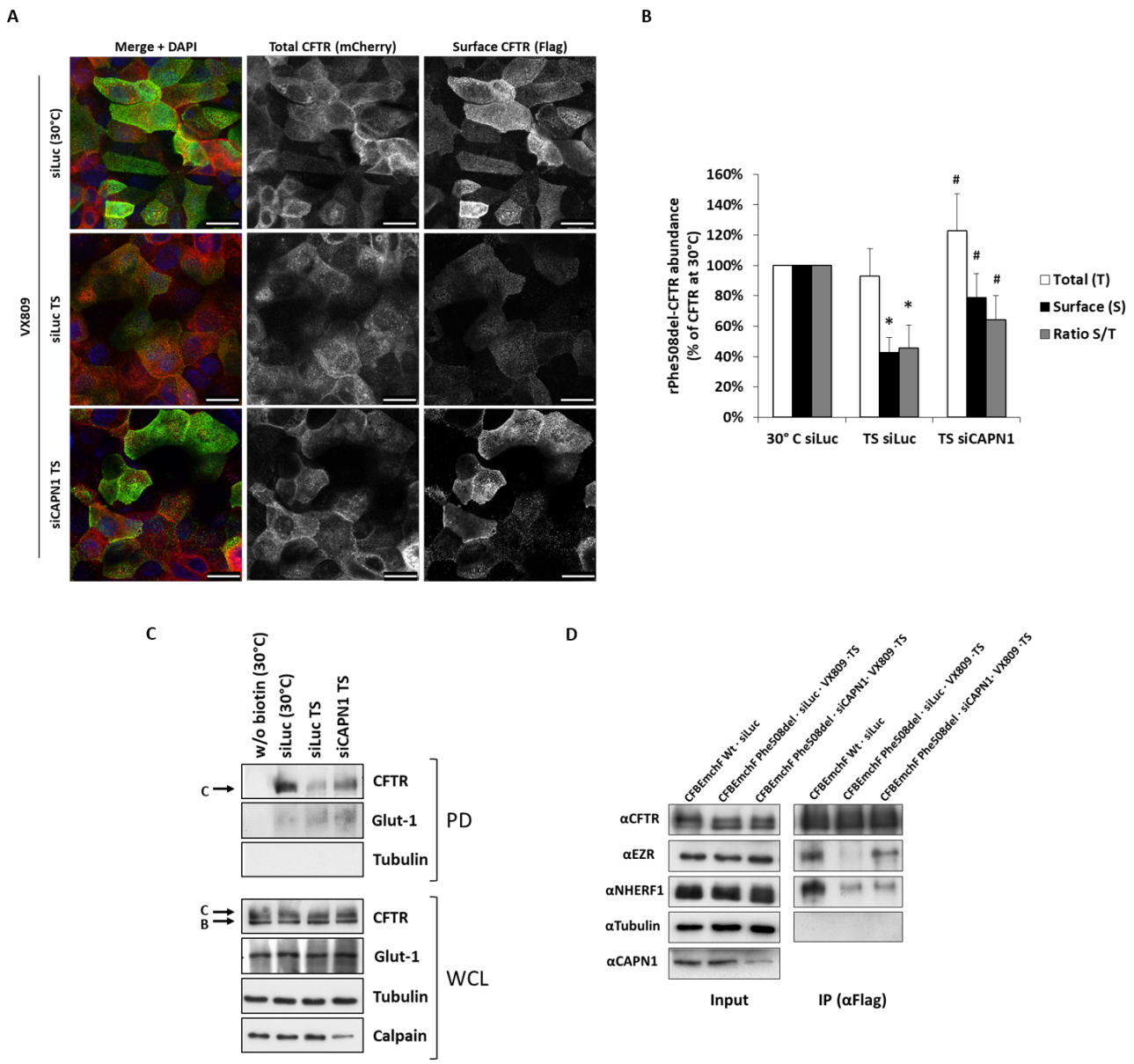

Figure 4.6 – CAPN1 downregulation outcome on the PM levels of EZR, NHERF1 and rescued Phe508del-CFTR upon thermal shift assay

A- Confocal images of Dox-induced-CFBEmChF-Phe508del cells, transfected with either siLuc or siCAPN1. Phe508del-CFTR was rescued to the PM by 48 h incubation with VX-809 at 30°C and subjected to a thermal shift (TS) of 4 h at 37˚C, except for siLuc low temperature control (30°C). Images are tripled labelled unpermeabilized cells, where mCherry fluorescence is proportional to the total amount of CFTR, AlexaFluor488 fluorescence is proportional to the amount of CFTR present at the cell surface, and nuclei were stained with DAPI. **B-** Analysis of single-cell fluorescence signals in three independent experiments. Data is presented as total (T), surface (S), or S/T ratio of rescued Phe508del-CFTR abundance, expressed as percentage of CFTR at 30°C (low temperature control). **C-** WB analysis of biotinylated cell surface proteins (biotin pull-down - PD) and whole cell lysates (WCL), treated as in (A). **D-** WB analysis of EZR and NHERF1 proteins co-precipitating with Wt- or Phe508del-CFTR at the cell surface. PM CFTR in Wt- or Phe508del-CFTR CFBEmChF cells, the treated for 48h with VX-809, were transfected with either siLuc or siCAPN1. The siLuc and siCAPN1 conditions were then subjected to a TS of 4 h at 37˚C to destabilize rescued CFTR. CFTR at the PM was labelled with α-Flag antibody in non-permeabilizing conditions, and immunoprecipitated. WB using specific antibodies detected co-precipitating NHERF1 and EZR proteins. All shown data represent means ± SEM.: *$p < 0.001$; #$p < 0.05$; rPhe508del-CFTR=rescued Phe508del-CFTR; PD=pull down; WCL=whole cell lysate [Images acquired jointly with Paulo Matos]

4.3.6. Acute chemical inhibition of endogenous Calpain 1 significantly increases VX-809-mediated Phe508del-CFTR functional rescue in bronchial epithelial cells

As described above, intersection of MS data with the ChEMBL database identified CAPN1 as a druggable candidate protein since its activity can be chemically inhibited by ALLM, a cell-permeable peptide aldehyde [223,224]. We thus tested the effect of ALLM co-treatment on the functional rescue of Phe508del-CFTR by VX-809 using the HS-YFP assay. CFBE-Phe508del cells co-expressing HS-YFP were incubated with 3 µM VX-809 for 48 hours and co-treated with either DMSO or 250 nM of ALLM for the last 4 hours. As before, cells were then stimulated with Fsk and Gen and analyzed by live confocal imaging after I^- addition (Figure 4.7A and B). Treatment with ALLM produced a striking response in fluorescence decay, which was CFTR-dependent, since it was completely reverted by the concomitant presence of CFTR inh172. Calculation of initial Iodide influx rates (as before) revealed that treatment with ALLM increase by ~4 fold the functional response of VX-809-rescued Phe508del-CFTR, when compared to DMSO treated cells (Figure 4.7B).

Analysis of PM abundance (Figure 4.7C and Supplementary Figure S4.2A) and surface thermal stabilization (Figure 4.7E and Supplementary Figure S4.2B) of rescued Phe508del-CFTR corroborate this enhanced functional response. ALLM treated cells presented a 5-fold increase in rescued Phe508del-CFTR PM levels [~8% to ~40%, compared to DMSO control cells (Figure 4.7C)]. Even considering the small enrichment in total CFTR induced by ALLM treatment, the Phe508del-CFTR retention at the membrane (surface/total ratio) reached nearly 4-fold that of control, DMSO treated cells (Figure 4.7C), which translated into a full thermal stabilization of the rescue channels present at the surface of these cells (Figure 4.7E). Again, these results were also observable through surface protein biotinylation followed by WB analysis (Figure 4.7D and F, respectively).

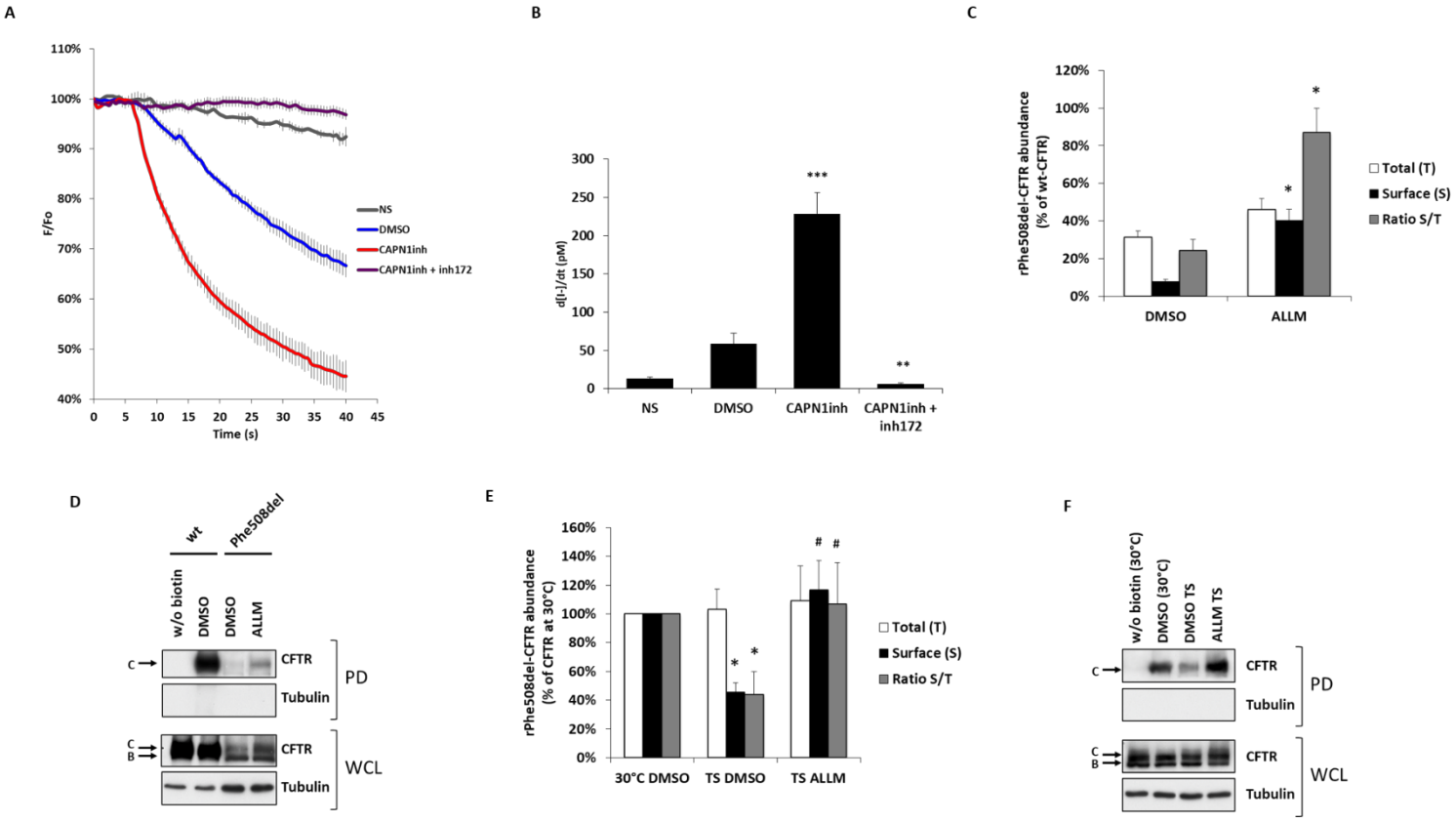

Figure 4.7 - Chemical inhibition of Calpain 1 improves rescued Phe508del-CFTR PM abundance, function and stability.
A - Traces of iodide-induced HS-YFP fluorescence decay of CFBE Phe508del-cells treated with 3 µM VX-809 for 48h, non-treated (NT) or co-treated with either DMSO or 250 nM ALLM CAPN1 inhibitor in the last 4 hours, co-treated or not with 25 µM of inh172 for 15 min prior to stimulation for 30 min in PBS with Fsk and Gen, in the presence or absence of inh172, followed by continuous fluorescence recording and addition of Iodide. **B-** Summary of iodide influx rates calculated by fitting the iodide assay results to exponential decay curves. **C-** Analysis of single-cell fluorescence signals in three independent experiments of Dox-induced CFBEmChF Wt or Phe508del cells, treated with 3 µM VX-809 for 48 h and co-treated with either DMSO or 250 nM ALLM CAPN1 inhibitor in the last 4 hours. Data is presented as total (T), surface (S), or S/T ratio of rescued Phe508del-CFTR abundance, expressed as percentage of Wt-CFTR values. **D-** WB analysis of biotinylated cell surface proteins (biotin pull-down - PD) and whole cell lysates (WCL), treated as in (C). **E-** Analysis of single-cell fluorescence signals in three independent experiments of Dox-induced CFBEmChF Phe508del cells, treated with 3 µM VX-809 for 48 h at 30°C and subjected to a thermal shift (TS) of 4 hours at 37˚C in the presence of either DMSO or 250 nM ALLM CAPN1 inhibitor, except for DMSO low temperature control (30°C). Data is presented as total (T), surface (S), or S/T ratio of rescued Phe508del-CFTR abundance, expressed as percentage of CFTR at 30°C (low temperature control). **F-** WB analysis of biotinylated cell surface proteins (biotin pull-down - PD) and whole cell lysates (WCL), treated as in (E). All shown data represent means ± SEM.: ***$p < 0.0003$, **$p < 0.001$;*$p < 0.001$; #$p < 0.001$; rPhe508del-CFTR=rescued Phe508del-CFTR; PD=pull down; WCL=whole cell lysate [Images acquired jointly with Paulo Matos]

4.4. Discussion

So far, several studies have identified numerous CFTR's interacting partners with essential roles in the processing, localization and function of the channel [8,98,99,101,102,107], nonetheless, the present work is the first to specifically characterize CFTR interactions particularly at the PM compartment. Previous studies have shown that several interactions between CFTR and its binding partners are mediated through the scaffolding protein NHERF1, which seems to be a central protein in the assembly of the CFTR-containing macromolecular complexes at the surface of airway cells [99,123,124]. EZR is also a key component in these complexes, mediating the tethering of NHERF1-bound CFTR proteins at the PM to the actin cytoskeleton, thus stabilizing the channel at the cell surface, blocking its endocytosis [104,105,225]. Moreover, we showed previously that the low cell surface stability of chemically rescued Phe508del-CFTR was, at least in part, caused by an impaired recruitment of EZR to Phe508del-CFTR/NHERF1 complexes at the PM, preventing their anchoring to actin and leading to their rapid internalization [40]. Moreover, we and others [37,226] showed that overexpression of constitutively active EZR coaxed the retention of rescued Phe508del-CFTR at the membrane, by causing a conformational change in NHERF1 that displaced CHIP ubiquitin ligase preventing CFTR ubiquitination and internalization [37]. This led us to hypothesize that EZR overexpression was somehow circumventing a mechanistic restrain that prevented its association with rPhe508del-CFTR/NHERF1 complexes in normal conditions. We thus reasoned that it would be highly likely that, as with CHIP, additional proteins, interacting specifically with rPhe508del- but not with wt-CFTR, could be preventing EZR binding thus causing the destabilization of rescued Phe508del-CFTR/NHERF1 complexes at the PM. These hypotheses guided the development of the assay to selective immunoprecipitate and characterize CFTR-containing complexes from the membrane. Notably, the whole CFTR interactome described by Pankow and colleagues [107], detected about 27% of the interactors identified by our PM-directed analysis. This is consistent with a compartment-specific enrichment of our dataset, supporting the selectivity of our experimental approach. Our hypothesis also guided the bioinformatic analysis of the gathered data, allowing us to converge our MS dataset from a network of 557 putative interactors to a subnetwork of 22 core proteins with a high probability to directly interact with rescued Phe508del-CFTR/NHERF1 but not wt-CFTR/NHERF1 complexes at the PM. Among these high confidence-scoring proteins, Calpain 1 stood out as a potentially druggable candidate, since chemical inhibitors for this protein were already commercially available. Of course this does not exclude that several other relevant regulators of CFTR PM stability may exist among the many identified interactors, leaving an open door for further studies of these additional candidate proteins.

Notwithstanding, we showed here that Calpain 1, an ubiquitous cytoskeleton and PM associated Ca^{2+} dependent cysteine protease [219], is present within the PM complex assembled around rescued Phe508del-CFTR, but not around wt-CFTR proteins. Moreover, we demonstrated that chemical inhibition of Calpain 1 with ALLM promotes the stabilization of VX-809-rescued Phe508del-CFTR at the PM of bronchial epithelial cells, leading to a near 4-fold improvement in the functional restoration of CFTR-mediated ion transport. Although ALLM has a higher specificity to inhibit Calpain 1 over other calpains, it is also a potent inhibitor of cathepsins, a group of Lysosome associated proteases [223].

Since degradation of rescued Phe508del-CFTR internalized from the PM was said to occur mainly at the lysosome compartment [36], we cannot exclude a partially contribution of cathepsin inhibition to the increased PM abundance of rescued CFTR after ALLM treatment. Indeed, while siRNA-mediated Calpain 1 knockdown produced a similar effect to ALLM treatment regarding PM abundance, stability and functional rescue of Phe508del-CFTR, the overall magnitude of the effects was lower than that achieved with the chemical inhibitor. Previous studies in peripheral blood mononuclear cells (PBMC) of patients homozygous for Phe508del-CFTR showed that elevated levels of intracellular Ca^{2+} led to an unbalance in the calpain/calpastatin system, resulting in a constitutive Calpain 1 protease activation due to a decrease in their specific inhibitory regulators, resulting in a reduction of mature CFTR in PBMCs [227]. These authors also showed that Calpain 1 was able to hydrolyze CFTR and NHERF1 localized at the PM, causing a disorganization of the CFTR functional complex, and that total EZR protein levels were lower in the PBMC of CF patients [227]. Although the expression of CFTR in PBMCs is still subject to controversy [228,229], Ca^{2+} was also found elevated in epithelial airway cells of CF patients [230–233], suggesting a similar upregulation of Calpain 1 activity in these cells. Moreover, while the authors did not fully elucidate the mechanism of PM CFTR destabilization in PBMCs [227], we have shown here that knockdown of Calpain 1 stabilizes Phe508del-CFTR by promoting the association of endogenous EZR with the CFTR/NHERF1 complex at the PM. This is consistent with our previous findings that it was possible to coax the anchoring and PM retention of chemically-rescued Phe508del-CFTR by promoting the activation and association of EZR to CFTR/NHERF1 complexes at the PM, by increasing endogenous RAC1 signaling through the stimulation of airway epithelial cells with HGF [40]. The binding of activated EZR induces a conformational change in NHERF1 that exposes a second PDZ domain for CFTR binding, which stabilizes the rescued channel at the cell surface, leading to a 3-fold increase in functional restoration achieved by corrector drugs such as VX-809 [37,40]. An equivalent extent of functional recovery was observed with Calpain 1 inhibition, either by siRNA-mediated Knockdown or by chemical inhibition with ALLM.

The physiological role of the calpains is still not fully clear but, in general, it is believed that the system has a regulatory rather than a degradative function, due to the fact that calpains cleave polypeptides at specific sites and in limited numbers, leaving large and, often, catalytically active fragments [219,234,235]. EZR is among the known Calpain 1 substrates, and remarkably, is the only member of the ezrin-radixin-moesin (ERM) family to be cleaved by this protease, again, pointing to a possible regulatory function [236]. These evidences led us to propose the following model (Figure 4.8): elevated Ca^{2+} intercellular levels coupled to the recruitment of Calpain 1 to rescued Phe508del-CFTR/NHERF1 PM complexes leads to the hydrolysis/displacement not of NHERF1 (who's PM levels did not change upon Calpain 1 downregulation) but of EZR from the complex, preventing its activation by endogenous signaling events (such as those mediated by RAC1 [40]), NHERF1 opening and the anchoring of rescued CFTR to the actin cytoskeleton. This leads to the accelerated internalization and degradation of rescued channels, as described by us and others [37,40,50]. Inhibition of Calpain 1, allows the activation and binding of EZR to Phe508del-CFTR/NHERF1 complexes at the PM, promoting the retention and stabilization of rescued channels at the cell surface.

Taken together, our results indicate that Calpain 1 association plays an important role in reducing the half-life of rescued Phe508del-CFTR at the PM, and that its pharmacological inhibition may have a relevant therapeutic application in combination therapies with other modulator drugs, namely correctors and potentiators. It should be noted that, even though there are no Calpain 1 inhibitors currently progressing into clinical trials, important advances are being made in their development and several preclinical studies demonstrated the potential therapeutic value of Calpain inhibitors [237,238]. In accordance, further *in vivo* studies will now be required to evaluate the therapeutic applicability of Calpain 1 inhibition in CF disease.

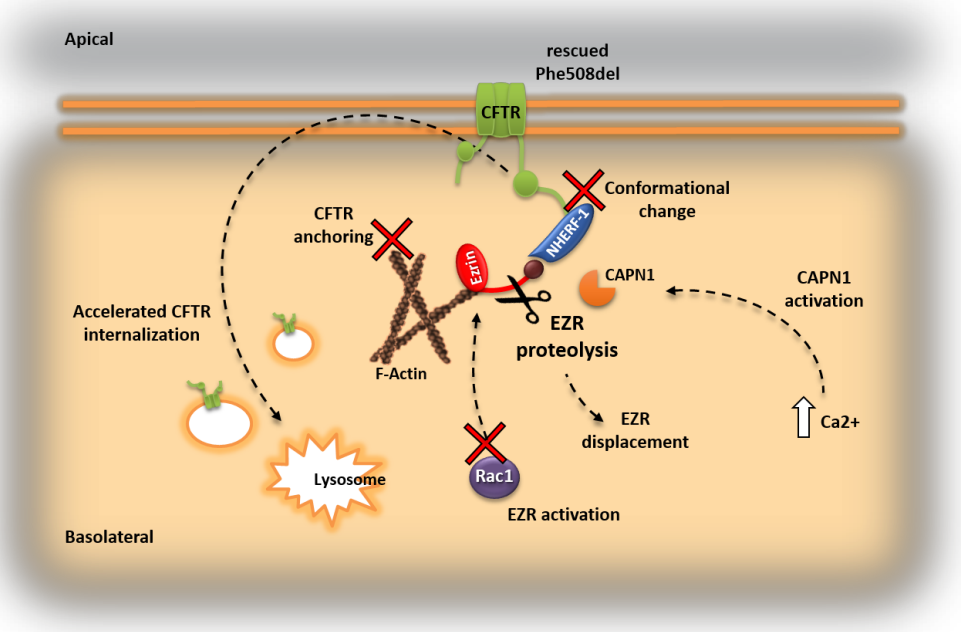

Figure 4.8 - Schematic representation of the proposed mechanism by which CAPN1 affects rescued Phe508del-CFTR PM abundance and retention. See text for details.

4.5. Materials and Methods

4.5.1. Cell culture, treatment and transfection

CFBEmChF cells were cultured in Minimum Essential Medium (MEM) (Gibco, Life Technologies) supplemented with 10% (v/v) heat inactivated fetal bovine serum (Gibco, Life Technologies), 10 mg/ml blasticidin (Santa Cruz Biotechnology) and 2 µg/ml puromycin (Gibco, Life Technologies) at 37˚C with 5% CO_2. CFBE Phe508del-CFTR cells constitutively expressing HS-YFP F46L/H148Q/I152L were cultured in Minimum Essential Medium (MEM) (Gibco, Life Technologies) supplemented with 10 % (v/v) heat inactivated fetal bovine serum (Gibco, Life Technologies), 0,4 mg/ml hygromycin B (Thermo Fisher Scientific) and 2 µg/ml puromycin (Gibco, Life Technologies) at 37˚C with 5% CO_2. Cells were transfected with LipofectAMINE 2000 (Invitrogen) using a solution of 220 pmol siRNA, 9 µl LipofectAMINE 2000 and 250 µL of OptiMEM (Gibco, Life Technologies) per 35mm petri dish. Stock solutions of forskolin (10 mM, Sigma-Aldrich), genistein (50 mM, Sigma-

Aldrich), CFTRinh-172 (CFFT USA, 10 mM), VX-809 (10 mM, GENTAUR) and ALLM (5 mg/ml, Merck Millipore) were prepared in DMSO.

4.5.2. Immunoprecipitation and Western blot procedures

Proteins were separated on 9% (w/v) SDS-PAGE gels (to assess CFTR expression these gels contained 1% (v/v) glycerol and were run at 4°C). For detection of specific proteins SDS-PAGE gels were transferred onto PVDF membranes (BioRad). Western blot (WB) membranes were blocked in TBS, 0.1% (v/v) Triton X-100, 5% (w/v) milk, and probed using the following primary antibodies: mouse α-CFTR clone 596 (CFF); goat α-CAPN1 clone N-19 (sc-7531, Santa Cruz Biotechnology); mouse α-EZR clone 1E11 (SAB1402391, Sigma-Aldrich); mouse α-NHERF-1 clone A7 (sc-271552, Santa Cruz Biotechnology); rabbit α-PDIA3 (HPA003230, Sigma-Aldrich); rabbit α-Glut1 Ab652 (Abcam); and mouse α-Tubulin clone B-5-1-2 (T5168, Sigma-Aldrich) - followed by a secondary peroxidase-conjugated antibody (α-goat IgG 31430, Sigma-Aldrich ; α-mouse IgG 1706516 BioRad; α-rabbit IgG 1706515, BioRad) and ECL. For densitometry analysis of WB bands, x-rays films were digitalized and images analyzed with ImageJ software (NIH).

4.5.3. Silver Staining of SDS-PAGE gels

SDS-PAGE gels intended for MS analysis were silver stained as described in [218]. Briefly, gels were transferred to a glass tray and fixed for 1 hour at room temperature in Fixer solution (40% ethanol, 10% glacial acetic acid, 50% ddH_2O), and washed overnight in ddH_2O. Gels were sensitized in 0.02% sodium thiosulfate (0.04 g $Na_2S_2O_3$, 200 ml ddH_2O) for 1 min and washed tree times with ddH_2O. Gels were then incubated in cold 0.1 % silver nitrate solution (0.2 g $AgNO_3$, 200 ml ddH_2O, 0.02% formaldehyde) for 20 min and washed twice with ddH_2O. Gels were transferred to a new tray and washed for 1 min before developing in 3 % sodium carbonate solution (7.5 g Na_2CO_3 in 250 ml ddH_2O, 0.05% formaldehyde) until distinct bands were visible. After ddH_2O washing, staining was completed in 5% acetic acid for 5 min and gels were stored at 4˚C in 1% acetic acid until MS analysis.

4.5.4. Immunofluorescence and confocal microscopy

CFBEmChF cells grown on coverslips were induced with Dox (1 µg/mL; Sigma-Aldrich) and treated as indicated below for biotinylation of cell surface proteins. Afterwards, cells were rinsed on ice with cold PBS-CM (PBS pH 8.0 containing 0.1 mM $CaCl_2$ and 1 mM $MgCl_2$) and incubated with M2 α-Flag antibody (1:500; Sigma-Aldrich) in PBS-CM for 1 hour at 4°C, without permeabilization. Cells were washed three times with ice cold PBS-CM and incubated with α-mouse AlexaFluor488 secondary antibody (1:500; Life Technologies) for 1 hour at 4°C. Cells were then fixed with 4 % formaldehyde for 15 min, thorough washed in PBS containing DAPI (4',6-diamidino-2-phenylindole) and mounted on microscope slides with Vectashield (Vector Laboratories). Images were acquired on a Leica TCS-SPE confocal microscope.

4.5.5. Precipitation of CFTR membrane association complex

CFBEmChF wt-CFTR cells were incubated at 37˚C for 48 hours after Dox-induced CFTR expression (1 µg/mL; Sigma-Aldrich), while CFBEmChF Phe508del-CFTR cells were incubated in three different conditions for 48 hours after Dox-induced CFTR expression: at 37˚C; at 26˚C for lower temperature CFTR correction; and at 30˚C with VX-809 mediated pharmacological correction (5µM; GENTAUR). For each condition cells near confluence on 100 mm culture dishes were gently, but thoroughly, washed with ice cold PBS-CM (PBS pH 8.0 containing 0.1 mM $CaCl_2$ and 1 mM $MgCl_2$). Cells were then placed on ice, washed three times with ice cold PBS-CM and left 5 min in cold PBS-CM to ensure arrest of endocytic traffic. Cells were incubated with agitation for 2 hours with M2 α-Flag antibody (1:500; Sigma-Aldrich) – all dishes except one, used for Flag-control assessment – and rinsed twice with ice-cold PBS-CM. Each condition was incubated with the crosslink solution DSP+SPDP (1:1 0.2 mM; Thermo Scientific) for 2 hours with agitation before being rinsed twice and left for 15 min with Tris-HCL (50 mM Tris/HCl pH 7.5) to quench the reaction. Cells were again washed three times with cold PBS-CM and lysed in 500 µl Lysis Buffer (50 mM Tris/HCl pH 7.5, 2 mM MgCl, 100 mM NaCl, 10% (v/v) glycerol, 1% (v/v) NP40, 0,01% (v/v) SDS, Protease inhibitor cocktail (Sigma)). Cell lysates were cleared at 6000x g for 5 min at 4˚C. ~450 µl lysate were added to 45 µl streptavidin-agarose beads (Sigma) to perform a pre-clearing of the cleared lysates, which were rotated for 1 hour at 4˚C, centrifuged for 1 min at 6000x g and recovered. ~400 µl of the pre-cleared lysates were added to 40 µl G-protein agarose beads (Roche) and rotated for 1 hour at 4˚C, centrifuged for 1 min at 6000x g and washed six times in cold Wash Buffer (50 mM Tris/HCl pH 7.5, 2 mM MgCl, 300 mM NaCl, 10% (v/v) glycerol, 1% (v/v) NP40, 0.1% (v/v) SDS). Captured proteins were recovered in 50 µl 2x Sample Buffer with DTT (100 mM). Captured proteins were separated on 9% (w/v) SDS-PAGE gels and run 1 cm. The obtained gel was silver stained as described above, and the whole samples were send to Mass Spectrometry analysis using a SCIEX TripleTOF 6600 system, outsourced to UniMs (ITQB institute, Oeiras, Portugal).

4.5.6. Bioinformatics

4.5.6.1. Confidence in protein detection

Precipitation of CFTR membrane association complex was performed in three replicates. In each replicate, identification of each protein in MS spectra was characterized by a protein confidence score (PCS), detected with ProteinPilot™ Software (Sciex). For PCS higher than 1.3, the confidence in the identification of that particular protein in the sample is equal or higher than 95%. To conjugate this individual score with the detection of the same protein across replicates we generated a combined confidence score (CCS), defined by five levels of confidence for protein detection: level 5 proteins are detected with PCS ≥ 1.3 in more than one replicate and not in the controls; level 4 proteins are detected in one replicate with PCS ≥ 1.3 and not in the controls; level 3 proteins are detected in more replicates than in controls, and with an average PCS higher than their respective the controls; level 2 proteins are detected in one replicate with PCS ≤ 1.3, and not in the controls; and level 1 proteins are detected in the same number of replicates and controls, with a replicate average PCS higher than the corresponding controls. All other cases are included in level 0, where proteins are not considered to be present in the set of replicates.

4.5.6.2. Human Interactome Network

Interactions between detected proteins were retrieved from a human interactome network, built from two data sources: Agile Protein Interactomes DataServer (APID, apid.dep.usal.es/) and The Human Reference Protein Interactome Mapping Project (HuRI, http://interactome.baderlab.org/). APID collects physical protein interactions reported in the literature. We used all the interactions available in APID between human proteins. HuRI gives access to interactions detected through unbiased high-throughput pairwise protein interaction experimental detection. Network analyses were conducted in R using functions from the iGraph package. Network visualizations were produced with Cytoscape.

4.5.6.3. CFTR-Ezrin-NHERF1 interaction interference score

To measure the capability of individual proteins to interfere with the formation of the interactions between CFTR-EZR-NHERF1, we developed a quantitative score. First, for a given subnetwork containing these three proteins, the number of paths linking two of these proteins through 2, 3 or 4 interactions (path length) is computed. For each protein in the network, it is determined the fraction of paths of each length that pass through its node. The final score is a weighted sum of these fractions, where fractions associated with higher lengths have lower weights (Equation 1).

Equation 1 Score = (% paths length 2) + 0.5 * (% paths length 3) + 0.25 * (% paths length 4)

4.5.7. Protein thermal destabilization assay

CFBEmChF-CFTR Phe508del cells were incubated for 48 hours after Dox-induced CFTR expression (1 µg/mL; Sigma-Aldrich) at 30˚C with VX-809 mediated pharmacological correction (5µM; GENTAUR). Cells were transferred for incubation at 37˚C for 4 hours to destabilize the rescued Phe508del-CFTR at the PM, as described in [36]. Cells were placed on ice, washed three times with ice cold PBS-CM (PBS pH 8.0 containing 0.1 mM $CaCl_2$ and 1 mM $MgCl_2$) and left 5 min in cold PBS-CM. Cells were then treated according to the proceeding downstream assay.

4.5.8. Co-Immunoprecipitation of CFTR membrane associated proteins

4.5.8.1. Hit proteins validation

CFBEmChF-CFTR wt cells were incubated at 37˚C for 48 hours after Dox-induced CFTR expression (1 µg/mL; Sigma-Aldrich), while CFBEmChF-CFTR Phe508del cells were incubated for 48 hours after Dox-induced CFTR expression at 30˚C with VX-809-mediated pharmacological correction (5 µM; GENTAUR). For both conditions cells were placed on ice, washed three times with ice cold PBS-CM, and left 5 min in cold PBS-CM. Cells were then incubated with agitation for 2 hours with M2 α-Flag antibody (1:500; Sigma-Aldrich) and rinsed twice with ice-cold PBS-CM. Cells were again washed three times with cold PBS-CM and lysed in 500 µl Lysis Buffer (50 mM Tris/HCl pH 7.5, 2 mM $MgCl_2$, 100 mM NaCl, 10% (v/v) glycerol, 1% (v/v) NP40, 0,01% (v/v) SDS, Protease inhibitor cocktail (Sigma-Aldrich)). Cell lysates were cleared at 6000x g for 5 min at 4˚C. ~450 µl lysate were added to 45 µl streptavidin-agarose beads (Sigma) to perform a pre-clearing of the cleared lysates, rotated for 1

hour at 4˚C, centrifuged for 1 min at 6000x g and recovered. ~400 µl of the pre-cleared lysates were added to 40 µl G-protein agarose beads (Roche) and rotated for 1 hour at 4˚C, centrifuged for 1 min at 6000x g and washed six times in cold Wash Buffer (50 mM Tris/HCl pH 7.5, 2 mM $MgCl_2$, 300 mM NaCl, 10% (v/v) glycerol, 1% (v/v) NP40, 0.1% (v/v) SDS). Captured proteins were recovered in 20 µl 2x Sample Buffer with DTT (100mM). Captured proteins were analyzed by Western blotting with specific antibodies, as described above.

4.5.8.2. PM abundance measurement

In assays for which rescued Phe508del-CFTR PM abundance was measured we performed an additional protein thermal destabilization step (See above). CFBEmChF-CFTR cells were either transfected with siCAPN1 (sc-29885, Santa Cruz Biotechnology) or siLuc (siRNA against the firefly luciferase - Thermo Scientific) and incubated for 48 hours after Dox-induced CFTR expression (1µg/mL; Sigma-Aldrich) at 30˚C with VX-809-mediated pharmacological correction (5 µM; GENTAUR), and placed at 37˚C for the last 4 hours for the protein thermal destabilization assay; or treated with the vehicle DMSO (Sigma-Aldrich) or 250 nM of the specific Calpain inhibitor I, ALLM (Merck Millipore) and placed at 37˚C for the last 4 hours for the protein thermal destabilization assay. For all conditions, cells were then treated as described for hit proteins validation.

4.5.9. Biotinylation of cell surface proteins

CFBEmChF-CFTR cells were either transfected with siCAPN1 (sc-29885, Santa Cruz Biotechnology) or siLuc (siRNA against the firefly luciferase - Thermo Scientific) and incubated for 48 hours after Dox-induced CFTR expression (1 µg/mL; Sigma-Aldrich) at 30˚C with VX-809-mediated pharmacological correction (5 µM; GENTAUR), and placed at 37˚C for the last 4 hours for the protein thermal destabilization assay; or treated with the vehicle DMSO (Sigma-Aldrich) or 250 nM of the specific Calpain inhibitor I, ALLM (Merck Millipore) before being placed at 37˚C for the last 4 hours for the protein thermal destabilization assay. For all conditions, cells were placed on ice, washed three times with ice cold PBS-CM (PBS pH 8.0 containing 0.1 mM $CaCl_2$ and 1 mM $MgCl_2$) and left 5 min in cold PBS-CM. Cells were then incubated for 45 min with 0.5 mg of EZ-Link Sulfo-NHS-SS-Biotin (Santa Cruz Biotechnology) to label all cell surface proteins. Cells were rinsed twice and left for 15 min on ice with ice-cold Tris-Q (100 mM Tris/HCl pH 8.0, 150 mM NaCl, 0.1 mM $CaCl_2$, 1 mM $MgCl_2$, 10 mM glycine, 1% (w/v) BSA) to quench the reaction. Cells were again washed three times with cold PBS-CM and lysed in 250 µl of pull-down buffer (50 mM Tris/HCl pH 7.5, 100 mM NaCl, 10% (v/v) glycerol, 1% (v/v) NP40, Protease inhibitor cocktail (Sigma-Aldrich)). Cell lysates were cleared at 16000x g for 5 min at 4˚C and an aliquot of 40 µl, representing input CFTR levels, was removed while 200 µl lysate were added to 15 µl of G-protein agarose beads (Roche) to perform a pre-clearing of the cleared lysates, rotated for 1 hour at 4˚C, centrifuged for 1 min at 6000x g and recovered. The pre-cleared lysates were added to 20 µl streptavidin-agarose beads (Sigma), previously incubated for 1 hour in 1 ml cold pull-down buffer containing 2% (w/v) milk, and washed three times in pull-down buffer. Lysate and beads were rotated for 1 hour at 4˚C, centrifuged for 1 min at 6000x g, and washed five times in cold wash buffer (100 mM Tris/HCl pH 7.5, 300 mM NaCl, 1% (v/v) Triton X-100). Captured

proteins were recovered in 20 µl of 2x Sample Buffer with 100 mM DTT and analyzed by Western blotting with specific antibodies, as described above.

4.5.10. Iodide Efflux Assay (CFTR functional assay)

CFBE CFTR Phe508del cells constitutively expressing EYFP F46L/H148Q/I152L [159] were seeded in 8 well Chamber Slides (Lab-Tek). Cells were either transfected with siCAPN1 (sc-29885, Santa Cruz Biotechnology) or siLuc (Thermo Scientific) and incubated with VX-809 (5 µM; GENTAUR) for 48 hours with an additional protein thermal destabilization assay for 4 hours at 37˚ C; or incubated for 48 hours at 30˚C with VX-809 and treated with the vehicle DMSO (Sigma-Aldrich) or 250 nM of the specific Calpain inhibitor I, ALLM (Merck Millipore) for the last 4 hours at 37˚C. Cells were carefully washed twice with isomolar PBS (WPBS; 137 mM NaCl, 2.7 mM KCl, 0.7 mM $CaCl_2$, 1.1 mM $MgCl_2$, 1.5 mM KH_2PO_4, 8.1 mM Na_2HPO_4, pH 7.4), and incubated for 30 minutes with WPBS containing compounds for CFTR stimulation/inhibition (forskolin 5 µM, genistein 20 µM, and CFTR-inh172 25 µM, all from Sigma-Aldrich). Cells were then transferred to a Leica TCS-SPE confocal microscope for time-lapse analysis. Each well was assayed individually for iodide influx by recording fluorescence continuously (500 ms per point) for 10 s (baseline), and then for 110 s after the rapid (≤1 s) addition of isomolar PBS in which 137mM Cl^- was replaced by I^- (IPBS; final NaI concentration of 100 mM/plate well). Assays were performed at room temperature. After background subtraction, cell fluorescence recordings were normalized for the initial average value measured before addition of I^-. Quantification of fluorescence decay was performed on at least 24 individual cells per well, using ImageJ (NIH) as previously described[37,159].

4.5.11. Statistical Analysis

Statistical analysis was performed using GraphPad Prism 5 software. Quantitative results are shown as means ± SEM of at least three independent experiments. To compare sets of data, we used two-tailed Student's *t* tests. In the HS-YFP–based functional assay, signal decay was fitted to an exponential decay function to derive the maximal slope that corresponds to initial influx of I^- into the cells [159,161]. Maximal slopes were converted into rates of variation of the intracellular I^- concentration (in pM/s) using the equation $d[I^-]/dt = K_d\ [d(F/F_0)/dt]$, where K_d is the affinity constant of YFP for I^- [159,161], and F/F_0 is the ratio of the cell fluorescence at a given time versus the initial fluorescence. For all statistical analysis, *p*-values bellow 0.05 were considered to be statistically significant.

4.6. Supplementary Material

Supplementary Table S4.1 - Gene ontology-based functional annotation analysis of the subnetwork of 22 proteins with putative direct interactions to CFTR, ezrin or NHERF1 in rescued Phe508del-CFTR at the PM. The analysis was performed on the Functional Annotation Tool DAVID Bioinformatics Resources 6.8, NIAID/NIH using the Gene Ontology terms: GOTERM_BP_DIRECT; GOTERM_CC_DIRECT; and GOTERM_MF_DIRECT.

TERM	PROTEIN COUNT	PERCENTAGE (%)	P-VALUE	FDR (BENJAMINI)
MEMBRANE	11	50	6.40E-05	1.10E-03
EXTRACELLULAR EXOSOME	19	86,4	1.90E-12	1.60E-10
CYTOSOL	15	68,2	1.40E-06	2.90E-05
MELANOSOME	6	27,3	9,00E-08	3.80E-06
FOCAL ADHESION	8	36,4	1.80E-07	5.00E-06
PROTEIN FOLDING	3	13,6	2.10E-02	5.60E-01
UNFOLDED PROTEIN BINDING	4	18,2	3.30E-04	6.90E-03
PROTEIN BIDING	22	100	1.10E-06	6.90E-05
POLY (A) RNA BINDING	8	36,4	3.00E-04	9.30E-03
MYELIN SHEATH	4	18,2	6.80E-04	9.60E-03

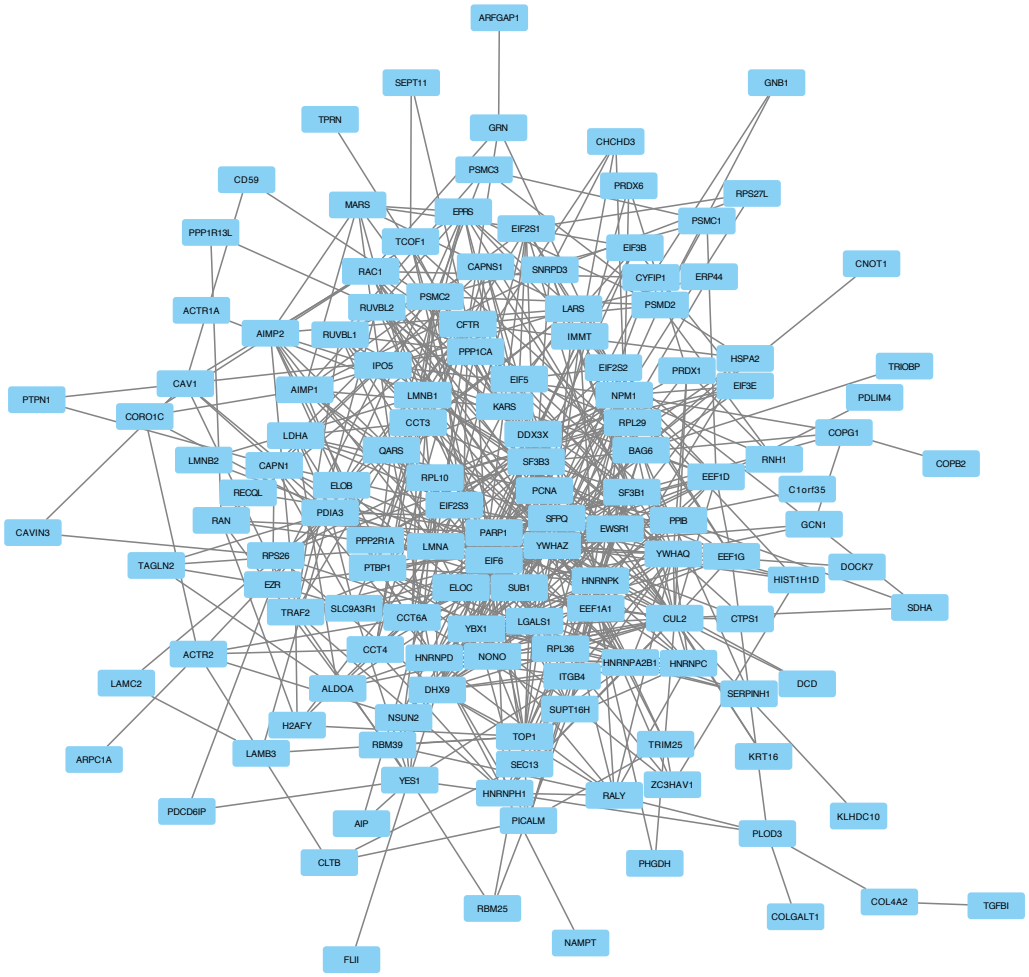

Supplementary Figure S4.1 - Subnetwork of proteins directly interacting with either CFTR, EZR or NHERF1 (SLC9A3R1) Schematic representation of the protein network with direct interactions to CFTR, EZR or NHERF1 that were detected interacting with rescued Phe508del-CFTR at the PM, both through the action of VX-809 or low temperature. [Bioinformatic analysis performed by Francisco Pinto and included with permission]

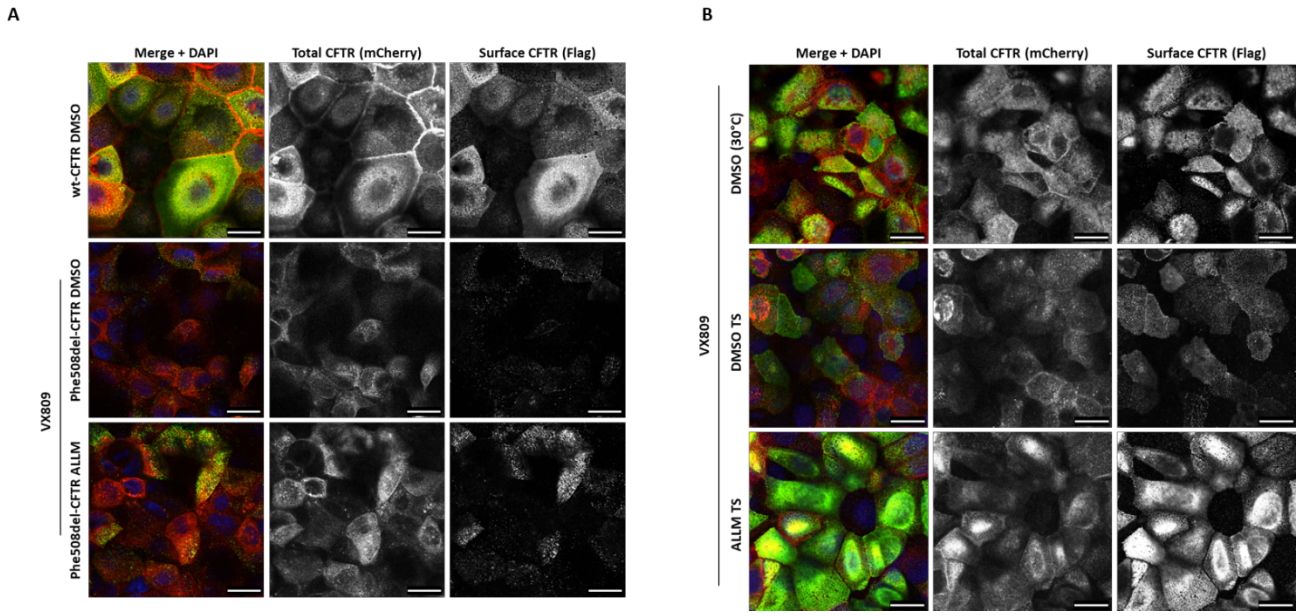

Supplementary Figure S4.2 - Chemical CAPN1 inhibition outcome on rescued PM Phe508del-CFTR abundance and stability

A- Confocal images of Dox-induced CFBEmChF Wt or Phe508del cells, treated with 3 µM VX-809 for 48 hours and co-treated with either DMSO or 250 nM ALLM CAPN1 inhibitor in the last 4 hours. Images are tripled labelled unpermeabilized cells, where mCherry fluorescence is proportional to the total amount of CFTR, AlexaFluor488 fluorescence is proportional to the amount of CFTR present at the cell surface, and nuclei were stained with DAPI. **B -** Confocal images of Dox-induced CFBEmChF Phe508del cells, treated with 3 µM VX-809 for 48 h at 30°C and subjected to a thermal shift (TS) of 4 hours at 37˚C in the presence of either DMSO or 250 nM ALLM CAPN1 inhibitor, except for DMSO low temperature control (30°C). Images acquired as in (A). [Images acquired jointly with Paulo Matos]

Chapter 5
General Discussion

In the field of CF personalized medicine it is imperative to always consider the multidimensional nature of the disease. Even for CF patients carring the Phe508del mutation, a universal treatment is not likely to become a reality, given the complexity of phenotypes observed among the several possible compound-genotypes and even among homozygous patients. The contribution of lung tissue integrity, modifier genes, environmental factors, etc., has to be accounted, while tuning drug combination therapies to each individual patient. This is even more relevant if one considers therapies to fit the plethora of CFTR mutations displaying distinct functional defects, as more than one type of CFTR-modulator drug has to be used [32,40]. In accordance, there are several CFTR-modulator drug combinations under study for the clinical treatment of CF patients with the Phe508del mutation [175,239]. Nonetheless, there are currently no corrective treatment for the reduced apical surface stability and consequential low CFTR PM levels reported for what is, by far, the most common CF mutation. Given the accelerated endocytic rate of Phe508del-CFTR [32,127,131,175], part of the incomplete effectiveness of the available corrector and potentiator compounds [17,42,136] may derive from an inability to sustain sufficient CFTR levels at the apical surface of epithelial cells. Indeed, a PM stabilizer, in combination with the corrector/potentiator combination therapies available [214], could help to overcome the modest benefits achieved with the present treatments [17,42,136]. Thus, with this work, we aimed to identify molecular strategies attaining the PM retention of functional rescued Phe508del-CFTR that can be applied to the benefit of Phe508del-CFTR CF patients.

This dissertation is based on the previous findings by the host lab [40], showing that the RAC1 signaling pathway can be stimulated *via* HGF, the ligand for the c-Met receptor [239,240], to increase the cell surface retention of rescued Phe508del-CFTR. HGF boosted, by ~3-fold, the functional restoration of Phe508del-CFTR rescued by first generation correctors C3 and Corr4a, supporting that a combination of CFTR-modulator drugs is important to restore Phe508del-CFTR multiple functional defects in patients. For that reason, in the present work, we investigated whether acute and prolonged (15-days) HGF co-administration with the FDA- and EMA-approved corrector/potentiator drug combination (VX-809 plus VX-770) [58,59], also enhanced the functional correction of Phe508del-CFTR in polarized airway cells. We found that acute HGF co-treatment with VX-809/VX-770 significantly increased, again by 3-fold, the functional rescue of Phe508del-CFTR. Since it is reported that exposure to VX-770 can interfere with Phe508del-CFTR cell surface stability [47,54], it was surprising that this effect was sustained after prolonged HGF co-treatment with VX-809/VX-770, revelling that HGF protects VX-809-rescued Phe508del-CFTR from VX-770 induced destabilization. The administration of HGF and VX-809/VX-770 for a longer period also allowed us to observe that HGF treatment also protected both airway and intestinal cells against a previously unreported dedifferentiative effect of prolonged exposure to VX-809. These two systems are the most affected by adverse symptoms in patients treated with the VX-809 drug [34,62] and our results suggest that the observed epithelial dedifferentiation effect after prolonged exposure to VX-809 may, at least partially, contribute to these adverse manifestations. Thus, the protective effect to epithelial integrity of prolonged HGF treatment may be of particular interest for patients with severe lung disease (predicted FEV_1 < 40%), which have considerably higher frequency and severity of therapy-related adverse effects [60,204,205]. While HGF is already under clinical trials for its regenerative effects in several conditions [207–209], there are still some concerns regarding its therapeutic administration. Most lie on

the fact that HGF/MET activates several signaling pathways often dysregulated in cancer, namely RAS, PI3K, MAPK/STAT, and β-catenin/Wnt, potentially promoting epithelial cell scattering, proliferation, resistance to apoptosis, increased invasive potential, and neo-angiogenesis [239,241,242]. Despite the fact we have showed here that prolonged administration of HGF had a protective and pro-differentiation effect in bronchial and colorectal epithelium-like monolayers, these observations occurred *in vitro* and have to be further evaluated *in vivo*. Meanwhile, we decided to further explore the mechanisms by which HGF/RAC1 signaling promotes rescued Phe508del-CFTR surface stabilization.

Identifying the different components of a disease-associated signaling pathway or molecular mechanism has often contributed to the development of drug therapies by targeting key elements in disease-related molecular processes [243,244]. From previous work by the host lab [40] we knew that the increased stabilization of apical Phe508del-CFTR occurred upon endogenous RAC1 activation by promoting the tethering of the CFTR/NHERF1/EZR molecular complex to the actin cytoskeleton, delaying the internalization of the rescued channels. Since RAC1 mediated CFTR anchoring requires EZR activation [245], it was acknowledged that this process is a crucial step for its surface retention. By further characterizing this mechanism we found that the PDZ adaptor protein NHERF1 undergoes a conformational change upon EZR activation and binding, inducing CFTR's C-terminal domain to switch its interaction from the NHERF1-PDZ1 to the NHERF1-PDZ2 [37]. This conformational switch precludes the recruitment of CHIP ubiquitin ligase, therefore avoiding rescued Phe508del-CFTR ubiquitination and internalization [36,37]. Remarkably, contrary to previous assumptions, we showed that actin anchoring is a consequence rather than the cause of CFTR surface stabilization, revealing that EZR mediated NHERF1 PDZ switch is the key step to PPQC evasion and decreased CFTR turnover [37]. These findings indicated that, like happens with CHIP, other protein interactions within the macromolecular complexes formed around NHERF1 and rescued CFTR at the membrane may be interfering with EZR recruitment and binding thus precluding CFTR retention and stability at the cell surface. This was further supported by the findings by us and other groups that EZR overexpression can overcome this interference, coaxing its association with rescued Phe508del-CFTR/NHERF1 PM complexes [37,40,226]. This let us to hypothesize that if we could identify what additional proteins are interacting specifically with rescued Phe508del, but not with wt-CFTR, we may be able to directly target the mechanism preventing PM recruitment and binding of active EZR to rescued Phe508del-CFTR/NHERF1 complexes. Therefore, we developed an assay to selectively immunoprecipitate CFTR-containing complexes from the membrane and determine, for the first time, CFTR's specific interactome at the PM compartment. We found 164 high-confidence putative interactors that could be interfering with rescued Phe508del-CFTR stability, which were not detected in wt-CFTR interactome. These were enriched mainly in chaperones and membrane-associated proteins, supporting the compartment-selectivity of our analysis. Also in agreement with this, only 27% of our candidate proteins were found among the whole cell Phe508del-CFTR interactome described by Pankow and colleagues [107], which was mostly enriched in proteins involved in ER quality control and ER-associated degradation pathway. Using a hypothesis-driven bioinformatic analysis we converged our dataset into a subnetwork of 25 core proteins with a high probability to directly interact with rescued Phe508del-CFTR/NHERF1/EZR complexes at the PM, from which Calpain 1 was highlighted as the candidate most

likely to allow pharmacological targeting. Indeed, we demonstrated that by inhibiting Calpain 1, an ubiquitous cytoskeleton and PM associated Ca^{2+} dependent cysteine protease [219], we were able to promote the stabilization of VX-809-rescued Phe508del-CFTR at the PM, leading to a ~4-fold improvement in the functional restoration of CFTR-mediated ion transport. This functional recovery is equivalent to our previous observations with HGF and VX-809 co-treated cells [37,40]. Moreover, we showed that knockdown of Calpain 1 stabilizes Phe508del-CFTR by promoting the association of endogenous EZR with the CFTR/NHERF1 complex at the PM. This again links to our previous findings, where PM retention of corrector-rescued Phe508del-CFTR was promoted by increased levels of active EZR associating to CFTR/NHERF1 complexes at the PM, as a consequence of upregulating endogenous RAC1 signaling by stimulation with HGF [40].

Taking all together, the results obtain in this dissertation have contributed to deepen the knowledge in the field of CF disease, particularly elucidating the molecules and mechanisms regulating the retention and stability of CFTR at the cell surface. It provided novel insights into CFTR interactions occurring at the PM and presents HGF and Calpain 1 inhibitors as two potentially viable modulators to enhance the retention and stability of pharmacologically rescued Phe508del-CFTR at the surface of epithelial cells in CF patients. Importantly, these findings may also have implications in other CF mutations that impair the CFTR PM stability (class VI).

In figure 5.1 is a summary of our main findings targeting the increased retention and stability of VX-809 rescued channels at the cell surface.

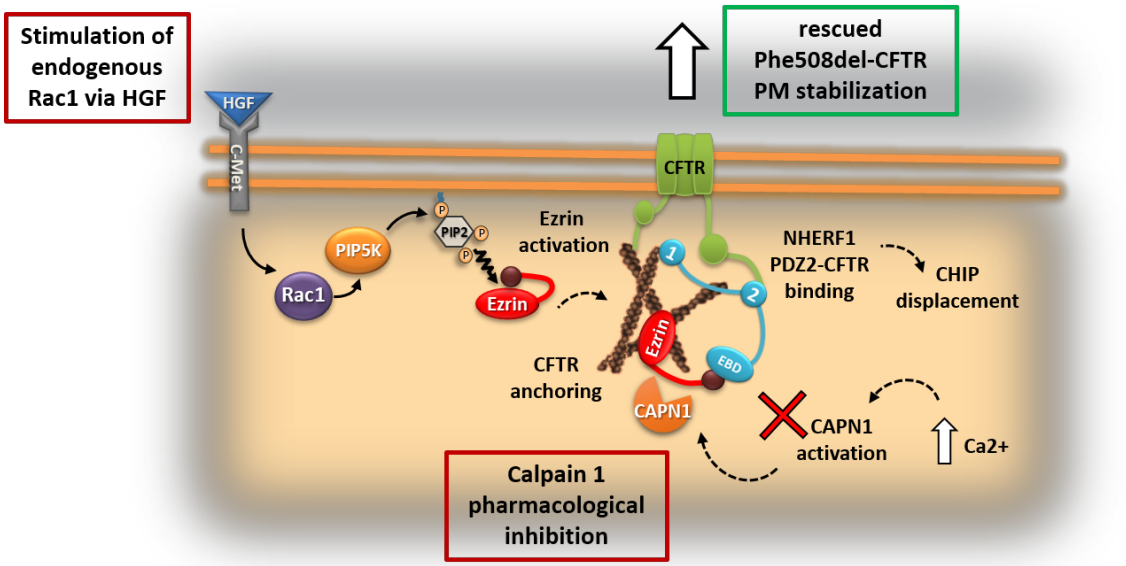

Figure 5.1 - Summary of our main findings targeting the increased retention and stability of rescued Phe508del-CFTR at the cell surface

PM Phe508del-CFTR stabilization can be induced by the stimulation of endogenous RAC1 *via* HGF, which leads to enhanced levels of activated EZR which subsequently coaxes its binding to Phe508del-CFTR/NHERF1 complexes at the PM. EZR binding triggers a conformational change in NHERF1, hindering the recruitment of CHIP ubiquitin ligase, hence evading rescued Phe508del-CFTR ubiquitination and internalization. Another regulator of EZR binding is the Ca^{2+} dependent protease Calpain 1, recruited to rescued Phe508del-CFTR PM complexes upon the characteristic CF elevated intracellular Ca^{2+} levels. At the complex, Calpain 1 may hydrolyse active EZR, impeding its interaction with the CFTR/NHERF1 complex, preventing NHERF1's conformational shift that allows rescued CFTR to bind to its 2nd PDZ leading to its anchoring to the actin cytoskeleton. These results in the accelerated internalization and degradation of rescued channels. By using HGF treatment or Calpain 1 chemical inhibitors one can increase the binding of active EZR to Phe508del-CFTR/NHERF1 complexes and promote the retention and stabilization of the rescued channels at the cell surface.

6. References

1. About Cystic Fibrosis | CF Foundation. Available at: https://www.cff.org/What-is-CF/About-Cystic-Fibrosis/. (Accessed: 28th December 2017)
2. Riordan, J. R. CFTR function and prospects for therapy. *Annu. Rev. Biochem.* **77,** 701–26 (2008).
3. Riordan, J. R. *et al.* Identification of the Cystic Fibrosis Gene : Cloning and Characterization of Complementary DNA. *Science (80-.).* **245,** 1066–73 (1989).
4. Sheppard, D. N. & Welsh, M. J. Structure and function of the CFTR chloride channel. *Physiol. Rev.* **79,** S23-45 (1999).
5. Liu, F. *et al.* Molecular Structure of the Human CFTR Ion Channel. *Cell* **169,** 85–95.e8 (2017).
6. Gunderson, K. L. & Kopito, R. R. Conformational states of CFTR associated with channel gating: The role of ATP binding and hydrolysis. *Cell* **82,** 231–239 (1995).
7. Farinha, C. M., Matos, P. & Amaral, M. D. Control of cystic fibrosis transmembrane conductance regulator membrane trafficking: not just from the endoplasmic reticulum to the Golgi. *FEBS J.* **280,** 4396–406 (2013).
8. Kunzelmann, K. CFTR: interacting with everything? *News Physiol. Sci.* **16,** 167–70 (2001).
9. Sheppard, M. N. & Nicholson, A. G. The pathology of cystic fibrosis. *Curr. Diagnostic Pathol.* **8,** 50–59 (2002).
10. Grossman, S. & Grossman, L. C. Pathophysiology of cystic fibrosis: implications for critical care nurses. *Crit. Care Nurse* **25,** 46–51 (2005).
11. Ehre, C., Ridley, C. & Thornton, D. J. Cystic fibrosis: an inherited disease affecting mucin-producing organs. *Int. J. Biochem. Cell Biol.* **52,** 136–45 (2014).
12. Kreda, S. M., Davis, C. W. & Rose, M. C. CFTR, Mucins, and Mucus Obstruction in Cystic Fibrosis. *Cold Spring Harb. Perspect. Med.* **2,** a009589–a009589 (2012).
13. Donaldson, S. H. & Boucher, R. C. Update on pathogenesis of cystic fibrosis lung disease. *Curr. Opin. Pulm. Med.* **9,** 486–491 (2003).
14. Quinton, P. M. Cystic fibrosis: impaired bicarbonate secretion and mucoviscidosis. *Lancet* **372,** 415–417 (2008).
15. Welcome to CFTR2 | CFTR2. Available at: https://www.cftr2.org/. (Accessed: 28th December 2017)
16. Cystic Fibrosis Mutation Database. Available at: http://www.genet.sickkids.on.ca/cftr/app. (Accessed: 23rd April 2018)
17. Amaral, M. D. & Farinha, C. M. Rescuing Mutant CFTR: A Multi-task Approach to a Better Outcome in Treating Cystic Fibrosis. *Curr. Pharm. Des.* **19,** 0–0 (2013).
18. Amaral, M. D. Novel personalized therapies for cystic fibrosis: treating the basic defect in all patients. *J. Intern. Med.* **277,** 155–166 (2015).
19. Amaral, M. D. & Kunzelmann, K. Molecular targeting of CFTR as a therapeutic approach to cystic fibrosis. *Trends Pharmacol. Sci.* **28,** 334–341 (2007).
20. De Boeck, K. & Amaral, M. D. Progress in therapies for cystic fibrosis. *Lancet. Respir. Med.* **4,** 662–674 (2016).
21. De Boeck, K., Zolin, A., Cuppens, H., Olesen, H. V & Viviani, L. The relative frequency of CFTR mutation classes in European patients with cystic fibrosis. *J. Cyst. Fibros.* **13,** 403–9 (2014).
22. Van Goor, F. *et al.* Rescue of CF airway epithelial cell function in vitro by a CFTR potentiator, VX-770. *Proc. Natl. Acad. Sci. U. S. A.* **106,** 18825–30 (2009).
23. Ramalho, A. S. *et al.* Deletion of CFTR Translation Start Site Reveals Functional Isoforms of the Protein in CF Patients. *Cell. Physiol. Biochem.* **24,** 335–346 (2009).
24. Farinha, C. M. & Amaral, M. D. Most F508del-CFTR is targeted to degradation at an early folding checkpoint and independently of calnexin. *Mol. Cell. Biol.* **25,** 5242–52 (2005).
25. Farinha, C. M. & Canato, S. From the endoplasmic reticulum to the plasma membrane: mechanisms of CFTR folding and trafficking. *Cell. Mol. Life Sci.* **74,** 39–55 (2017).
26. Amaral, M. D. Processing of CFTR: traversing the cellular maze--how much CFTR needs to go through to avoid cystic fibrosis? *Pediatr. Pulmonol.* **39,** 479–91 (2005).
27. Lukacs, G. L. & Verkman, A. S. CFTR: folding, misfolding and correcting the ΔF508 conformational defect. *Trends Mol. Med.* **18,** 81–91 (2012).
28. Pedemonte, N. & Galietta, L. J. V. Pharmacological correctors of mutant CFTR mistrafficking. *Front. Pharmacol.* **3 OCT,** 1–7 (2012).
29. Denning, G. M. *et al.* Processing of mutant cystic fibrosis transmembrane conductance regulator is temperature-sensitive. *Nature* **358,** 761–764 (1992).
30. Kunzelmann, K. & Mall, M. Pharmacotherapy of the Ion Transport Defect in Cystic Fibrosis. *Am. J. Respir. Med.*

2, 299–309 (2003).
31. Kerem, E. Pharmacological induction of CFTR function in patients with cystic fibrosis: mutation-specific therapy. *Pediatr. Pulmonol.* **40,** 183–196 (2005).
32. Drug Development Pipeline | CFF Clinical Trials Tool. Available at: https://www.cff.org/Trials/Pipeline. (Accessed: 14th December 2017)
33. Ren, H. Y. *et al.* VX-809 corrects folding defects in cystic fibrosis transmembrane conductance regulator protein through action on membrane-spanning domain 1. *Mol. Biol. Cell* **24,** 3016–24 (2013).
34. Clancy, J. P. *et al.* Results of a phase IIa study of VX-809, an investigational CFTR corrector compound, in subjects with cystic fibrosis homozygous for the F508del-CFTR mutation. *Thorax* **67,** 12–8 (2012).
35. Ramsey, B. W. *et al.* A CFTR Potentiator in Patients with Cystic Fibrosis and the *G551D* Mutation. *N. Engl. J. Med.* **365,** 1663–1672 (2011).
36. Okiyoneda, T. *et al.* Peripheral protein quality control removes unfolded CFTR from the plasma membrane. *Science* **329,** 805–10 (2010).
37. Loureiro, C. A. *et al.* A molecular switch in the scaffold NHERF1 enables misfolded CFTR to evade the peripheral quality control checkpoint. *Sci. Signal.* **8,** ra48-ra48 (2015).
38. Gentzsch, M. *et al.* Endocytic Trafficking Routes of Wild Type and ⌬ F508 Regulator □. *Mol. Biol. Cell* **15,** 2684–2696 (2004).
39. Ashlock, M. A. & Olson, E. R. Therapeutics Development for Cystic Fibrosis: A Successful Model for a Multisystem Genetic Disease. *Annu. Rev. Med.* **62,** 107–125 (2011).
40. Moniz, S. *et al.* HGF stimulation of Rac1 signaling enhances pharmacological correction of the most prevalent cystic fibrosis mutant F508del-CFTR. *ACS Chem. Biol.* **8,** 432–42 (2013).
41. D. Amaral, M. & M. Farinha, C. Rescuing Mutant CFTR: A Multi-task Approach to a Better Outcome in Treating Cystic Fibrosis. *Curr. Pharm. Des.* **19,** 3497–3508 (2013).
42. Farinha, C. M. & Matos, P. Repairing the basic defect in cystic fibrosis - one approach is not enough. *FEBS J.* **283,** 246–264 (2016).
43. Investigational Medicines (Pipeline) | Vertex Pharmaceuticals. Available at: https://www.vrtx.com/pipeline-medicines/investigational-medicines-pipeline. (Accessed: 12th December 2017)
44. Konstan, M. W. *et al.* Design and powering of cystic fibrosis clinical trials using rate of FEV(1) decline as an efficacy endpoint. *J. Cyst. Fibros.* **9,** 332–8 (2010).
45. Kerem, E. *et al.* Factors associated with FEV1 decline in cystic fibrosis: analysis of the ECFS Patient Registry. *Eur. Respir. J.* **43,** 125–133 (2014).
46. Flume, P. A. *et al.* Ivacaftor in subjects with cystic fibrosis who are homozygous for the F508del-CFTR mutation. *Chest* **142,** 718–724 (2012).
47. Cholon, D. M. *et al.* Potentiator ivacaftor abrogates pharmacological correction of ΔF508 CFTR in cystic fibrosis. *Sci. Transl. Med.* **6,** 246ra96 (2014).
48. Van Goor, F. *et al.* Correction of the F508del-CFTR protein processing defect in vitro by the investigational drug VX-809. *Proc. Natl. Acad. Sci. U. S. A.* **108,** 18843–8 (2011).
49. Farinha, C. M. *et al.* Revertants, low temperature, and correctors reveal the mechanism of F508del-CFTR rescue by VX-809 and suggest multiple agents for full correction. *Chem. Biol.* **20,** 943–55 (2013).
50. Okiyoneda, T. *et al.* Mechanism-based corrector combination restores ΔF508-CFTR folding and function. *Nat. Chem. Biol.* **9,** 444–454 (2013).
51. Sloane, P. A. & Rowe, S. M. Cystic fibrosis transmembrane conductance regulator protein repair as a therapeutic strategy in cystic fibrosis. *Curr. Opin. Pulm. Med.* **16,** 591–597 (2010).
52. Boyle, M. P. *et al.* A CFTR corrector (lumacaftor) and a CFTR potentiator (ivacaftor) for treatment of patients with cystic fibrosis who have a phe508del CFTR mutation: a phase 2 randomised controlled trial. *Lancet. Respir. Med.* **2,** 527–38 (2014).
53. Wainwright, C. E. *et al.* Lumacaftor–Ivacaftor in Patients with Cystic Fibrosis Homozygous for Phe508del *CFTR*. *N. Engl. J. Med.* **373,** 220–231 (2015).
54. Veit, G. *et al.* Some gating potentiators, including VX-770, diminish ⌬F508-CFTR functional expression. *Sci. Transl. Med.* **6,** 246ra97-246ra97 (2014).
55. Matthes, E. *et al.* Low free drug concentration prevents inhibition of F508del CFTR functional expression by the potentiator VX-770 (ivacaftor). *Br. J. Pharmacol.* (2015). doi:10.1111/bph.13365
56. Stanton, B. A. Effects of *Pseudomonas aeruginosa* on CFTR chloride secretion and the host immune response. *Am. J. Physiol. - Cell Physiol.* **312,** C357–C366 (2017).
57. Stanton, B. A., Coutermarsh, B., Barnaby, R. & Hogan, D. Pseudomonas aeruginosa Reduces VX-809 Stimulated F508del-CFTR Chloride Secretion by Airway Epithelial Cells. *PLoS One* **10,** e0127742 (2015).
58. ORKAMBI® (lumacaftor/ivacaftor) Tablets. Available at: https://www.orkambi.com/. (Accessed: 2nd January

2018)
59. Our Approved Medicines | Vertex Pharmaceuticals. Available at: https://www.vrtx.com/pipeline-medicines/our-approved-medicines. (Accessed: 29th December 2017)
60. Hubert, D. *et al.* Real-life initiation of lumacaftor/ivacaftor combination in adults with cystic fibrosis homozygous for the Phe508del CFTR mutation and severe lung disease. *J. Cyst. Fibros.* **16,** 388–391 (2017).
61. Konstan, M. W. *et al.* Assessment of safety and efficacy of long-term treatment with combination lumacaftor and ivacaftor therapy in patients with cystic fibrosis homozygous for the F508del-CFTR mutation (PROGRESS): a phase 3, extension study. *Lancet Respir. Med.* **5,** 107–118 (2017).
62. Jennings, M. T. *et al.* An Observational Study of Outcomes and Tolerances in Patients with Cystic Fibrosis Initiated on Lumacaftor/Ivacaftor. *Ann. Am. Thorac. Soc.* **14,** 1662–1666 (2017).
63. Eckford, P. D. W. *et al.* VX-809 and Related Corrector Compounds Exhibit Secondary Activity Stabilizing Active F508del-CFTR after Its Partial Rescue to the Cell Surface. *Chem. Biol.* **21,** 666–678 (2014).
64. Donaldson, S. H. *et al.* Tezacaftor/Ivacaftor in Subjects with Cystic Fibrosis and F508del/F508del-CFTR or F508del/G551D-CFTR. *Am. J. Respir. Crit. Care Med.* rccm.201704-0717OC (2017). doi:10.1164/rccm.201704-0717OC
65. Rowe, S. M. *et al.* Tezacaftor–Ivacaftor in Residual-Function Heterozygotes with Cystic Fibrosis. *N. Engl. J. Med.* **377,** 2024–2035 (2017).
66. Taylor-Cousar, J. L. *et al.* Tezacaftor–Ivacaftor in Patients with Cystic Fibrosis Homozygous for Phe508del. *N. Engl. J. Med.* **377,** 2013–2023 (2017).
67. Vertex Announces Positive Phase 1 & Phase 2 Data from Three Different Triple Combination Regimens in People with Cystic Fibrosis Who Have One F508del Mutation and One Minimal Function Mutation (F508del/Min) (NASDAQ:VRTX). Available at: http://investors.vrtx.com/releasedetail.cfm?releaseid=1033559. (Accessed: 14th December 2017)
68. A Study Evaluating the Safety and Efficacy of VX-440 Combination Therapy in Subjects With Cystic Fibrosis - Full Text View - ClinicalTrials.gov. Available at: https://clinicaltrials.gov/ct2/show/NCT02951182. (Accessed: 12th December 2017)
69. A Study Evaluating the Safety of VX-152 Combination Therapy in Adults With Cystic Fibrosis - Full Text View - ClinicalTrials.gov. Available at: https://clinicaltrials.gov/ct2/show/NCT02951195. (Accessed: 2nd December 2018)
70. A Study to Evaluate Safety and Pharmacokinetics of VX-659 in Healthy Subjects and in Adults With Cystic Fibrosis - Full Text View - ClinicalTrials.gov. Available at: https://clinicaltrials.gov/ct2/show/NCT03029455. (Accessed: 12th December 2017)
71. Beumer, W. *et al.* WS01.2 QR-010, an RNA therapy, restores CFTR function using in vitro and in vivo models of ΔF508 CFTR. *J. Cyst. Fibros.* **14,** S1 (2015).
72. Zamecnik, P. C., Raychowdhury, M. K., Tabatadze, D. R. & Cantiello, H. F. Reversal of cystic fibrosis phenotype in a cultured 508 cystic fibrosis transmembrane conductance regulator cell line by oligonucleotide insertion. *Proc. Natl. Acad. Sci.* **101,** 8150–8155 (2004).
73. Solomon, G. M., Marshall, S. G., Ramsey, B. W. & Rowe, S. M. Breakthrough therapies: Cystic fibrosis (CF) potentiators and correctors. *Pediatr. Pulmonol.* **50,** S3–S13 (2015).
74. Nivalis Therapeutics Announces Results from Phase 2 Clinical Trial of Cavosonstat Added to Ivacaftor for Treatment of Cystic Fibrosis Nasdaq:NVLS. Available at: https://globenewswire.com/news-release/2017/02/23/927232/0/en/Nivalis-Therapeutics-Announces-Results-from-Phase-2-Clinical-Trial-of-Cavosonstat-Added-to-Ivacaftor-for-Treatment-of-Cystic-Fibrosis.html. (Accessed: 8th January 2018)
75. Grasemann, H., Gaston, B., Fang, K., Paul, K. & Ratjen, F. Decreased levels of nitrosothiols in the lower airways of patients with cystic fibrosis and normal pulmonary function. *J. Pediatr.* **135,** 770–2 (1999).
76. Hutt, D. M. *et al.* Reduced histone deacetylase 7 activity restores function to misfolded CFTR in cystic fibrosis. *Nat. Chem. Biol.* **6,** 25–33 (2010).
77. Bergougnoux, A. *et al.* The HDAC inhibitor SAHA does not rescue CFTR membrane expression in Cystic Fibrosis. *Int. J. Biochem. Cell Biol.* **88,** 124–132 (2017).
78. Proteostasis Therapeutics Announces Progression of PTI-428 and PTI-801 to Longer Duration Studies in CF Subjects | Proteostasis Therapeutics. Available at: http://ir.proteostasis.com/news-releases/news-release-details/proteostasis-therapeutics-announces-progression-pti-428-and-pti. (Accessed: 8th January 2018)
79. Wang, X. *et al.* Discovery of 4-[(2 *R* ,4 *R*)-4-({[1-(2,2-Difluoro-1,3-benzodioxol-5-yl)cyclopropyl]carbonyl}amino)-7-(difluoromethoxy)-3,4-dihydro-2 *H* -chromen-2-yl]benzoic Acid (ABBV/GLPG-2222), a Potent Cystic Fibrosis Transmembrane Conductance Regulator (CFTR) Corrector for the Treatment of Cystic Fibrosis. *J. Med. Chem.* acs.jmedchem.7b01339 (2018). doi:10.1021/acs.jmedchem.7b01339
80. Mijnders, M., Kleizen, B. & Braakman, I. Correcting CFTR folding defects by small-molecule correctors to cure

cystic fibrosis. *Curr. Opin. Pharmacol.* **34,** 83–90 (2017).
81. Zawistoski, M. *et al.* 32 Properties of a novel F508del-CFTR corrector FDL169. *J. Cyst. Fibros.* **15,** S59–S60 (2016).
82. QBW251 Is a Safe and Efficacious CFTR Potentiator for Patients with Cystic Fibrosis.
83. French, P. J. *et al.* Genistein activates CFTR Cl- channels via a tyrosine kinase- and protein phosphatase-independent mechanism. *Am. J. Physiol. Physiol.* **273,** C747–C753 (1997).
84. Wang, W., Bernard, K., Li, G. & Kirk, K. L. Curcumin Opens Cystic Fibrosis Transmembrane Conductance Regulator Channels by a Novel Mechanism That Requires neither ATP Binding nor Dimerization of the Nucleotide-binding Domains. *J. Biol. Chem.* **282,** 4533–4544 (2007).
85. Eckford, P. D. W., Li, C., Ramjeesingh, M. & Bear, C. E. Cystic Fibrosis Transmembrane Conductance Regulator (CFTR) Potentiator VX-770 (Ivacaftor) Opens the Defective Channel Gate of Mutant CFTR in a Phosphorylation-dependent but ATP-independent Manner. *J. Biol. Chem.* **287,** 36639–36649 (2012).
86. Wang, G. The Inhibition Mechanism of Non-phosphorylated Ser 768 in the Regulatory Domain of Cystic Fibrosis Transmembrane Conductance Regulator. *J. Biol. Chem.* **286,** 2171–2182 (2011).
87. Moran, O., Galietta, L. J. V. & Zegarra-Moran, O. Binding site of activators of the cystic fibrosis transmembrane conductance regulator in the nucleotide binding domains. *C. Cell. Mol. Life Sci.* **62,** 446–460 (2005).
88. Sohma, Y., Yu, Y.-C. & Hwang, T.-C. Curcumin and genistein: the combined effects on disease-associated CFTR mutants and their clinical implications. *Curr. Pharm. Des.* **19,** 3521–8 (2013).
89. Dekkers, J. F. *et al.* Potentiator synergy in rectal organoids carrying S1251N, G551D, or F508del CFTR mutations. *J. Cyst. Fibros.* **15,** 568–578 (2016).
90. Wang, G. Molecular Basis for Fe(III)-Independent Curcumin Potentiation of Cystic Fibrosis Transmembrane Conductance Regulator Activity. *Biochemistry* **54,** 2828–2840 (2015).
91. Wang, G., Linsley, R. & Norimatsu, Y. External Zn 2+ binding to cysteine-substituted cystic fibrosis transmembrane conductance regulator constructs regulates channel gating and curcumin potentiation. *FEBS J.* **283,** 2458–2475 (2016).
92. Wang, G. Interplay between Inhibitory Ferric and Stimulatory Curcumin Regulates Phosphorylation-Dependent Human Cystic Fibrosis Transmembrane Conductance Regulator and ΔF508 Activity. *Biochemistry* **54,** 1558–1566 (2015).
93. Gonçalves, C. *et al.* Curcumin/poly(2-methyl-2-oxazoline-b-tetrahydrofuran-b-2-methyl-2-oxazoline) formulation: An improved penetration and biological effect of curcumin in F508del-CFTR cell lines. *Eur. J. Pharm. Biopharm.* **117,** 168–181 (2017).
94. Davies, G. *et al.* T4 Safety and expression of a single dose of lipid-mediated CFTR gene therapy to the upper and lower airways of patients with Cystic Fibrosis. *Thorax* **66,** A2–A2 (2011).
95. Alton, E. W. F. W. *et al.* Repeated nebulisation of non-viral CFTR gene therapy in patients with cystic fibrosis: a randomised, double-blind, placebo-controlled, phase 2b trial. *Lancet. Respir. Med.* **3,** 684–691 (2015).
96. Sousa, M. *et al.* HGF Stimulation of Rac1 Signaling Enhances Pharmacological Correction of the Most Prevalent Cystic Fibrosis Mutant F508del- CFTR. (2012).
97. Zeng, L. *et al.* The cellular kinetics of lung alveolar epithelial cells and its relationship with lung tissue repair after acute lung injury. *Respir. Res.* **17,** 164 (2016).
98. Wang, S. & Li, M. Molecular studies of CFTR interacting proteins. *Pflugers Arch. Eur. J. Physiol.* **443,** 62–64 (2001).
99. Li, C. & Naren, A. P. Macromolecular complexes of cystic fibrosis transmembrane conductance regulator and its interacting partners. *Pharmacol. Ther.* **108,** 208–223 (2005).
100. Okiyoneda, T. & Lukacs, G. L. Cell surface dynamics of CFTR: the ins and outs. *Biochim. Biophys. Acta* **1773,** 476–9 (2007).
101. Li, C. & Naren, A. P. CFTR chloride channel in the apical compartments: spatiotemporal coupling to its interacting partners. *Integr. Biol. (Camb).* **2,** 161–77 (2010).
102. Moyer, B. D. *et al.* The PDZ-interacting domain of cystic fibrosis transmembrane conductance regulator is required for functional expression in the apical plasma membrane. *J. Biol. Chem.* **275,** 27069–74 (2000).
103. Li, C. & Naren, A. P. Analysis of CFTR Interactome in the Macromolecular Complexes. doi:10.1007/978-1-61779-117-8_17
104. Reczek, D. & Bretscher, A. The Carboxyl-terminal Region of EBP50 Binds to a Site in the Amino-terminal Domain of Ezrin That Is Masked in the Dormant Molecule. *J. Biol. Chem.* **273,** 18452–18458 (1998).
105. Short, D. B. *et al.* An Apical PDZ Protein Anchors the Cystic Fibrosis Transmembrane Conductance Regulator to the Cytoskeleton. *J. Biol. Chem.* **273,** 19797–19801 (1998).
106. Wang, X. *et al.* Hsp90 Cochaperone Aha1 Downregulation Rescues Misfolding of CFTR in Cystic Fibrosis. *Cell* **127,** 803–815 (2006).
107. Pankow, S. *et al.* ΔF508 CFTR interactome remodelling promotes rescue of cystic fibrosis. *Nature* **advance on,**

(2015).
108. Pankow, S., Bamberger, C., Calzolari, D., Bamberger, A. & Yates Iiird, J. R. Deep interactome profiling of membrane proteins by Co- interacting Protein Identification Technology (CoPIT) HHS Public Access. *Nat Protoc* **11,** 2515–2528 (2016).
109. Haggie, P. M., Kim, J. K., Lukacs, G. L. & Verkman, A. S. Tracking of Quantum Dot-labeled CFTR Shows Near Immobilization by C-Terminal PDZ Interactions □ D □ V. *Mol. Biol. Cell* **17,** 4937–4945 (2006).
110. Wang, S., Raab, R. W., Schatz, P. J., Guggino, W. B. & Li, M. Peptide binding consensus of the NHE-RF-PDZ1 domain matches the C-terminal sequence of cystic fibrosis transmembrane conductance regulator (CFTR). *FEBS Lett.* **427,** 103–108 (1998).
111. Bretscher, A., Chambers, D., Nguyen, R. & Reczek, D. ERM-Merlin and EBP50 Protein Families in Plasma Membrane Organization and Function. *Annu. Rev. Cell Dev. Biol.* **16,** 113–143 (2000).
112. Li, J., Callaway, D. J. E. & Bu, Z. Ezrin induces long-range interdomain allostery in the scaffolding protein NHERF1. *J. Mol. Biol.* **392,** 166–80 (2009).
113. Morales, F. C., Takahashi, Y., Kreimann, E. L. & Georgescu, M.-M. Ezrin-radixin-moesin (ERM)-binding phosphoprotein 50 organizes ERM proteins at the apical membrane of polarized epithelia. *Proc. Natl. Acad. Sci. U. S. A.* **101,** 17705–10 (2004).
114. Reczek, D., Berryman, M. & Bretscher, A. Identification of EBP50: A PDZ-containing phosphoprotein that associates with members of the ezrin-radixin-moesin family. *J. Cell Biol.* **139,** 169–79 (1997).
115. Fievet, B. T. *et al.* Phosphoinositide binding and phosphorylation act sequentially in the activation mechanism of ezrin. *J. Cell Biol.* **164,** 653–659 (2004).
116. Hao, J.-J. *et al.* Phospholipase C-mediated hydrolysis of PIP2 releases ERM proteins from lymphocyte membrane. *J. Cell Biol.* **184,** 451–62 (2009).
117. Fiévet, B., Louvard, D. & Arpin, M. ERM proteins in epithelial cell organization and functions. *Biochim. Biophys. Acta - Mol. Cell Res.* **1773,** 653–660 (2007).
118. Bosk, S., Braunger, J. A., Gerke, V. & Steinem, C. Activation of F-Actin Binding Capacity of Ezrin: Synergism of PIP 2 Interaction and Phosphorylation. *Biophysj* **100,** 1708–1717 (2011).
119. Crepaldi, T., Gautreau, A., Comoglio, P. M., Louvard, D. & Arpin, M. Ezrin Is an Effector of Hepatocyte Growth Factor–mediated Migration and Morphogenesis in Epithelial Cells. *J. Cell Biol.* **138,** 423–434 (1997).
120. Matsui, T. *et al.* Rho-kinase phosphorylates COOH-terminal threonines of ezrin/radixin/moesin (ERM) proteins and regulates their head-to-tail association. *J. Cell Biol.* **140,** 647–57 (1998).
121. Simons, P. C., Pietromonaco, S. F., Reczek, D., Bretscher, A. & Elias, L. C-Terminal Threonine Phosphorylation Activates ERM Proteins to Link the Cell's Cortical Lipid Bilayer to the Cytoskeleton. *Biochem. Biophys. Res. Commun.* **253,** 561–565 (1998).
122. Ng, T. *et al.* Ezrin is a downstream effector of trafficking PKC-integrin complexes involved in the control of cell motility. *EMBO J.* **20,** 2723–41 (2001).
123. Cushing, P. R., Fellows, A., Villone, D., Boisguérin, P. & Madden, D. R. The Relative Binding Affinities of PDZ Partners for CFTR: A Biochemical Basis for Efficient Endocytic Recycling †. *Biochemistry* **47,** 10084–10098 (2008).
124. Bhattacharya, S. *et al.* A conformational switch in the scaffolding protein NHERF1 controls autoinhibition and complex formation. *J. Biol. Chem.* **285,** 9981–94 (2010).
125. Guggino, W. B. & Stanton, B. A. New insights into cystic fibrosis: molecular switches that regulate CFTR. *Nat. Rev. Mol. Cell Biol.* **7,** 426–436 (2006).
126. Bertrand, C. A. & Frizzell, R. A. The role of regulated CFTR trafficking in epithelial secretion. *Am. J. Physiol. Physiol.* **285,** C1–C18 (2003).
127. Prince, L. S., Workman, R. B. & Marchase, R. B. Rapid endocytosis of the cystic fibrosis transmembrane conductance regulator chloride channel. *Proc. Natl. Acad. Sci. U. S. A.* **91,** 5192–6 (1994).
128. Lukacs, G. L., Segal, G., Kartner, N., Grinstein, S. & Zhang, F. Constitutive internalization of cystic fibrosis transmembrane conductance regulator occurs via clathrin-dependent endocytosis and is regulated by protein phosphorylation. *Biochem J.* **361,** 353–361 (1997).
129. Hu, W., Howard, M. & Lukacs, G. L. Multiple endocytic signals in the C-terminal tail of the cystic fibrosis transmembrane conductance regulator. *Biochem. J.* **354,** 561–72 (2001).
130. Cheng, J., Wang, H. & Guggino, W. B. Modulation of mature cystic fibrosis transmembrane regulator protein by the PDZ domain protein CAL. *J. Biol. Chem.* **279,** 1892–8 (2004).
131. Swiatecka-Urban, A. *et al.* The Short Apical Membrane Half-life of Rescued ΔF508-Cystic Fibrosis Transmembrane Conductance Regulator (CFTR) Results from Accelerated Endocytosis of ΔF508-CFTR in Polarized Human Airway Epithelial Cells. *J. Biol. Chem.* **280,** 36762–36772 (2005).
132. Ganeshan, R., Nowotarski, K., Di, A., Nelson, D. J. & Kirk, K. L. CFTR surface expression and chloride currents are

decreased by inhibitors of N-WASP and actin polymerization.
133. Ridley, A. J. Rho GTPases and actin dynamics in membrane protrusions and vesicle trafficking. *Trends Cell Biol.* **16,** 522–529 (2006).
134. Jaffe, A. B. & Hall, A. RHO GTPASES: Biochemistry and Biology. *Annu. Rev. Cell Dev. Biol.* **21,** 247–269 (2005).
135. Guerra, L. *et al.* Na+/H+ exchanger regulatory factor isoform 1 overexpression modulates cystic fibrosis transmembrane conductance regulator (CFTR) expression and activity in human airway 16HBE14o- cells and rescues DeltaF508 CFTR functional expression in cystic fibrosis ce. *J. Biol. Chem.* **280,** 40925–33 (2005).
136. Ameen, N., Silvis, M. & Bradbury, N. A. Endocytic trafficking of CFTR in health and disease. *J. Cyst. Fibros.* **6,** 1–14 (2007).
137. Wolde, M. *et al.* Targeting CAL as a negative regulator of DeltaF508-CFTR cell-surface expression: an RNA interference and structure-based mutagenetic approach. *J. Biol. Chem.* **282,** 8099–109 (2007).
138. Chaudhuri, T. K. & Paul, S. Protein-misfolding diseases and chaperone-based therapeutic approaches. *FEBS Journal* (2006). doi:10.1111/j.1742-4658.2006.05181.x
139. Conn, P. M. & Ulloa-Aguirre, A. Pharmacological Chaperones for Misfolded Gonadotropin-Releasing Hormone Receptors. *Adv. Pharmacol.* (2011). doi:10.1016/B978-0-12-385952-5.00008-7
140. Bell, S. C., De Boeck, K. & Amaral, M. D. New pharmacological approaches for cystic fibrosis: Promises, progress, pitfalls. *Pharmacol. Ther.* (2014). doi:10.1016/j.pharmthera.2014.06.005
141. Two 24-Week Phase 3 Studies of Lumacaftor in Combination with Ivacaftor Met Primary Endpoint with Statistically Significant Improvements in Lung Function (FEV1) in People with Cystic Fibrosis who have Two Copies of the F508del Mutation | Vertex Pharmaceuticals. Available at: https://investors.vrtx.com/news-releases/news-release-details/two-24-week-phase-3-studies-lumacaftor-combination-ivacaftor-met. (Accessed: 1st October 2018)
142. Van Goor, F., Yu, H., Burton, B. & Hoffman, B. J. Effect of ivacaftor on CFTR forms with missense mutations associated with defects in protein processing or function. *J. Cyst. Fibros.* (2014). doi:10.1016/j.jcf.2013.06.008
143. Sharma, M. *et al.* Misfolding diverts CFTR from recycling to degradation: quality control at early endosomes. *J. Cell Biol.* **164,** 923–33 (2004).
144. Apaja, P. M., Xu, H. & Lukacs, G. L. Quality control for unfolded proteins at the plasma membrane. *J. Cell Biol.* (2010). doi:10.1083/jcb.201006012
145. Hall, A. Rho family GTPases. *Biochem. Soc. Trans.* (2012). doi:10.1042/BST20120103
146. Nakamura, T., Sakai, K., Nakamura, T. & Matsumoto, K. Hepatocyte growth factor twenty years on: Much more than a growth factor. *J. Gastroenterol. Hepatol.* (2011). doi:10.1111/j.1440-1746.2010.06549.x
147. Panganiban, R. A. M. & Day, R. M. Hepatocyte growth factor in lung repair and pulmonary fibrosis. *Acta Pharmacol. Sin.* **32,** 12–20 (2011).
148. Birukova, A. a, Moldobaeva, N., Xing, J. & Birukov, K. G. Magnitude-dependent effects of cyclic stretch on HGF- and VEGF-induced pulmonary endothelial remodeling and barrier regulation. *Am. J. Physiol. Lung Cell. Mol. Physiol.* (2008). doi:10.1152/ajplung.90236.2008
149. Birukova, A. a, Alekseeva, E., Mikaelyan, A. & Birukov, K. G. HGF attenuates thrombin-induced endothelial permeability by Tiam1-mediated activation of the Rac pathway and by Tiam1/Rac-dependent inhibition of the Rho pathway. *FASEB J.* (2007). doi:10.1096/fj.06-7660com
150. Li, J., Dai, Z., Jana, D., Callaway, D. J. E. & Bu, Z. Ezrin controls the macromolecular complexes formed between an adapter protein Na+/H+ exchanger regulatory factor and the cystic fibrosis transmembrane conductance regulator. *J. Biol. Chem.* **280,** 37634–37643 (2005).
151. Smyth, E. C., Sclafani, F. & Cunningham, D. Emerging molecular targets in oncology: clinical potential of MET/hepatocyte growth-factor inhibitors. *Onco. Targets. Ther.* (2014). doi:10.2147/OTT.S44941
152. Stam, J. C. *et al.* Targeting of Tiam1 to the plasma membrane requires the cooperative function of the N-terminal pleckstrin homology domain and an adjacent protein interaction domain. *J. Biol. Chem.* (1997). doi:10.1074/jbc.272.45.28447
153. Hallows, K. R. *et al.* Up-regulation of AMP-activated kinase by dysfunctional cystic fibrosis transmembrane conductance regulator in cystic fibrosis airway epithelial cells mitigates excessive inflammation. *J. Biol. Chem.* (2006). doi:10.1074/jbc.M511029200
154. Almaça, J. *et al.* Functional genomics assays to study CFTR traffic and ENaC function. *Methods Mol. Biol.* **742,** 249–64 (2011).
155. Swiatecka-Urban, A. *et al.* PDZ domain interaction controls the endocytic recycling of the cystic fibrosis transmembrane conductance regulator. *J. Biol. Chem.* **277,** 40099–40105 (2002).
156. Guerra, L. *et al.* Na+/H+ exchanger regulatory factor isoform 1 overexpression modulates cystic fibrosis transmembrane conductance regulator (CFTR) expression and activity in human airway 16HBE14o- cells and rescues ??F508 CFTR functional expression in cystic fibrosis cells. *J. Biol. Chem.* (2005).

doi:10.1074/jbc.M505103200
157. Morales, F. C. *et al.* NHERF1/EBP50 head-to-tail intramolecular interaction masks association with PDZ domain ligands. *Mol. Cell. Biol.* **27,** 2527–37 (2007).
158. Bossard, F. *et al.* β1, β2, and β3 adrenoceptors and Na+/H + Exchanger Regulatory Factor 1 expression in human bronchi and their modifications in cystic fibrosis. *Am. J. Respir. Cell Mol. Biol.* (2010). doi:10.1165/rcmb.2009-0372OC
159. Galietta, L. J. ., Haggie, P. M. & Verkman, A. . Green fluorescent protein-based halide indicators with improved chloride and iodide affinities. *FEBS Lett.* **499,** 220–224 (2001).
160. Yang, H. *et al.* Nanomolar affinity small molecule correctors of defective Delta F508-CFTR chloride channel gating. *J. Biol. Chem.* **278,** 35079–85 (2003).
161. Caputo, A. *et al.* Mutation-specific potency and efficacy of cystic fibrosis transmembrane conductance regulator chloride channel potentiators. *J. Pharmacol. Exp. Ther.* **330,** 783–91 (2009).
162. Farinha, C. M., Nogueira, P., Mendes, F., Penque, D. & Amaral, M. D. The human DnaJ homologue (Hdj)-1/heat-shock protein (Hsp) 40 co-chaperone is required for the in vivo stabilization of the cystic fibrosis transmembrane conductance regulator by Hsp70. *Biochem. J.* (2002). doi:10.1042/bj20011717
163. Saxena, A. *et al.* Human heat shock protein 105/110 kDa (Hsp105/110) regulates biogenesis and quality control of misfolded cystic fibrosis transmembrane conductance regulator at multiple levels. *J. Biol. Chem.* (2012). doi:10.1074/jbc.M111.297580
164. He, L. *et al.* Correctors of ??F508 CFTR restore global conformational maturation without thermally stabilizing the mutant protein. *FASEB J.* (2013). doi:10.1096/fj.12-216119
165. Arora, K. *et al.* Stabilizing Rescued Surface-Localized ΔF508 CFTR by Potentiation of Its Interaction with Na + /H + Exchanger Regulatory Factor 1. (2014). doi:10.1021/bi401263h
166. Bradford, E. M., Sartor, M. A., Gawenis, L. R., Clarke, L. L. & Shull, G. E. Reduced NHE3-mediated Na+ absorption increases survival and decreases the incidence of intestinal obstructions in cystic fibrosis mice. *AJP Gastrointest. Liver Physiol.* (2009). doi:10.1152/ajpgi.90520.2008
167. Georgescu, Morales, Molina & Hayashi. Roles of NHERF1/EBP50 in cancer. *Curr. Mol. Med.* (2008). doi:10.2174/156652408785748031
168. Botelho, H. M. *et al.* Protein traffic disorders: an effective high-throughput fluorescence microscopy pipeline for drug discovery. *Sci. Rep.* **5,** 9038 (2015).
169. Matos, P. *et al.* B-RafV600ECooperates With Alternative Spliced Rac1b to Sustain Colorectal Cancer Cell Survival. *Gastroenterology* (2008). doi:10.1053/j.gastro.2008.05.052
170. Elborn, J. S. Cystic fibrosis. *The Lancet* (2016). doi:10.1016/S0140-6736(16)00576-6
171. Harutyunyan, M. *et al.* Personalized Medicine in CF: From Modulator Development to Therapy for Cystic Fibrosis Patients with Rare CFTR Mutations. *Am. J. Physiol. Cell. Mol. Physiol.* (2017). doi:10.1152/ajplung.00465.2017
172. Ren, C. L. *et al.* Cystic Fibrosis Foundation Pulmonary Guidelines. Use of Cystic Fibrosis Transmembrane Conductance Regulator Modulator Therapy in Patients with Cystic Fibrosis. *Ann. Am. Thorac. Soc.* **15,** 271–280 (2018).
173. Char, J. E. *et al.* A little CFTR goes a long way: CFTR-dependent sweat secretion from G551D and R117H-5T cystic fibrosis subjects taking ivacaftor. *PLoS One* (2014). doi:10.1371/journal.pone.0088564
174. Schneider, E. K., Reyes-Ortega, F., Li, J. & Velkov, T. Can Cystic Fibrosis Patients Finally Catch a Breath With Lumacaftor/Ivacaftor? *Clinical Pharmacology and Therapeutics* (2017). doi:10.1002/cpt.548
175. Heda, G. D., Tanwani, M. & Marino, C. R. The {Delta}F508 mutation shortens the biochemical half-life of plasma membrane CFTR in polarized epithelial cells. *Am J Physiol Cell Physiol* **280,** C166-174 (2001).
176. Goździk-Spychalska, J. *et al.* C-MET inhibitors in the treatment of lung cancer. *Curr. Treat. Options Oncol.* **15,** 670–682 (2014).
177. Mo, H.-N. & Liu, P. Targeting MET in cancer therapy. *Chronic Dis. Transl. Med.* (2017). doi:10.1016/j.cdtm.2017.06.002
178. Sun, X. & Kaufman, P. D. Ki-67: more than a proliferation marker. *Chromosoma* (2018). doi:10.1007/s00412-018-0659-8
179. Darzynkiewicz, Z. *et al.* Initiation and termination of DNA replication during S phase in relation to cyclins D1, E and A, p21WAF1, Cdt1 and the p12 subunit of DNA polymerase δ revealed in individual cells by cytometry. *Oncotarget* **6,** 11735–50 (2015).
180. Talamo Guevara, M. & McColley, S. A. The safety of lumacaftor and ivacaftor for the treatment of cystic fibrosis. *Expert Opin. Drug Saf.* **16,** 1305–1311 (2017).
181. Sood, R. *et al.* Regulation of CFTR expression and function during differentiation of intestinal epithelial cells. *EMBO J.* **11,** 2487–2494 (1992).

182. Mailhot, G. *et al.* CFTR knockdown stimulates lipid synthesis and transport in intestinal Caco-2/15 cells. *Am. J. Physiol. Gastrointest. Liver Physiol.* **297,** G1239-1249 (2009).
183. Mailhot, G., Rabasa-Lhoret, R., Moreau, A., Berthiaume, Y. & Levy, E. CFTR depletion results in changes in fatty acid composition and promotes lipogenesis in intestinal Caco 2/15 cells. *PLoS One* **5,** e10446 (2010).
184. Valdivieso, A. G. *et al.* The Mitochondrial Complex I Activity Is Reduced in Cells with Impaired Cystic Fibrosis Transmembrane Conductance Regulator (CFTR) Function. *PLoS One* **7,** e48059 (2012).
185. Jantarajit, W., Lertsuwan, K., Teerapornpuntakit, J., Krishnamra, N. & Charoenphandhu, N. CFTR-mediated anion secretion across intestinal epithelium-like Caco-2 monolayer under PTH stimulation is dependent on intermediate conductance K+channels. *Am. J. Physiol. Cell Physiol.* **313,** C118–C129 (2017).
186. Sambuy, Y. *et al.* The Caco-2 cell line as a model of the intestinal barrier: influence of cell and culture-related factors on Caco-2 cell functional characteristics. *Cell Biol. Toxicol.* **21,** 1–26 (2005).
187. Gerdes, J. *et al.* Cell cycle analysis of a cell proliferation-associated human nuclear antigen defined by the monoclonal antibody Ki-67. *J. Immunol.* (1984).
188. Bruno, S. & Darzynkiewicz, Z. Cell cycle dependent expression and stability of the nuclear protein detected by Ki-67 antibody in HL-60 cells. *Cell Prolif.* (1992). doi:10.1111/j.1365-2184.1992.tb01435.x
189. Fukada, S. *et al.* Molecular signature of quiescent satellite cells in adult skeletal muscle. *Stem Cells* (2007). doi:10.1634/stemcells.2007-0019
190. Kaihara, T. *et al.* Dedifferentiation and decreased expression of adhesion molecules, E-cadherin and ZO-1, in colorectal cancer are closely related to liver metastasis. *J. Exp. Clin. Cancer Res.* (2003).
191. Kwak, J. M. *et al.* The prognostic significance of E-cadherin and liver intestine-cadherin expression in colorectal cancer. *Dis. Colon Rectum* (2007). doi:10.1007/s10350-007-9034-1
192. Wang, H. *et al.* Epithelial-Mesenchymal Transition (EMT) Induced by TNF-α Requires AKT/GSK-3β-Mediated Stabilization of Snail in Colorectal Cancer. *PLoS One* (2013). doi:10.1371/journal.pone.0056664
193. Fortier, A.-M., Asselin, E. & Cadrin, M. Keratin 8 and 18 loss in epithelial cancer cells increases collective cell migration and cisplatin sensitivity through claudin1 up-regulation. *J. Biol. Chem.* **288,** 11555–11571 (2013).
194. Eriksson, J. E. *et al.* Introducing intermediate filaments: from discovery to disease. *J. Clin. Invest.* **119,** 1763–1771 (2009).
195. Zhang, B. *et al.* Cytokeratin 18 knockdown decreases cell migration and increases chemosensitivity in non-small cell lung cancer. *J. Cancer Res. Clin. Oncol.* (2016). doi:10.1007/s00432-016-2253-x
196. Zhang, H. *et al.* EGR1 decreases the malignancy of human non-small cell lung carcinoma by regulating KRT18 expression. *Sci. Rep.* (2014). doi:10.1038/srep05416
197. Majumdar, D., Tiernan, J. P., Lobo, A. J., Evans, C. A. & Corfe, B. M. Keratins in colorectal epithelial function and disease. *Int. J. Exp. Pathol.* (2012). doi:10.1111/j.1365-2613.2012.00830.x
198. Lähdeniemi, I. A. K. *et al.* Keratins regulate colonic epithelial cell differentiation through the Notch1 signalling pathway. *Cell Death Differ.* (2017). doi:10.1038/cdd.2017.28
199. Kermorgant, S., Dessirier, V., Lewin, M. J. & Lehy, T. HGF upregulates and modifies subcellular distribution of proteins in colon cancer cell enterocytic differentiation. *Am. J. Physiol. Gastrointest. Liver Physiol.* (2001).
200. Farrell, J. *et al.* HGF induces epithelial-to-mesenchymal transition by modulating the mammalian Hippo/MST2 and ISG15 pathways. *J. Proteome Res.* (2014). doi:10.1021/pr5000285
201. Van Goor, F. *et al.* Rescue of CF airway epithelial cell function in vitro by a CFTR potentiator, VX-770. *Proc. Natl. Acad. Sci.* (2009). doi:10.1073/pnas.0904709106
202. Rowe, S. M. *et al.* Tezacaftor-Ivacaftor in Residual-Function Heterozygotes with Cystic Fibrosis. *N. Engl. J. Med.* **377,** 2024–2035 (2017).
203. Burgener, E. B. & Moss, R. B. Cystic fibrosis transmembrane conductance regulator modulators: precision medicine in cystic fibrosis. *Curr. Opin. Pediatr.* (2018). doi:10.1097/MOP.0000000000000627
204. Popowicz, N., Wood, J., Tai, A., Morey, S. & Mulrennan, S. Immediate effects of lumacaftor/ivacaftor administration on lung function in patients with severe cystic fibrosis lung disease. *J. Cyst. Fibros. Off. J. Eur. Cyst. Fibros. Soc.* **16,** 392–394 (2017).
205. Murer, C. *et al.* First experience in Switzerland in Phe508del homozygous cystic fibrosis patients with end-stage pulmonary disease enrolled in a lumacaftor-ivacaftor therapy trial - preliminary results. *Swiss Med. Wkly.* **148,** w14593 (2018).
206. Yaekashiwa, M. *et al.* Simultaneous or delayed administration of hepatocyte growth factor equally represses the fibrotic changes in murine lung injury induced by bleomycin. A morphologic study. *Am. J. Respir. Crit. Care Med.* **156,** 1937–1944 (1997).
207. Ido, A. *et al.* Safety and pharmacokinetics of recombinant human hepatocyte growth factor (rh-HGF) in patients with fulminant hepatitis: a phase I/II clinical trial, following preclinical studies to ensure safety. *J. Transl. Med.* **9,** 55 (2011).

208. Hirano, S. *et al.* A phase I/II exploratory clinical trial for intracordal injection of recombinant hepatocyte growth factor for vocal fold scar and sulcus. *J. Tissue Eng. Regen. Med.* (2017). doi:10.1002/term.2603
209. Matsumoto, K., Funakoshi, H., Takahashi, H. & Sakai, K. HGF-Met Pathway in Regeneration and Drug Discovery. *Biomedicines* **2,** 275–300 (2014).
210. Sosnay, P. R. *et al.* Defining the disease liability of variants in the cystic fibrosis transmembrane conductance regulator gene. *Nat. Genet.* **45,** 1160–1167 (2013).
211. Carvalho-Oliveira, I. *et al.* CFTR Localization in Native Airway Cells and Cell Lines Expressing Wild-type or F508del-CFTR by a Panel of Different Antibodies. *J. Histochem. Cytochem.* **52,** 193–203 (2004).
212. Bronsveld, I. *et al.* Residual chloride secretion in intestinal tissue of deltaF508 homozygous twins and siblings with cystic fibrosis. The European CF Twin and Sibling Study Consortium. *Gastroenterology* **119,** 32–40 (2000).
213. Kälin, N., Claaß, A., Sommer, M., Puchelle, E. & Tümmler, B. ΔF508 CFTR protein expression in tissues from patients with cystic fibrosis. *J. Clin. Invest.* **103,** 1379–1389 (1999).
214. Matos, A. M. & Matos, P. Combination therapy in Phe508del CFTR: how many will be enough? *J Lung Heal. Dis* **2,** 9–16 (2018).
215. Grasemann, H. CFTR Modulator Therapy for Cystic Fibrosis. *N. Engl. J. Med.* **377,** 2085–2088 (2017).
216. Elborn, J. S. *et al.* Efficacy and safety of lumacaftor/ivacaftor combination therapy in patients with cystic fibrosis homozygous for Phe508del CFTR by pulmonary function subgroup: a pooled analysis. *Lancet Respir. Med.* **4,** 617–626 (2016).
217. Kristensen, A. R., Gsponer, J. & Foster, L. J. A high-throughput approach for measuring temporal changes in the interactome. *Nat. Methods* **9,** 907–909 (2012).
218. Shevchenko, A., Wilm, M., Vorm, O. & Mann, M. Mass Spectrometric Sequencing of Proteins from Silver-Stained Polyacrylamide Gels. *Anal. Chem.* **68,** 850–858 (1996).
219. Goll, D. E., Thompson, V. F., Li, H., Wei, W. & Gong, J. The Calpain System. *Physiol Rev* **83,** 731–801 (2003).
220. Averna, M. *et al.* Calpain Inhibition Promotes the Rescue of F508del-CFTR in PBMC from Cystic Fibrosis Patients. *PLoS One* **8,** e66089 (2013).
221. Yao, X., Thibodeau, A. & Forte, J. G. Ezrin-calpain I interactions in gastric parietal cells. *Am. J. Physiol. - Cell Physiol.* **265,** (1993).
222. Shcherbina, A., Bretscher, A., Kenney, D. M. & Remold-O'Donnell, E. Moesin, the major ERM protein of lymphocytes and platelets, differs from ezrin in its insensitivity to calpain. *FEBS Lett.* **443,** 31–36 (1999).
223. Sasaki, T. *et al.* Inhibitory effect of di- and tripeptidyl aldehydes on calpains and cathepsins. *J. Enzyme Inhib.* **3,** 195–201 (1990).
224. Shenoy, A. M. & Brahmi, Z. Inhibition of the calpain-mediated proteolysis of protein kinase C enhances lytic activity in human NK cells. *Cell. Immunol.* **138,** 24–34 (1991).
225. Li, J., Dai, Z., Jana, D., Callaway, D. J. E. & Bu, Z. Ezrin Controls the Macromolecular Complexes Formed between an Adapter Protein Na^+/H^+ Exchanger Regulatory Factor and the Cystic Fibrosis Transmembrane Conductance Regulator. *J. Biol. Chem.* **280,** 37634–37643 (2005).
226. Ezrin activation helps restore CFTR function. *J. Cell Sci.* **129,** (2016).
227. Averna, M. *et al.* Evidence for alteration of calpain/calpastatin system in PBMC of cystic fibrosis patients. *Biochim. Biophys. Acta - Mol. Basis Dis.* **1812,** 1649–1657 (2011).
228. van Meegen, M. A. *et al.* Analysis of CFTR expression in immune cell subsets of peripheral blood. *J. Cyst. Fibros.* **8,** S56 (2009).
229. Johansson, J. *et al.* Detection of CFTR Protein in Human Leukocytes by Flow Cytometry.
230. Antigny, F., Norez, C., Becq, F. & Vandebrouck, C. Calcium homeostasis is abnormal in cystic fibrosis airway epithelial cells but is normalized after rescue of F508del-CFTR. *Cell Calcium* **43,** 175–183 (2008).
231. Antigny, F., Norez, C., Cantereau, A., Becq, F. & Vandebrouck, C. Abnormal spatial diffusion of Ca2+ in F508del-CFTR airway epithelial cells. *Respir. Res.* **9,** 70 (2008).
232. Norez, C., Antigny, F., Becq, F. & Vandebrouck, C. Maintaining Low Ca2+ Level in the Endoplasmic Reticulum Restores Abnormal Endogenous F508del-CFTR Trafficking in Airway Epithelial Cells. *Traffic* **7,** 562–573 (2006).
233. Ribeiro, C. M. P., Paradiso, A. M., Carew, M. A., Shears, S. B. & Boucher, R. C. Cystic Fibrosis Airway Epithelial $Ca^{2+}{}_i$ Signaling. *J. Biol. Chem.* **280,** 10202–10209 (2005).
234. Ono, Y. & Sorimachi, H. Calpains — An elaborate proteolytic system. *Biochim. Biophys. Acta - Proteins Proteomics* **1824,** 224–236 (2012).
235. Piatkov, K. I., Oh, J.-H., Liu, Y. & Varshavsky, A. Calpain-generated natural protein fragments as short-lived substrates of the N-end rule pathway. *Proc. Natl. Acad. Sci. U. S. A.* **111,** E817-26 (2014).
236. Hoskin, V. *et al.* Ezrin regulates focal adhesion and invadopodia dynamics by altering calpain activity to promote breast cancer cell invasion. *Mol. Biol. Cell* **26,** 3464–79 (2015).
237. Donkor, I. O. Calpain inhibitors: a survey of compounds reported in the patent and scientific literature. *Expert*

Opin. Ther. Pat. **21,** 601–636 (2011).
238. Donkor, I. O. An updated patent review of calpain inhibitors (2012 – 2014). *Expert Opin. Ther. Pat.* 1–15 (2014). doi:10.1517/13543776.2014.982534
239. Sherbet, G. V. & Sherbet, G. V. 5 – Hepatocyte Growth Factor. in *Growth Factors and Their Receptors in Cell Differentiation, Cancer and Cancer Therapy* 65–70 (2011). doi:10.1016/B978-0-12-387819-9.00005-0
240. Nakamura, T. & Mizuno, S. The discovery of hepatocyte growth factor (HGF) and its significance for cell biology, life sciences and clinical medicine. *Proc. Jpn. Acad. Ser. B. Phys. Biol. Sci.* **86,** 588–610 (2010).
241. Matsumoto, K. & Nakamura, T. Roles of HGF as a pleiotropic factor in organ regeneration. *EXS* **65,** 225–49 (1993).
242. Nakamura, T. Structure and function of hepatocyte growth factor. *Prog. Growth Factor Res.* **3,** 67–85 (1991).
243. MD Aksam, V. K., Chandrasekaran, V. M. & Pandurangan, S. Identification of cluster of proteins in the network of MAPK pathways as cancer drug targets. *Informatics Med. Unlocked* **9,** 86–92 (2017).
244. Zhu, P., Aliabadi, H. M., Uludağ, H. & Han, J. Identification of Potential Drug Targets in Cancer Signaling Pathways using Stochastic Logical Models. *Sci. Rep.* **6,** 23078 (2016).
245. Auvinen, E., Kivi, N. & Vaheri, A. Regulation of ezrin localization by Rac1 and PIPK in human epithelial cells. *Exp. Cell Res.* **313,** 824–833 (2007).
246. Jiang, L. *et al.* CLIC proteins, ezrin, radixin, moesin and the coupling of membranes to the actin cytoskeleton: A smoking gun? *Biochim. Biophys. Acta - Biomembr.* **1838,** 643–657 (2014).